

# UNCLASSIFIED

AD NUMBER
AD919079
NEW LIMITATION CHANGE
TO Approved for public release, distribution unlimited
FROM Distribution authorized to U.S. Gov't. agencies only; Test and Evaluation; OCT 1973. Other requests shall be referred to Air Force Rocket Propulsion Lab., Edwards AFB, CA 93523.
AUTHORITY
AFRPL ltr, 15 May 1986

THIS PAGE IS UNCLASSIFIED

AD 919 079

AUTHORITY:

AFRPL.

15 MAY 86



THIS REPORT HAS BEEN DELIMITED  
AND CLEARED FOR PUBLIC RELEASE  
UNDER DOD DIRECTIVE 5200.20 AND  
NO RESTRICTIONS ARE IMPOSED UPON  
ITS USE AND DISCLOSURE.

DISTRIBUTION STATEMENT A

APPROVED FOR PUBLIC RELEASE;  
DISTRIBUTION UNLIMITED.

✓ AFRPL-TR-73-114

# **MORE-STORABLE FUELS FOR GAS DYNAMIC LASER APPLICATIONS**

AD919079

PREPARED FOR:

AIR FORCE WEAPONS LABORATORY  
KIRTLAND AFB, NEW MEXICO 87117

CURTIS C. SELPH

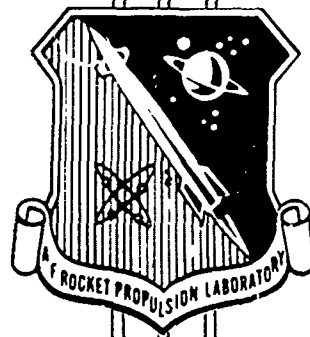
MICHAEL F. POWELL, ET AL

FEBRUARY 1974

FINAL REPORT FOR PERIOD AUGUST 1969 - JUNE 1973

DISTRIBUTION LIMITED TO U.S. GOVERNMENT AGENCIES ONLY:  
TEST AND EVALUATION, OCTOBER 1973. OTHER REQUESTS FOR  
THIS DOCUMENT MUST BE REFERRED TO AFRPL (ST'INFO/DOZ),  
EDWARDS, CALIFORNIA 93523.

AIR FORCE ROCKET PROPULSION LABORATORY  
DIRECTOR OF SCIENCE AND TECHNOLOGY  
AIR FORCE SYSTEMS COMMAND  
EDWARDS, CALIFORNIA 93523



## NOTICES

When US Government drawings, specifications, or other data are used for any purpose other than a definitely related Government procurement operation, the Government thereby incurs no responsibility nor any obligation whatsoever, and the fact that the Government may have formulated, furnished, or in any way supplied the said drawings, specifications or other data, is not to be regarded by implication or otherwise, or in any manner licensing the holder or any other person or corporation, or conveying any rights or permission to manufacture use, or sell any patented invention that may in any way be related thereto.

## APPROVAL

This technical report has been reviewed and is approved.

FOR THE COMMANDER

CHARLES E. SIEBER, Lt Col, USAF  
Chief, Liquid Rocket Division

REPORT DOCUMENTATION PAGE		READ INSTRUCTIONS BEFORE COMPLETING FORM
1 REPORT NUMBER AFRPL-TR-73-114	2 GOVT ACCESSION NO.	3. RECIPIENT'S CATALOG NUMBER
4 TITLE (and Subtitle) More Storable Fuels for Gas Dynamic Laser Application		5 TYPE OF REPORT & PERIOD COVERED Final AUG 69 - JUN 73
		6 PERFORMING ORG. REPORT NUMBER AFRPL TR-73-114
7 AUTHOR(s) Curtis C. Selph Michael F. Powell et al		8 CONTRACT OR GRANT NUMBER(s)
9 PERFORMING ORGANIZATION NAME AND ADDRESS Air Force Rocket Propulsion Laboratory (LK) Edwards, CA 93523		10 PROGRAM ELEMENT, PROJECT, TASK AREA & WORK UNIT NUMBERS 62302F/5730/07
11 CONTROLLING OFFICE NAME AND ADDRESS AFWL/LRL Kirtland AFB NM 87117		12 REPORT DATE February 1974
		13 NUMBER OF PAGES 161
14 MONITORING AGENCY NAME & ADDRESS (if different from Controlling Office)		15. SECURITY CLASS (of this report) UNCLASSIFIED
		15a DECLASSIFICATION DOWNGRADING SCHEDULE N/A
16 DISTRIBUTION STATEMENT (of this Report) Distribution limited to U.S. Government agencies only; test and evaluation; Oct 1973. Other requests for this document must be referred to AFRPL (STINFO/DOZ), Edwards CA 93523		
17. DISTRIBUTION STATEMENT (of the abstract entered in Block 20, if different from Report)  APPROVED FOR PUBLIC RELEASE: DISTRIBUTION UNLIMITED		
18 SUPPLEMENTARY NOTES Documents work under AFRPL in-house Project number 317J06SB		
19 KEY WORDS (Continue on reverse side if necessary and identify by block number) Storable laser reactants, synthesis, thermochemical characterization, gas dynamic laser, combustion evaluation		
20. ABSTRACT (Continue on reverse side if necessary and identify by block number) Chemical and physical characterization of a number of potential GDL fuel candidates was accomplished, including previously known molecules and also molecules synthesized especially with GDL applications in mind. The strongest candidate was dicyanofuroxan, DCFO, $C_4N_4O_2$ , which was finally discarded on safety grounds. The approach was revised to emphasize storable diluent compounds, based on the substitution of carbon monoxide for a portion of the nitrogen in the GDL medium. A by-product of this approach is the alleviation of problems associated with the fuel. Carbonyl diisocyanate, CDI, $C_2O_3N_2$ ,		

SECURITY CLASSIFICATION OF THIS PAGE(When Data Entered)

20. ABSTRACT:

was characterized as a possible storable diluent, and its combustion characteristics were determined in a small combustion facility.

SECURITY CLASSIFICATION OF THIS PAGE(When Data Entered)

## SUMMARY

The objective of finding a storable Gas Dynamic Laser (GDL) fuel can be summed up as a search for compounds which have no elements other than carbon, hydrogen, nitrogen, or oxygen, and with the further constraint that the atom ratio of carbon to hydrogen be about five or greater. Since the fuel must heat a large quantity of nitrogen to  $\sim 1600$ - $1800^\circ\text{K}$ , high energy is essential. Other desired characteristics are low vapor pressure, low melting point, good stability, low toxicity, and favorable cost and availability. No compounds with a large share of these qualities were found.

The compound which received the greatest attention was dicyanofuroxan, DCFO,  $\text{C}_4\text{N}_4\text{O}_2$ , which came closest to meeting the requirements. New techniques were devised which greatly improved our ability to make DCFO in quantity. Chemical and physical characterization of DCFO were well underway, leading towards combustion tests, when a series of accidents here and elsewhere raised questions about the safety of DCFO. New hazards testing was undertaken which showed that DCFO could be detonated with explosive charges and would also propagate powerful detonations in tube sizes at least as small as  $1/8$ " i.d. Work with neat DCFO was abandoned.

Earlier studies on low melting eutectic mixtures containing DCFO were renewed in hopes of eliminating the detonation hazard. Low hydrogen compounds, malononitrile and maleic anhydride, were mixed with DCFO. Progressive reduction in hazard was noted, but a completely safe system was not obtained until the DCFO content was at or below 50 percent by weight. The resulting compositions had a carbon to hydrogen ratio about 2.5/1, which was determined by the AFWL to be insufficiently attractive to warrant further work.

Synthesis efforts were intensified to find a safe alternative to DCFO. These were centered around a previously unreported compound, dicyano-oxazole,  $\text{C}_5\text{HN}_3\text{O}$ , and were rewarded by the synthesis of a low melting, high boiling solid with good stability. Yields were very low, however, and remained unsatisfactory after strenuous effort. Even the modest quantities required by this project could not be obtained, and the effort was discontinued.

In the absence of attractive fuel candidates, the storable heat source avenue of investigation was abandoned. The project was temporarily halted, pending definition of an approach that would provide a reasonable continuation. An approach was devised involving the use of carbonyl diisocyanate, CDI,  $\text{C}_3\text{O}_3\text{N}_2$ , which theoretically could satisfy the role of both fuel and diluent, leading to the elimination of all the hard cryogens from the GDL reactant system. The use of carbonyl diisocyanate in such a role is predicated on a theoretical argument with two main assumptions. One is that the compound may be pyrolyzed by burning a portion of it with



$\text{N}_2\text{O}$  to a gaseous mixture of carbon monoxide and nitrogen, and the second is that such a mixture is substitutable for nitrogen in the GDL medium. The kinetic substitutability of carbon monoxide for nitrogen was accepted as a reasonable risk based on the currently available information (2). The demonstration of the pyrolysis of CDI to CO and  $\text{N}_2$  was in turn accepted as a reasonable revised program goal, if its thermodynamic feasibility could be proved. The dearth of similar compounds made its heat of formation highly uncertain, and a final commitment was delayed while a measurement was obtained. A heat of formation of -83.3 kcal/mole was determined by hydrolysis in a reaction calorimeter. This was 15-20 kilocalories more negative than expected, and made it necessary to propose supplemental energy from the burning of a higher energy material. Although the simplicity of a combined fuel and diluent was lost, an important advantage remained: the fuel could have a much lower carbon to hydrogen ratio. This results from the small amount of fuel needed, and from the fact that the reducing conditions of the medium prevent much of the hydrogen from oxidizing to water. Thus, exotic hydrogen-free fuels like DCFO would not be required. A combined system of CDI plus  $\text{N}_2\text{O}$  plus benzonitrile was shown theoretically to produce a useful medium, worth characterizing experimentally.

A micro-engine designed originally for studying DCFO and similar materials was adapted for CDI. The main characteristic of the engine is its ability to work at very low flow rates to conserve scarce reactants. Lasing tests were not provided for, due to practical difficulties at the low flow rates. Flame temperature and species collection were main analytical tools. A photocell record of chamber luminosity was included as a check on particulate matter. A positive displacement feed system allowed accurate control of the small flows. Large heat losses characteristic of such low flow rate devices were avoided through the use of high temperature refractory liners around the combustion zone, and a regenerative back flow of diluent.

The basic design changes to accommodate CDI related to the introduction of CDI at midchamber. A swirl cup injector with 1/8" feed tubes was welded into a 1/4" concentric outer tube carrying cooling water. The chamber walls and liners were modified for the installation at midchamber of this injector. The CDI spray fan (15° half  $\Delta$ ) pointed downstream and the droplets were entrained into a combustion medium produced upstream by the burning of CO and  $\text{O}_2$ . The upstream liners were cooled by a regenerative back-flow of a CO plus  $\text{H}_2$  mixture which was injected into the chamber either at the combustor head end or at midchamber with CDI, depending on how the liners were installed for a particular test. The mixture ratios were adjusted to give burnt compositions and temperature similar to those expected from a  $\text{N}_2\text{O}$ /CDI/benzonitrile laser system, except that  $\text{N}_2$  was low. Effectively the only  $\text{N}_2$  present originated in the CDI, and this was used as a gauge of the pyrolysis of the CDI.

The combustion results verify the decomposition of CDI to CO and N<sub>2</sub> with one possibly significant exception. Substantial amounts of HCN were produced from reaction of CDI or its intermediates with the H<sub>2</sub> brought in with the liner coolant.

Simultaneous combustion of N<sub>2</sub>O/CDI/benzonitrile was found not to be feasible in this device due to very low benzonitrile flow rates required for a reasonable simulation. A separate combustion experiment for N<sub>2</sub>O/benzonitrile has been planned to supplement the results of the CDI experiments, and these results will be given in a later report.

## PREFACE

The work reported herein was accomplished under a cooperative project between the Air Force Weapons Laboratory (AFWL) and the Air Force Rocket Propulsion Laboratory (AFRPL) between August 1969 and June 1973. Funds and broad guidance were supplied by AFWL/LRL while the manpower and facility requirements were supplied primarily by the AFRPL. Project Monitors at AFWL over the course of the project included Major Raymond Oglukian, Mr. Kay Rimer, Capt Roger Miller, Capt George Rhodes, Capt Fred Damm, and Lt. Robert Hemm. The work described was accomplished either by or under the direction of personnel of the Engine Components Branch, Liquid Rocket Division. AFRPL resources from tasks 314802 and 573007 and AFWL funds from projects 644A and 317J were utilized under AFRPL in-house project 317J06SB to implement this effort. The Program Manager was Mr. Bernard R. Bornhorst, and the Project Engineer was Mr. Curtis Selph who was assisted by Lt. Arthur Pope and Mr. Michael Powell.

Major portions of the combustion facility were designed within the Test and Support Division by Messrs Tyrone Williams and Doug Haas; and the facility buildup, activation and operation were accomplished by the Test and Support Division with Captain Pony Rice and Sgt Ed Soteropoulos serving as Test Engineers at different times during the Project.

The synthesis effort was carried out at the Chemical and Materials Branch of the Technology Division, with contributions from Dr. Claude Merrill, Dr. Michael Barnes, and Sgt Richard Watson. These individuals co-authored the Synthesis section of the report.

Reactant characterization and combustion sample analysis were carried out at the Chemical and Materials Branch by Mr. Berge Goshgarian, Capt. Neal Lupton, Mr. Tom Owens, Mr. Mike Citro, Mr. Bill Robbs, Mr. George Shoemaker, Mr. Louis Dee, Lt. Avanzino, Lt. Hess, Lt. Doug Curry and Mr. Herman Martens.

## TABLE OF CONTENTS

<u>Section</u>		<u>Page</u>
I	INTRODUCTION. . . . .	9
II	SURVEY OF POTENTIAL FUEL CANDIDATES . . . . .	11
III	SYNTHESIS. . . . .	17
IV	CHEMICAL AND PHYSICAL CHARACTERIZATION . . .	27
V	HARDWARE AND TEST FACILITY FOR COMBUSTION TESTS . . . . .	71
VI	COMBUSTION TESTS . . . . .	115
VII	CONCLUSIONS AND RECOMMENDATIONS. . . . .	153
	REFERENCES. . . . .	155
	AUTHOR'S BIOGRAPHY . . . . .	160

## LIST OF FIGURES

<u>Figure #</u>	<u>Title</u>	<u>Page</u>
1.	Specific Gravity of Dicyanofuroxan (DCFO) . . . . .	31
2.	Infrared Spectrum of DCFO . . . . .	32
3.	Kinematic Viscosity of DCFO . . . . .	33
4.	Surface Tension of DCFO . . . . .	35
5.	DCFO/Malononitrile Mixtures Critical Diameter for Detonation . . . . .	39
6.	Vapor pressure of Dicyanofurazan (DCFA) . . . . .	44
7.	Density of Dicyanofurazan (DCFA) . . . . .	46
8.	Infrared Spectrum of "Bottoms" . . . . .	48
9.	Flame Temperature vs CO <sub>2</sub> in the system CDI + N <sub>2</sub> O(L) + 1% H <sub>2</sub> O . . . . .	56
10.	Flame Temperature vs CO <sub>2</sub> at 1% H <sub>2</sub> O for the system CDI + Benzonitrile + N <sub>2</sub> O(L) . . . . .	58
11.	Rate of Viscosity Change of CDI . . . . .	60
12.	Initial Viscosity of CDI vs Temperature . . . . .	61
13.	Effect of Materials on Polymerization of CDI at 30°C . . . . .	62
14.	Vapor Pressure of CDI . . . . .	68
15.	Density of CDI vs Temperature . . . . .	69/70
16.	Schematic of the Mini Combustor - Fuels Configuration . .	74
17.	Mini Combustor - Disassembled . . . . .	75
18.	Inner Refractory Liner . . . . .	77
19.	Mini Combustor - CDI Configuration . . . . .	81

# LIST OF FIGURES (Cont'd)

<u>Figures</u>	<u>Title</u>	<u>Page</u>
20.	Gaseous O <sub>2</sub> /CO Corxial Injector . . . . .	84
21.	Gaseous O <sub>2</sub> Inlet Pressure vs Flowrate . . . . .	85
22.	Calculated Chamber Centerline O <sub>2</sub> Concentration vs Distance . . . . .	87
23.	CO Injection Annulus O. D. vs Inlet Pressure . . . . .	88
24.	O <sub>2</sub> Pintle; Post Firing . . . . .	90
25.	Section Drawing of CDI Injector . . . . .	91
26.	CDI Injector . . . . .	92
27.	Droplet Size and Nozzle Diameter vs $\Delta P$ , CDI Injector . . . . .	94
28.	Water Flow Pressure Drop vs Flowrate, CDI Injector . . . . .	95
29.	Water Spray Pattern From CDI Injector . . . . .	96
30.	Pressure Drop through Water Coolant Circuit, CDI Injector . . . . .	97
31.	Instrumentation Block Section . . . . .	99
32.	Chamber and Instrumentation Block Installed . . . . .	100
33.	Positive Expulsion Feed System . . . . .	103
34.	Schematic of the Sampling Probe . . . . .	108
35.	Spectral Response Curve of Photocell . . . . .	110
36.	Refractory Liners after CDI Series . . . . .	122
37.	Chamber Temperature - Run 3 . . . . .	125
38.	Chamber Temperature - Run 7 . . . . .	126
39.	Chamber Temperature - Run 13 . . . . .	128
40.	Chamber Pressure - Run 3 . . . . .	129

## LIST OF TABLES

<u>Table</u>		<u>Page</u>
1.	Low Hydrogen Compounds . . . . .	12
2.	Elemental Analysis of DCFO . . . . .	28
3.	Mass Spectrum of DCFO . . . . .	29
4.	Specific Heat of DCFO. . . . .	30
5.	Reactivity of GDL Fuels . . . . .	41
6.	Compatibility of Polymers with DCFA . . . . .	45
7.	Eutectic Mixtures of Low Hydrogen Fuels. . . . .	50
8.	Mass Spectrum of CDI. . . . .	67
9.	Composition of Reactants. . . . .	116
10.	Identity of Reactants used in Various Runs . . . . .	116
11.	Timing of Events in CDI Firings . . . . .	130
12.	Ballistic Data from CDI combustion Tests . . . . .	133
13.	Ballistic Efficiency for Mid-Chamber Injection of Gaseous Diluent. . . . .	137
14.	Ballistic Efficiency for Upper-Chamber Injection of Gaseous Diluent. . . . .	137
15.	Chemical Analysis of CDI Combustion Products . . . . .	139
16.	Averaged Sampling Results (without CDI Flow) . . . . .	144
17.	Averaged Sampling Results (with CDI Flow) . . . . .	145
18.	Ratio of Photocell Intensities (Before CDI/During CDI) .	147
19.	Quasi-Kinetic Calculations for Run 7. . . . .	150

## SECTION I

### INTRODUCTION

The objective of this project was to find and characterize storable gas generator reactants for use in combustion driven  $\text{CO}_2$  gas dynamic lasers (GDL). A literature search, assisted by theoretical computations of flame temperature and gas composition, was undertaken to identify candidate reactants. Quantities of several of the more promising materials were obtained and characterized with respect to their pertinent physical and chemical properties. Original synthesis of several new molecules which meet the nominal compositional requirements of the GDL application was accomplished; and improved synthesis routes were devised for two previously known compounds. A liquid micro-engine facility was designed and built to study the combustion characteristics of candidate fuels; and combustion data was obtained for a compound, carbonyl diisocyanate, which in combination with nitrous oxide and benzonitrile, offers the promise of a reactant system outside of the hard cryogen category of current propellants.

The general principles of gas dynamic laser operation have been reviewed by Gerry (1). Briefly, a population inversion in carbon dioxide molecules is produced between the first level of the asymmetric stretch mode and the first level of the symmetric stretch mode, an energy difference of about  $1000 \text{ cm}^{-1}$ . In the GDL such a condition is brought about by rapid expansion of a hot mixture of  $\text{CO}_2$ ,  $\text{N}_2$  and a catalyst,  $\text{H}_2\text{O}$ , or He. Through a fortuitous combination of kinetic rates, the lower energy symmetric mode is relaxed at a greater rate by these two catalysts than is the higher energy asymmetric mode. The function of the  $\text{N}_2$  is to replenish the upper level of  $\text{CO}_2$  through a very rapid transfer of energy from the first excited vibrational level.  $\text{N}_2$  is well suited to this role because of its long lifetime and near resonance with the upper level of  $\text{CO}_2$ .



Compositions and stagnation temperatures known to be effective for lasing are summarized below:

T	1200 - 1800°K
CO <sub>2</sub>	5-15 Mole %
H <sub>2</sub> O	0.5 - 1.5 Mole %
N <sub>2</sub>	Balance

When helium is used as catalyst, much higher concentrations (~30 percent) are required because of its lesser activity. Water is easier to incorporate into the system, and its only important drawback is the narrow range of useful concentration. At too low a concentration, the terminal laser level is not adequately unloaded. On the other hand, too high a water concentration leads to rapid quenching of the upper laser level. Since water is formed from hydrogen in the propellant, the water concentration limits, in conjunction with the CO<sub>2</sub> levels desired, suggest a carbon to hydrogen ratio of five or greater as being most appropriate for laser fuels. Lower ratios are tolerable at low CO<sub>2</sub> concentrations, but low CO<sub>2</sub> implies low temperatures, since most of the heat is released by the formation of CO<sub>2</sub>. In general, higher temperatures lead to better laser performance. The optimum temperature is above the 1800°K value indicated, but diminishing returns for the extra engineering problems suggest 1800°K as a reasonable upper limit. Above the optimum temperature, which varies with composition, laser performance actually falls off for a variety of reasons, including dissociation phenomena and enhanced deactivation rates in the nozzle and cavity.

The theoretical survey was undertaken with these constraints in mind and with two contrasting objectives. The more limited objective was the development of a storable, high energy fuel to replace the currently employed CO. The second, longer range objective was to devise an all-storable system in which the elemental nitrogen diluent, characteristic of the GDL, is also replaced.

## SECTION II

### SURVEY OF POTENTIAL FUEL CANDIDATES

At the outset of the project, the relative merit of a solid propellant versus a liquid propellant approach was an open question. The chief difficulty in either case is the low tolerance for hydrogen. For the liquid reactant approach this creates the most problems in the fuels area, since the oxidizer function is adequately filled by such hydrogen-free compounds as  $N_2O_4$ ,  $N_2O$ , and possibly  $C(NO_2)_4$ . For solid reactants a much greater choice of fuels may be proposed, but the possibilities for a very low-hydrogen oxidizer are limited, and there is the additional problem of the need for a binder, which typically contains considerable hydrogen. After considering the various possibilities, an early choice was made in favor of liquid reactants; and the various candidates were measured against the requirements of an assumed liquid system.

Table I shows a list of compounds encountered in the literature with carbon to hydrogen ratios equal to or greater than 5:1. Despite the size of the list the number of serious candidates is quite restricted and is a function of the rigor with which the ground rules are applied. Ultimately each of the compounds listed has one or more shortcomings, and further selection becomes somewhat subjective.

As a class the compounds are specialty chemicals, available only in experimental quantities, if at all. Nevertheless, there are differences in the relative ease of synthesis which becomes a special consideration in some cases.

Melting point is an important consideration in an application that assumes liquid injection. Obviously, compounds with melting points below ambient are wanted, but strict observance of this criterion would eliminate nearly all the candidates. The tendency to high melting points is characteristic of most substituents for hydrogen. Inclusion of intermediate melting compounds is possible if some complexity in the storage and feed system is accepted, or if a suitable low melting eutectic mixture

TABLE 1. LOW HYDROGEN COMPOUNDS

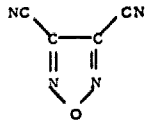
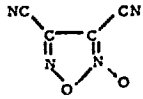
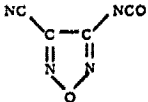
<u>Formula</u> <u>Name</u>	<u>Structure</u>	<u>mp(bp)</u> <u>(°C)</u>	<u>Remarks</u>	<u>Ref</u>
1. C Carbon	Varied	6000 (4200)	Cheap, non-toxic, hard to burn	3
2. CO Carbon monoxide	C=O	-207 (-190)	Toxic, cryogenic cheap, low energy	3
3. CN <sub>4</sub> Cyanogen azide	N <sub>3</sub> CN	Solid	Extremely shock sensitive	4
4. C <sub>2</sub> N <sub>2</sub> Cyanogen	NC-CN	-34.4 (-20.5)	Very toxic	3
5. C <sub>2</sub> N <sub>4</sub> Azodicarbonitrile	NC-N=N-CN	37	Shock sensitive	5
6. C <sub>2</sub> N <sub>4</sub> O <sub>6</sub> Trinitroacetonitrile	C(NO <sub>2</sub> ) <sub>3</sub> CN	30	Thermally unstable, shock sensitive, toxic	4
7. C <sub>2</sub> N <sub>8</sub> Cyanimidocarbonylazide	(N <sub>3</sub> ) <sub>2</sub> C=N-CN	42	Extremely shock sensitive	6
8. C <sub>3</sub> N <sub>2</sub> O Carbonyl Cyanide	CO(CN) <sub>2</sub>	(63)	Very toxic, volatile hydrolyses to HCN	7
9. C <sub>3</sub> N <sub>2</sub> O <sub>3</sub> Carbonyl Diisocyanate	CO(NCO) <sub>2</sub>	-50(105)	Polymerizes	8
10. C <sub>3</sub> O <sub>2</sub> Carbon suboxide	O=C=C=C=O	liq (7)	Toxic, unstable	9
11. C <sub>4</sub> N <sub>2</sub> Dicyanaocetylene	NC C≡C CN	liq (76)	Thermally unstable Toxic	10
12. C <sub>4</sub> N <sub>2</sub> O <sub>2</sub> Oxalylcyanide	NC COCOCN	61-2	Hydrolyses to HCN	11
13. C <sub>4</sub> N <sub>4</sub> O Dicyanofurazan		37(146)	Low yields, volatile, toxic	12
14. C <sub>4</sub> N <sub>4</sub> O <sub>2</sub> Dicyanofuroxan		42(200)	Toxic	13
15. C <sub>4</sub> N <sub>4</sub> O <sub>2</sub> Cyanoisocyanofurazan		liq (60 at 12mm)	Probably toxic, difficult synthesis	14

TABLE 1 (Cont'd)

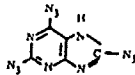
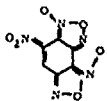
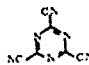
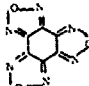
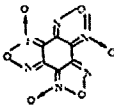
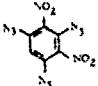
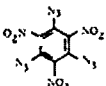
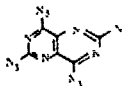
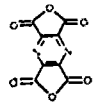
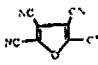
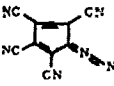
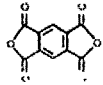
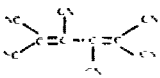
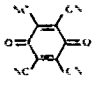
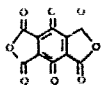
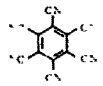
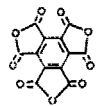
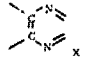
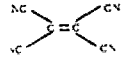
Formula Name	Structure	Mp(bp) (°C)	Remarks	Ref
16. $C_5H_3N_3$ Tricyanoethylene	$CH(CN)=C(CN)_2$	42	Thermally unstable	15
17. $C_5H_3N_5$ Triazidopurine		-	Probably explosive	16
18. $C_6H_3N_5O_6$ Nitrobenzodifuroxan		158	Explosive	4
19. $C_6N_2$ Dicyanodiacetylene	$NC-C\equiv C-C\equiv C-CN$	liq(76)	Thermally unstable	17
20. $C_6N_6$ Tricyanotriazine		Solid	Toxic, hydrolyses to HCN	
21. $C_6N_6O_3$ Benzotrifurazan		62	Poor synthesis	18
22. $C_6N_6O_6$ Benzotrifuroxan		194	Explosive	4
23. $C_6H_3N_5O_4$ Dinitrotriazidobenzene		106-8	Explosive	19
24. $C_6N_{12}O_6$ Triazidotrinitrobenzene		130	Explosive	4
25. $C_6N_{16}$ Tetrazidohomopurine		Solid	Explosive	16
26. $C_8N_2O_6$ Pyrazinetetracarboxylic anhydride		300	Low energy	20
27. $C_8N_4O$ Tetracyanofuran		126	Complex synthesis	21
28. $C_8N_6$ Hexacyanoethane	$C(CN)_3C(CN)_3$	Solid	Thermally unstable	22
29. $C_9N_6$ Diazotetracyanocyclopentadiene		Solid, d. 200	Likely Explosive	23

TABLE 1 (Cont'd)

<u>Formula Name</u>	<u>Structure</u>	<u>mp(bp) (°C)</u>	<u>Remarks</u>	<u>Ref</u>
30. $C_{10}H_2O_6$ Pyromellitic dianhydride		285	Low energy	24
31. $C_{10}N_6$ Hexacyanobutadiene		-	Likely very high melting	26
32. $C_{10}N_4O_2$ Tetracyanoquinone		-	Likely very high melting	12
33. $C_{10}O_8$ Quinonetetracarboxylic acid anhydride		-	Low energy	27
34. $C_{12}N_6$ Hexacyanobenzene		370		28
35. $C_{12}O_9$ Mellitic anhydride		-	Very high melting Low energy	24
36. $(CN)_x$ Paracyanogen		Solid dec 800		3
37. $C_6N_4$ Tetracyanoethylene		200°		2

of two or more compounds is found. Several compounds are shown with melting points in the range 30-50°C, and these have possibilities for binary eutectic mixtures with melting points in the 0°C range. Even higher melting compounds have utility in more complex eutectic mixtures. In general, attention has been concentrated on the intermediate melting compounds (30-50°C).

Toxicity is a major consideration, since it was an important factor in defeating cyanogen as a viable contender. However, it is not clear how toxic hazard can be avoided since none of the structural moieties for hydrogen replacement are free of toxic characteristics. Toxicity criteria were thus applied in a relative way, and usually without relative data. This was accomplished in general by equating toxic hazard with vapor pressure, since inhalation of vapors is regarded as the main danger. Reports of strong odor in a compound were also welcomed on detection arguments. As interest in a compound develops, of course, a more detailed accounting of toxic characteristics becomes necessary, and experimental work is justified.

Other safety related criteria are flammability and explosive hazards. Most of the compounds listed in Table 1 are only modest fire hazards due to low vapor pressure and attendant difficulty in forming vapor mixtures with air that lie within the ignition limits. Explosive hazard varies considerably, however, due to the varying nature of the substituents. Many of the compounds listed are organic azides, and in the absence of contrary information, may be assumed to be shock sensitive. A somewhat more tolerant view may be assumed for nitro substituted compounds, although at the highly substituted level required to displace significant hydrogen, explosive hazard becomes a problem. Cyano groups, on the other hand, introduce no explosive hazard. The importance attached to explosive hazard assumed dominant proportions during the later stages of the project. Initially, several candidates were explored which gave positive results in drop weight tests, in view of the successful use of sensitive compounds in solid propellants. Subsequent to an explosion at

AFRPL under another project, and at AVCO Corporation, both involving dicyanofurozan, more stringent criteria were applied. Thereafter, any candidate was required to pass a series of safety tests going beyond drop weight testing.

As suggested by the above discussion, the ultimate selection of candidates for experimental study was based on subjective judgment of the best combination of qualities, rather than by "filtration" of the candidates through a strictly defined mesh. Several of the candidates studied were in fact "targets of opportunity" -- accidentally made more available as by-products of the dicyanofuroxan synthesis.

Prior to this change in goals, a substantial effort had been expended on synthesis and characterization of compounds intended as high energy fuels, and this is reported in the following section.

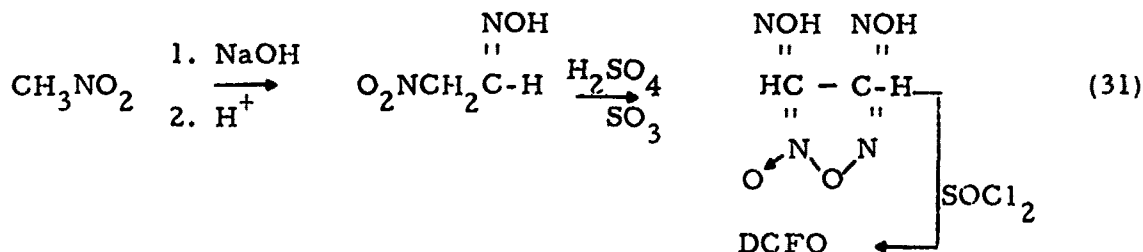
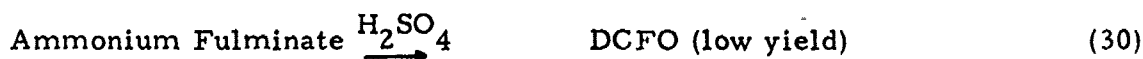
### SECTION III SYNTHESIS

The synthesis phase of this project had three main objectives: a) to supply the project with quantities of known compounds which could not be obtained commercially, b) to devise improved synthesis techniques for known compounds of interest, and c) to synthesize new compounds whose structures suggested properties which would meet the requirements set forth for GDL fuels.

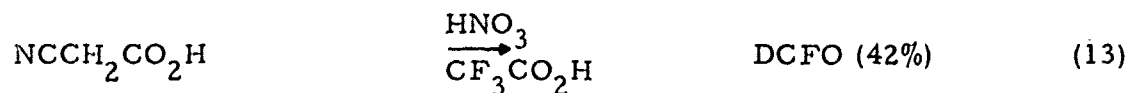
Most prominent among the compounds studied was dicyanofuroxan, DCFO, whose characterization is detailed in another section. An improved synthesis was developed which increased the yield and eliminated an expensive solvent. A related compound of interest was dicyanofurazan, DCFA; an alternate synthesis was developed for this material, with better yield. The details of these syntheses are given below, as well as those of a number of previously unreported hydrogen-free or hydrogen-poor molecules.

#### Dicyanofuroxan

Dicyanofuroxan (DCFO) has been prepared by several different schemes (see below): the most convenient of these methods is the one developed by Parker et al. (13) which involves the reaction of cyanoacetic acid with 100 percent white fuming nitric acid in trifluoroacetic acid solvent.



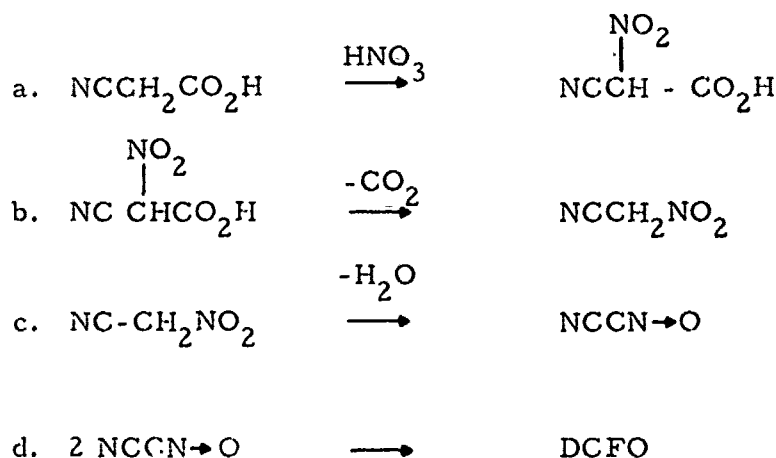




The parker method has two distinct disadvantages, especially for the preparation of larger than laboratory quantities of DCFO. These are:

1. Yield. Although Parker claimed a yield of 42 percent, this work and that in other laboratories has shown the average yield is closer to 30 percent.
2. Expense. Trifluoroacetic acid as solvent is relatively expensive. Its recovery after workup would be difficult, if not impossible.

A possible reaction mechanism of formation of DCFO from cyanoacetic acid by nitration is shown below:



Under the conditions of the Parker reaction, steps a, b and d are kinetically fast (see Ref 32, and 33 for examples). However, step c, the dehydration of a nitro compound to a nitrile oxide usually requires a dehydrating agent (34).

When the Parker reaction was carried out in the presence of various dehydrants, increased yields of DCFO were realized in almost every case. The most effective and convenient reagent was phosphorous pentoxide.

Two variations of the "P<sub>2</sub>O<sub>5</sub> Parker" reaction were devised (86). One variation was a solventless version wherein P<sub>2</sub>O<sub>5</sub> was added in small

increments to an equimolar solution of cyanoacetic acid and inhibited red fuming nitric acid (7%  $N_2O_4$ , 0.4%  $HF$ , 92.6%  $HNO_3$ ; this was much less expensive than the 100 percent white fuming nitric acid utilized by Parker.) Following each  $P_2O_5$  addition, the temperature of the reaction mixture was elevated to  $45^\circ C$  where a vigorous reaction occurred. Cooling requirements were considerable during this period to maintain the temperature less than  $50^\circ C$ . Above this temperature the reaction mixture is unstable and will "run away" with considerable foaming and heat. The crude yield of DCFO by this method was 63 percent. Gas chromatographic analysis showed this mixture to be 98 percent DCFO; however, upon distillation only about two-thirds of the crude mixture could be recovered as pure DCFO. The remaining material was an unidentified high boiling residue which did not show up in the analysis.

A variation that made the reaction much more controllable and requires less operator attention was the addition of the equimolar cyanoacetic-nitric acid mixture into a refluxing slurry of phosphorous pentoxide-methylene chloride. Pot temperatures were controlled by the refluxing action to less than  $40^\circ C$ .

Crude yields were somewhat lower using this method, averaging around 50 percent, but could be increased to 75 percent by using 1.5 to 2 times the theoretical amount of phosphorous pentoxide. The composition of the "crude" was 66 percent DCFO, 10-15 percent trinitroacetonitrile and the remainder was high boiling residue.

Purification was easily achieved by vacuum distillation which removed the volatile trinitroacetonitrile into the vacuum trap and left the residue in the distillation pot. Yields of analytically pure DCFO from cyanoacetic acid by this method averaged 50 percent.

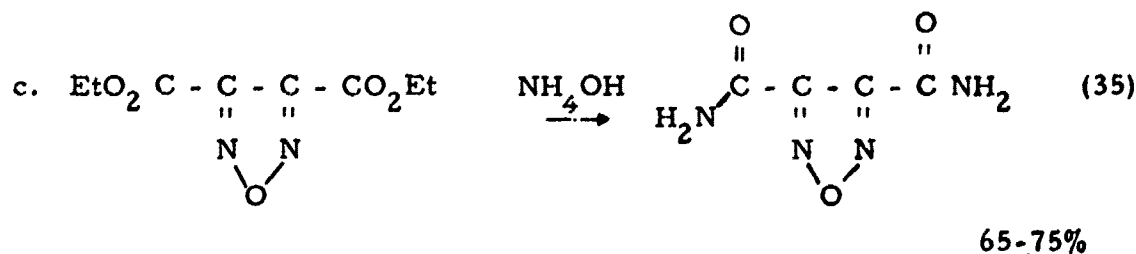
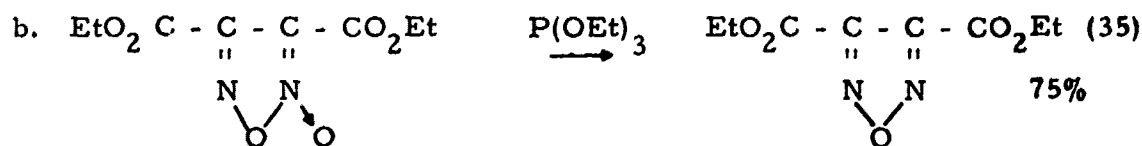
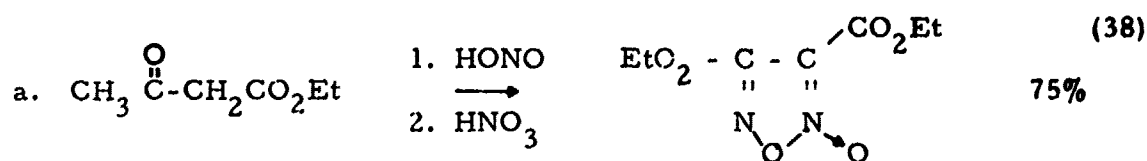
The use of other dehydrating agents in the modified Parker reaction was only briefly studied. It was found that this reaction could be effectively performed in trifluoroacetic anhydride and acetic anhydride. In the former case there is no advantage, as trifluoroacetic anhydride is expensive, and in the latter case separation of product and solvent proved to be

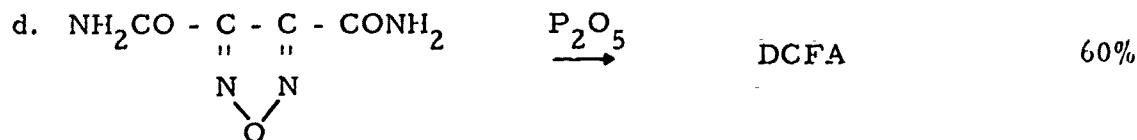
unexpectedly difficult. Phosphoryl chloride was surprisingly ineffective (86) but thionyl chloride gave a good yield of crude product (ca. 50 percent). Thionyl chloride is inexpensive on an industrial scale and this reagent may eventually prove to be the one of choice. It does, however, have the disadvantage of being most disagreeable to work with.

### Dicyanofurazan

Dicyanofurazan (DCFA) has been reported to have been prepared by deoxygenation of DCFO with triethyl phosphite in a 75 percent "crude" yield (35). The yield of purified material after distillation and crystallization was "lower due to the extraordinary volatility of the compound" (35). Even when this volatility is taken into account, this work and that in other laboratories (Ref 36, 37) has shown the yield of purified material is only about 20 percent. Thus, the overall yield of DCFA from commercially available starting materials is 10 percent.

An alternative scheme for the preparation of DCFA was devised as outlined below:





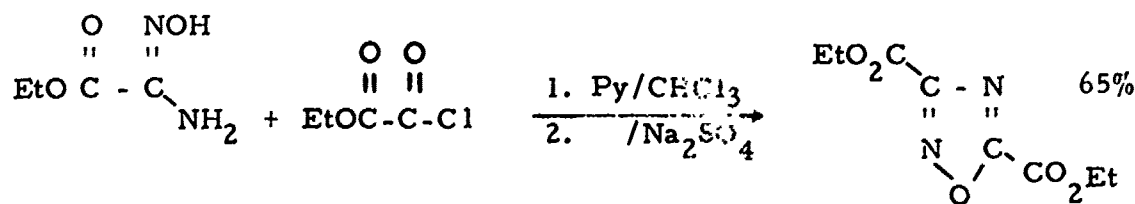
The overall yield of DCFA from commercially available ethyl acetoacetate is thus 30-35 percent. This process, although it is four steps compared to the two steps of the literature process, is quite convenient to carry out as steps b and c are very simple and do not require purification of the intermediates.

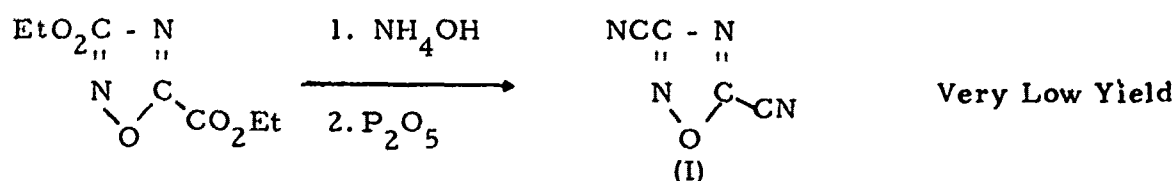
Several other reagents were tried without success for the conversion of furazandicarboxamide to DCFA (step d). There were: thionyl chloride, thionyl chloride in dimethylformamide (Ref 38), phosphoryl chloride (Ref 39), phosphoryl chloride in pyridine (Ref 39), and triphenyl phosphine-carbon tetrachloride (Ref 40).

### 3,5-Dicyano, 1, 2, 4 - Oxadiazole

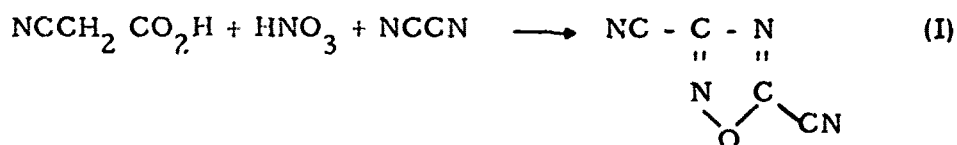
An isomer of DCFA is the previously unprepared 3,5-dicyano-1, 2, 4-oxadiazole (1). It was felt that this compound would be liquid or low melting and further, several attractive schemes existed for its synthesis (see Ref 41 for an excellent review on 1, 2, 4-oxadiazoles). This compound was prepared by two alternate routes as given below:

#### Scheme II





Scheme III

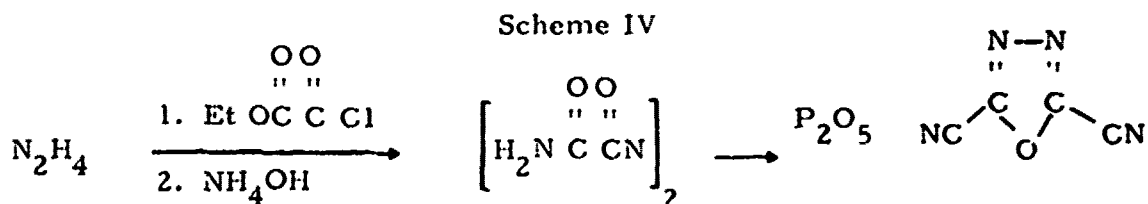


Scheme III is the Parker reaction with cyanogen added as an extra ingredient. Cyanogen traps the intermediate cyanogen mono-N-oxide formed in the Parker reaction to form compound (I). This reaction is definitely the preferred route as it is a one pot reaction.

Compound I was not obtained in a pure state. Its identity is based on infrared and mass spectra of the unpurified product.

#### 2, 5-Dicyano, 1, 3, 4-Oxadizole

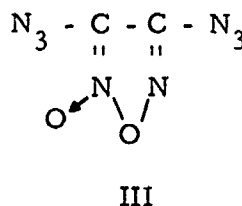
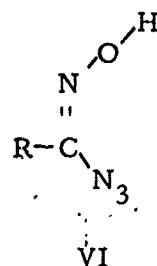
The other possible isomeric dicyano-oxadiazole is 2, 5-dicyano-1, 3, 4-oxadiazole (II). Its synthesis was attempted as given in Scheme IV.



A mixture was obtained whose infrared spectrum indicated the possible formation of II along with other products. The yield was low and the mixture sufficiently complex that this route was abandoned.

### Diazidofuroxan

The attempt synthesis of diazidofuroxan (III) was prompted by the report of Eloy (42) azidoximes (VI) are "surprisingly stable." As the basic structural elements (see below) of azidoximes are present in diazidofuroxan, it was felt that this too would be a stable structure.



The target compound was synthesized by the oxidation of diazidoglyoxime (42) with red fuming nitric acid. It was obtained as a red oil and identified as III by its infrared spectrum. It decomposed at room temperature as evidenced by gassing. It was very shock sensitive, and therefore no attempt was made to purify it. After this work was completed, a footnote in a paper by Grundmann (43) was found which refuted Eloy's claim that azidoximes are stable.

### 4, 5-Dicyano Oxazole

When DCFO was found to be detonable, emphasis was shifted away from oxodiazole chemistry in general. Another ring structure which was considered to offer better safety possibilities was the oxazole ring, and a concerted effort was made (44) to synthesize 4, 5-dicyano oxazole.

Initially, the synthesis of 4, 5-dicyano oxazole was achieved in poor yields by the synthesis route described below. Experimental details for the synthesis of 4, 5-dicarboxamide oxazole are found in the previously referenced works (45). Dehydration of the diamide, the final step, was performed on a small scale using 10 grams of the amide mixed thoroughly with 30 grams of  $\text{P}_2\text{O}_5$  which was subsequently heated to  $140^\circ$  in a vacuum

distillation apparatus at between 1 and 10 mm Hg pressure. The product was thus distilled from the reaction mass and collected in the receiving flask, usually in about 4 percent yields. The 4, 5-dicyano oxazole prepared by this method contained cyanamide,  $\text{H}_2\text{NCOCN}$ , which occurred as a result of diethyl -oxo- -hydroxy-succinate starting material being contaminated with diethyl oxalate.

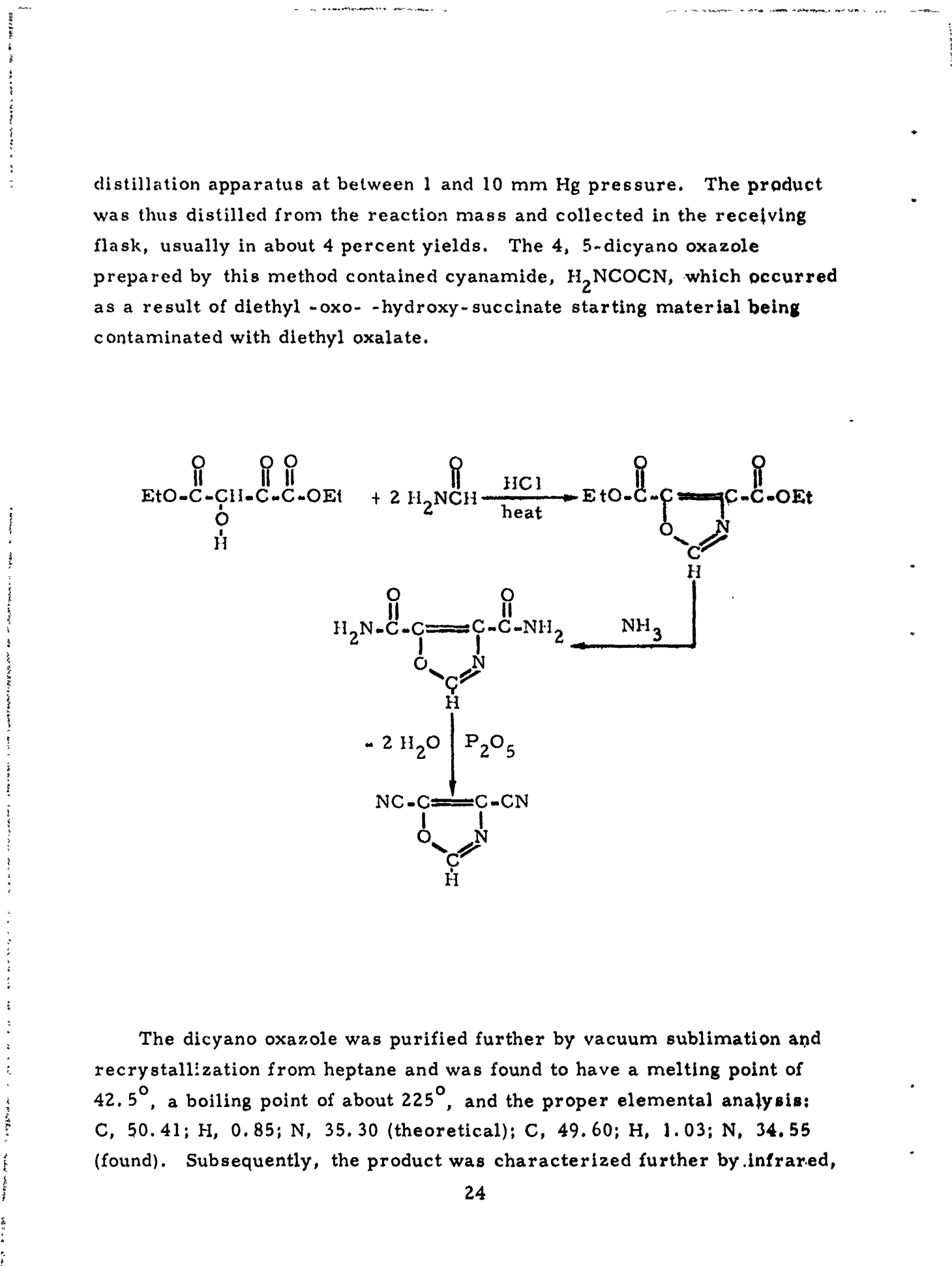
$$\text{EtO}-\overset{\overset{\text{O}}{\parallel}}{\text{C}}-\underset{\underset{\text{H}}{\mid}}{\text{CH}}-\overset{\overset{\text{O}}{\parallel}}{\text{C}}-\overset{\overset{\text{O}}{\parallel}}{\text{C}}-\text{OEt} + 2 \text{H}_2\text{N}-\overset{\overset{\text{O}}{\parallel}}{\text{C}}-\text{H} \xrightarrow[\text{heat}]{\text{HCl}} \text{EtO}-\overset{\overset{\text{O}}{\parallel}}{\text{C}}-\text{C}=\text{C}-\overset{\overset{\text{O}}{\parallel}}{\text{C}}-\text{OEt}$$

$$\begin{array}{c} \text{O} \quad \text{O} \\ \parallel \quad \parallel \\ \text{H}_2\text{N}-\text{C}-\text{C}=\text{C}-\text{C}-\text{NH}_2 \\ \mid \quad \mid \\ \text{O} \quad \text{N} \\ \text{H} \end{array} \xleftarrow{\text{NH}_3}$$

$$\begin{array}{c} \text{O} \quad \text{O} \\ \parallel \quad \parallel \\ \text{H}_2\text{N}-\text{C}-\text{C}=\text{C}-\text{C}-\text{NH}_2 \\ \mid \quad \mid \\ \text{O} \quad \text{N} \\ \text{H} \end{array} \xrightarrow[\text{P}_2\text{O}_5]{- 2 \text{H}_2\text{O}} \begin{array}{c} \text{NC}-\text{C}=\text{C}-\text{CN} \\ \mid \quad \mid \\ \text{O} \quad \text{N} \\ \text{H} \end{array}$$

The dicyano oxazole was purified further by vacuum sublimation and recrystallization from heptane and was found to have a melting point of  $42.5^\circ$ , a boiling point of about  $225^\circ$ , and the proper elemental analysis: C, 50.41; H, 0.85; N, 35.30 (theoretical); C, 49.60; H, 1.03; N, 34.55 (found). Subsequently, the product was characterized further by infrared,

24



distillation apparatus at between 1 and 10 mm Hg pressure. The product was thus distilled from the reaction mass and collected in the receiving flask, usually in about 4 percent yields. The 4, 5-dicyano oxazole prepared by this method contained cyanamide,  $\text{H}_2\text{NCOCN}$ , which occurred as a result of diethyl -oxo- -hydroxy-succinate starting material being contaminated with diethyl oxalate.

$$\begin{array}{c}
 \text{EtO}-\text{C}(=\text{O})-\text{CH}(\text{OH})-\text{C}(=\text{O})-\text{COEt} + 2 \text{H}_2\text{N}-\text{C}(=\text{O})-\text{NH}_2 \xrightarrow[\text{heat}]{\text{HCl}} \text{EtO}-\text{C}(=\text{O})-\text{C}_2\text{N}(\text{H})-\text{C}(=\text{O})-\text{COEt} \\
 \downarrow \text{NH}_3 \\
 \text{H}_2\text{N}-\text{C}(=\text{O})-\text{C}_2\text{N}(\text{H})-\text{C}(=\text{O})-\text{NH}_2 \xrightarrow{-2 \text{H}_2\text{O}, \text{P}_2\text{O}_5} \text{NC}-\text{C}_2\text{N}(\text{H})-\text{CN}
 \end{array}$$

The dicyano oxazole was purified further by vacuum sublimation and recrystallization from heptane and was found to have a melting point of  $42.5^\circ$ , a boiling point of about  $225^\circ$ , and the proper elemental analysis: C, 50.41; H, 0.85; N, 35.30 (theoretical); C, 49.60; H, 1.03; N, 34.55 (found). Subsequently, the product was characterized further by infrared,

24

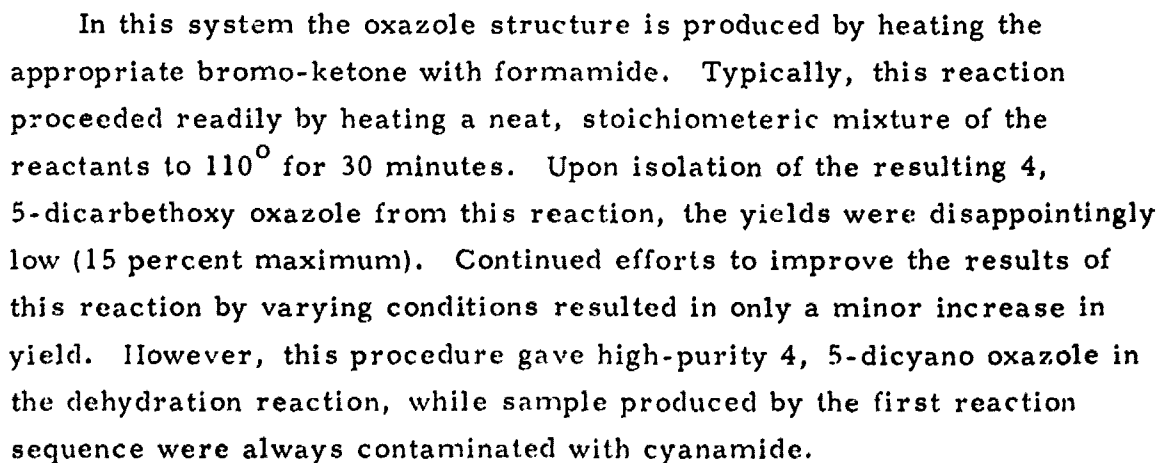
the principal bands being: 3290 (s), 2980 (m), 2250 (m), 1500 (s), 1340 (m), 1230 (s), 1095 (s), 1073 (s), 937 (ms), 887 (m), 637 (m), 621 (m)  $\text{cm}^{-1}$ . The NMR spectrum consisted of a single signal at 8.16 ppm from tetramethyl silane and the mass spectrum gave the following mass/charge signals and corresponding relative intensities: 119 ( $\text{C}_5\text{HN}_3\text{O}^+$ , parent, 17.51) 91 ( $\text{C}_4\text{HN}_3^+$ , 100), 64 ( $\text{C}_3\text{N}_2^+$ , 31.2), 65 ( $\text{C}_2\text{HN}_2^+$ , 54 ( $\text{C}_2\text{NO}^+$ , 18.0), 39 ( $\text{C}_2\text{HN}^+$ , 25.0), 38 ( $\text{C}_2\text{N}^+$ , 60.0), thus confirming the desired structure.

Two problem areas were manifest in the described synthesis route: (1) consistently low yields (about 4 percent) in the dehydration of the diamide stemming from the coagulation of the reaction mass observed during the distillation, which presumably results in the entrapment and pyrolysis of the product, (2) lower yields observed in the synthesis of the diamide precursors than reported in the literature, particularly in the preparation of diethyl -oxo- -hydroxy-succinate.

It was observed that increasing the quantity of the reactants in further attempts at dehydration of 4, 5-dicarboxamide oxazole resulted in even lower yields than those observed with smaller quantities. No more than 1.5 to 2.5 grams of 4, 5-dicyano oxazole were obtained per run although the quantities of oxazole dicarboxamide employed ranged between 5 and 50 grams. In order to minimize the problem of forming coagulated masses, the reaction was diluted with sand and the apparatus outfitted with a mechanical stirrer. In practice, this technique did tend to minimize the coagulation problem, although the reaction mixture still set up as a hard mass. However, the yields were only slightly improved by the procedure.

In an attempt to circumvent the low yields observed in this particular synthesis of oxazole-4, 5-dicarboxamide, a new synthesis route leading to the diamide was considered. The new route was patterned after previously known reactions resulting in oxazole derivatives (46) and is outlined as follows:





## SECTION IV

### CHEMICAL AND PHYSICAL CHARACTERIZATION

Most of the chemical and physical characterization reported below was accomplished at the AFRPL Chemical and Materials Laboratory. Certain of the safety related tests on DCFO were accomplished under Contract F04611-71-C-0035 by Rocketdyne, as were the safety and compatibility tests on CDI. For purposes of comparison or completeness a number of properties for DCFO are taken from AVCO work. Unless otherwise identified, the property measurements may be taken to be those of AFRPL, and in most cases these will be identified by reference to an AFRPL chemical laboratory test report number.

#### DCFO

The samples of DCFO characterized under the project were obtained from several sources. The earliest work was accomplished with two small samples donated by Rocketdyne for characterization, hereafter denoted as samples D1 and D2. Later work was done with portions of a one pound delivery purchased under a supply contract with Rocketdyne, hereafter denoted C-LB (contract - large bottle) and C-SB (contract - small bottle). Additional comparison characterization was later done on samples donated by AVCO, denoted 1039-125 and 1039-138 after the AVCO bottle labels. Limited characterization was done on AFRPL synthesized material. Aside from the differences in sources, the samples represent an evolution in synthesis and purification technique. Measurable, and sometimes significant differences were encountered in properties, although company proprietary interests prevent an accurate tracing of the origins of the differences. A satisfactory analytical technique for gaging DCFO purity was not developed, but all samples gave evidence of impurities.

Elemental Analysis: The elemental analysis was of limited value in distinguishing samples. Carbon and nitrogen analyses were 0.5 to 1 percent low. Oxygen was usually obtained by difference, but was found to be exactly the theoretical value for a single neutron activation determination run on Sample C-SB. All samples were found to contain hydrogen, typically 0.2 percent.

A summary of the elemental analyses for samples of various origins is given below, including a triply recrystallized sample synthesized in-house (IH).

TABLE 2 ELEMENTAL ANALYSIS OF DCFO

	<u>D1</u>	<u>D2</u>	<u>C-SB</u>	<u>1039-125</u>	<u>1039-138</u>	<u>IH</u>	<u>Theory</u>
C	39.5	40.6	40.5	40.4	40.4	41.3	41.1
N	33.5	34.6	34.4	34.5	34.5	35.3	35.3
H	0.2	0.2	0.2	0.2	0.2	0.11	0.0
O	----	----	23.6	----	----	----	23.6

Gas Chromatography: Using a silicone column and a thermal conductivity cell detector, the only impurity peak observed was trinitroacetoneitrile at levels of a few tenths of a percent. AVCO has reported (47) an earlier peak due to trinitroacetoneitrile in several of their samples, corresponding to about 1/3 percent. Earlier communications (48) reported an impurity peak of 6 percent. It is possible, if not likely, that additional impurities exist that are retained in the column.

Mass Spectrum: The mass spectrum of DCFO was taken (49) with the CES 21-110 using an ionization voltage of 68 ev. The ionization chamber was heated to 200°C and the electron current was 100 ma. The liquid was injected into a passivated glass reservoir at 110°C (total pressure 100 microns). The mass 76 peak was taken as reference, due to observed variation in parent peak (136) between several samples.

Density: The density of several samples of DCFO of various origins was measured in the liquid state at AFRPL over a period of time with only fair agreement. The results are shown in Figure 1.

As indicated, the top-most curve was run by AVCO, and is at surprising variance with all AFRPL measurements. To what extent the differences are due to sample purity or to experimental technique is not

TABLE 3. MASS SPECTRUM OF DCFO

M/e	ION	Relative Intensity	M/e	Ion	RI	M/e	Ion	RI
12	C	6.0	32	i	2.0	52	C <sub>2</sub> N <sub>2</sub>	40.0
14	N	2.0	36	C <sub>3</sub>	9.3	54	C <sub>2</sub> NO	3.0
16	O	2.0	38	C <sub>2</sub> N	120.0	60	N <sub>2</sub> O <sub>2</sub>	27.0
18	H <sub>2</sub> O	3.5	39	i	3.0	62	NO <sub>3</sub>	6.0
24	C <sub>2</sub>	15.0	42	CN <sub>0</sub>	3.0	64	C <sub>3</sub> N <sub>2</sub>	19.0
26	CN	21.0	43	HCNO	6.0	68	C <sub>2</sub> N <sub>2</sub> O	16.0
27	HCN	7.5	44	CO <sub>2</sub>	9.0	76	C <sub>4</sub> N <sub>2</sub>	100.0
28	CO	25.0	44	CH <sub>2</sub> NO	0.9	77	i	5.3
29	N <sub>2</sub>	25.0	46	NO <sub>2</sub>	4.2	90	C <sub>4</sub> N <sub>3</sub>	2.3
30	NO	850.0	48	C <sub>4</sub>	13.0	120	C <sub>4</sub> N <sub>4</sub> O	1.7
31	i	3.5	50	C <sub>3</sub> N	51.0	136	P	45.0
32	O <sub>2</sub>	4.0	51	i	2.0	137	i	2.9

Standard Pattern for C<sub>2</sub>F<sub>5</sub>Cl

31	32	66	6	100	6
35	4	69	78	119	45
47	4	85	100	135	38
50	20	87	29	137	14

known, but a 6 percent impurity was indicated by AVCO using GC analysis. The subsequent AVCO sample run at AFRPL had a single GC peak.

Infrared Analysis: The existence of impurities in the DCFO samples is most clearly demonstrated by the infrared spectra recorded. Three of these are shown in Figure 2. Basically the spectra are very similar, but each has one or more distinguishing peaks, indicated by arrows, which suggest different impurities from one sample to another, at least in magnitude.

Viscosity: The viscosity of DCFO was measured (49) by timing the flow through a tube by gravity for various temperatures (Fig 3).

Specific Heat: AVCO also determined (50) values for specific heat of solid and liquid as follows:

TABLE 4. SPECIFIC HEAT OF  
DCFO

<u>Temperature (<math>^{\circ}\text{C}</math>)</u>	<u>Specific Heat (cal/gram<math>^{\circ}\text{C}</math>)</u>
20-35	.150 - .200
72-110	.205 - .217

Vapor Pressure: The vapor pressure of dicyanofuroxan was determined (49) using a glass tube containing the sample attached to a calibrated transducer. The entire system was placed in a regulated temperature oven ( $\pm 0.1^{\circ}\text{C}$  regulation) and the data recorded continuously. When the recorded pressure reached a constant value at a given temperature, that point was taken as the sample vapor pressure at that temperature.

The sample was initially melted and any dissolved or trapped gases were removed prior to collection of data. This was necessary, since some gassing was noted when the samples initially melted.

LEGEND			
SYMBOL	SAMPLE ORIGIN	IDENTIFIER	REFERENCE
□	AVCO	-----	48
●	ROCKETDYNE	C-88	50
▲	AVCO	1038-125	50
○	ROCKETDYNE	C-LB	51
▼	ROCKETDYNE (RESUBLIMED)	D-2	52
✱	ROCKETDYNE	D-2	53

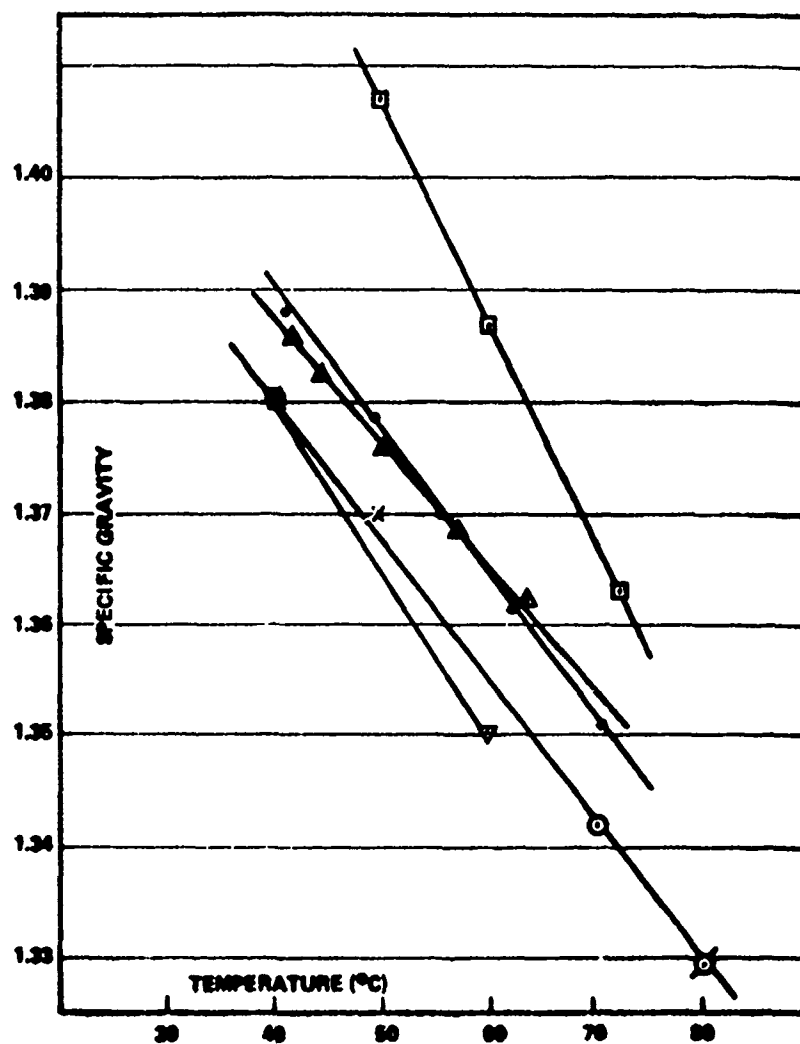
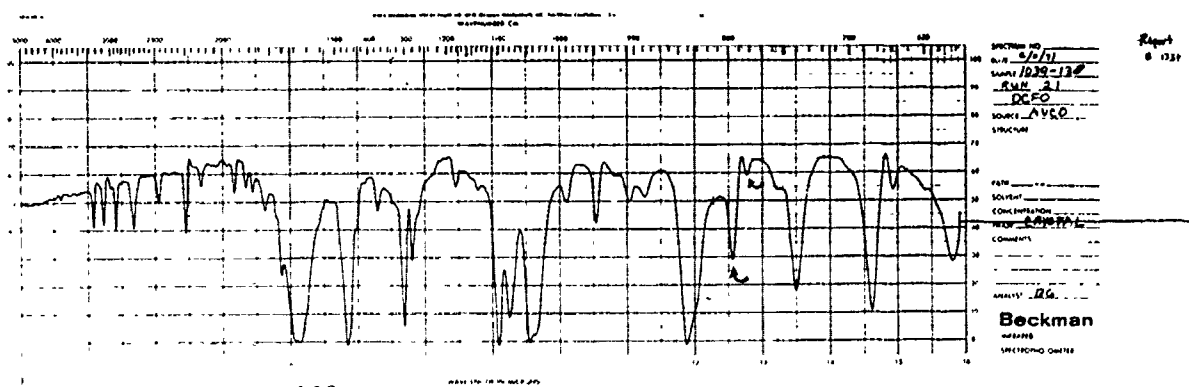
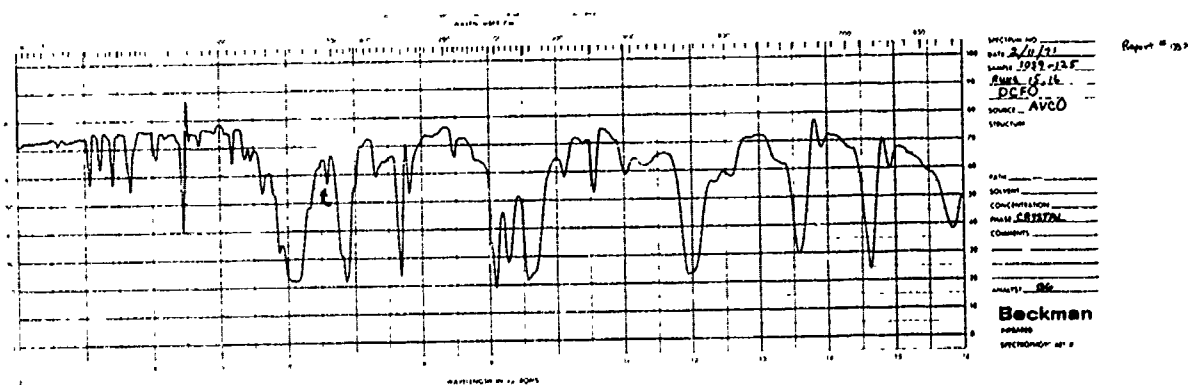


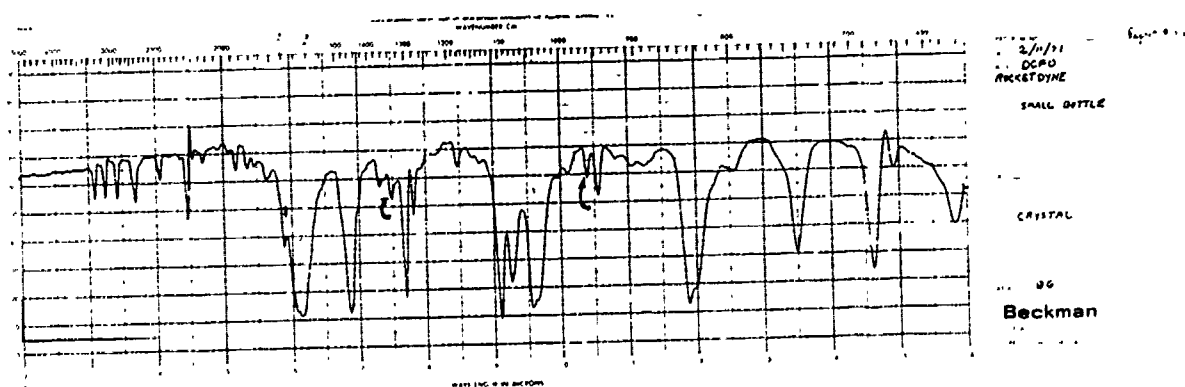
Figure 1. Specific Gravity of Dicyanofuroxan (DCFO)



2a. Sample 1039-138



2b. Sample 1039-125



2c. Sample CSB

Figure 2. Infrared Spectrum of DCFO

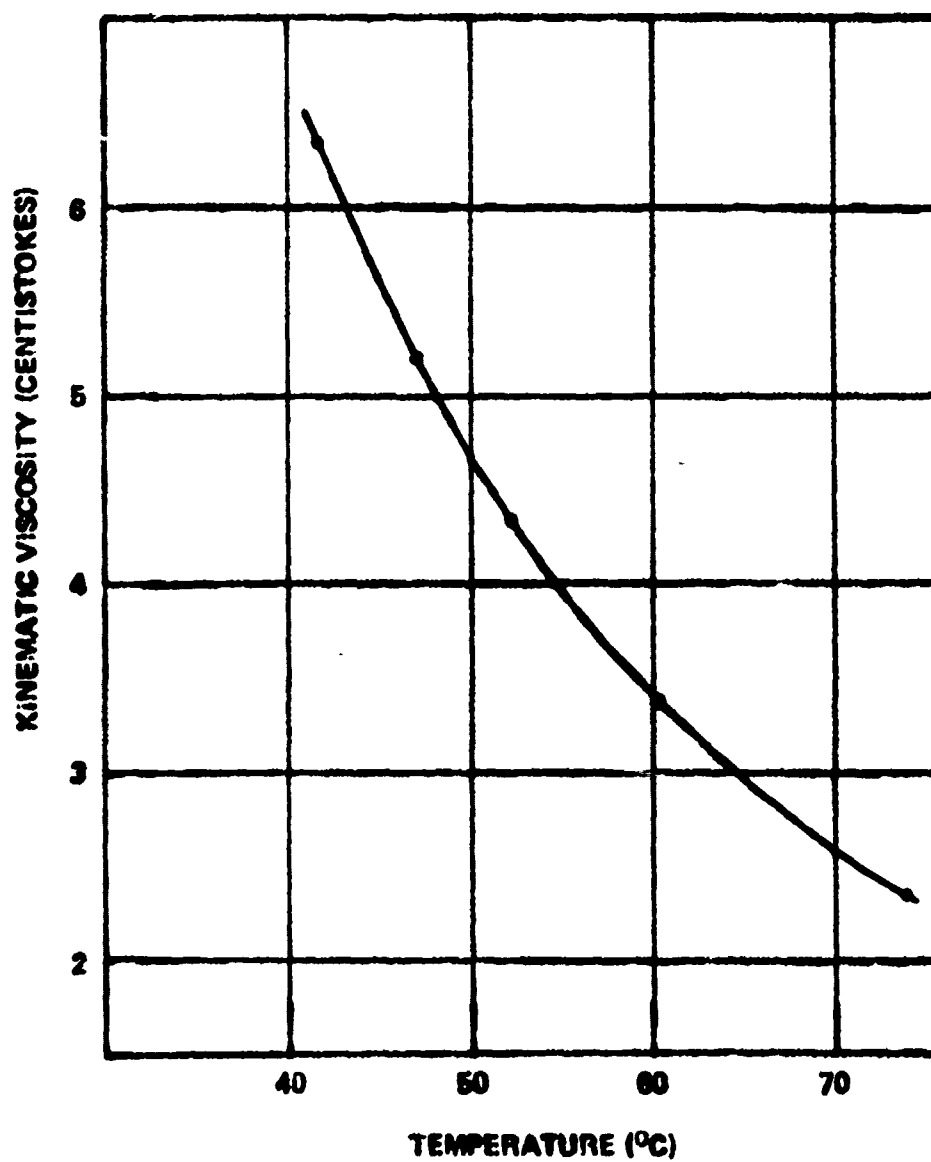


Figure 3. Kinematic Viscosity of Dicyanofuroxan (DCFO)



Data acquisition was terminated at 90°C, the sample was solidified, and the residual gas pressure analyzed (average pressure of residual gas was 1 mm at 25 °C). N<sub>2</sub>, NO, CO<sub>2</sub>, and C<sub>2</sub>N<sub>2</sub> were identified.

The vaporization data were fitted to the following equation:

$$\log P_{(\text{mmHg})} = 9.351 - \frac{3040}{T(\text{°K})}$$

From this data, an extrapolated boiling point of 197°C and a heat of vaporization of 13.9 k cal/mole are computed.

Heat of Vaporization: 13.9 k cal/mole, was derived from the vapor pressure curve.

Surface Tension: The surface tension was measured by the capillary rise method, and the results are shown in Figure 4.(54)

Heat of Fusion: The heat of fusion was determined by differential scanning calorimetry to be 25.1 ± 0.7 cal/gram (55). AVCO reported ΔH fusion = 20 cal/gram (48).

Heat of Combustion: The heat of combustion of solid DCFO was measured (56) by oxygen bomb calorimetry to be 3.579 ± .003 k cal/gram. AVCO reported ΔH combustion = 3.550 k cal/gram (48).

Heat of Formation: The heat of formation for DCFO is calculated from the heat of combustion to be 110.9 ± .46 k cal/mole, assuming the sample to be pure DCFO.

Materials Compatibility: DCFO was contacted with various polymers for a period of eleven days at 50°C (57). These tests showed teflon and silicone rubber to be compatible with DCFO.

Viton A, Neoprene, and JM-76 Impregnated Asbestos were found to undergo significant changes in weight, dimensions, and hardness during the test. In general, the DCFO showed no evidence of decomposition, although the impregnated asbestos caused some discoloration.

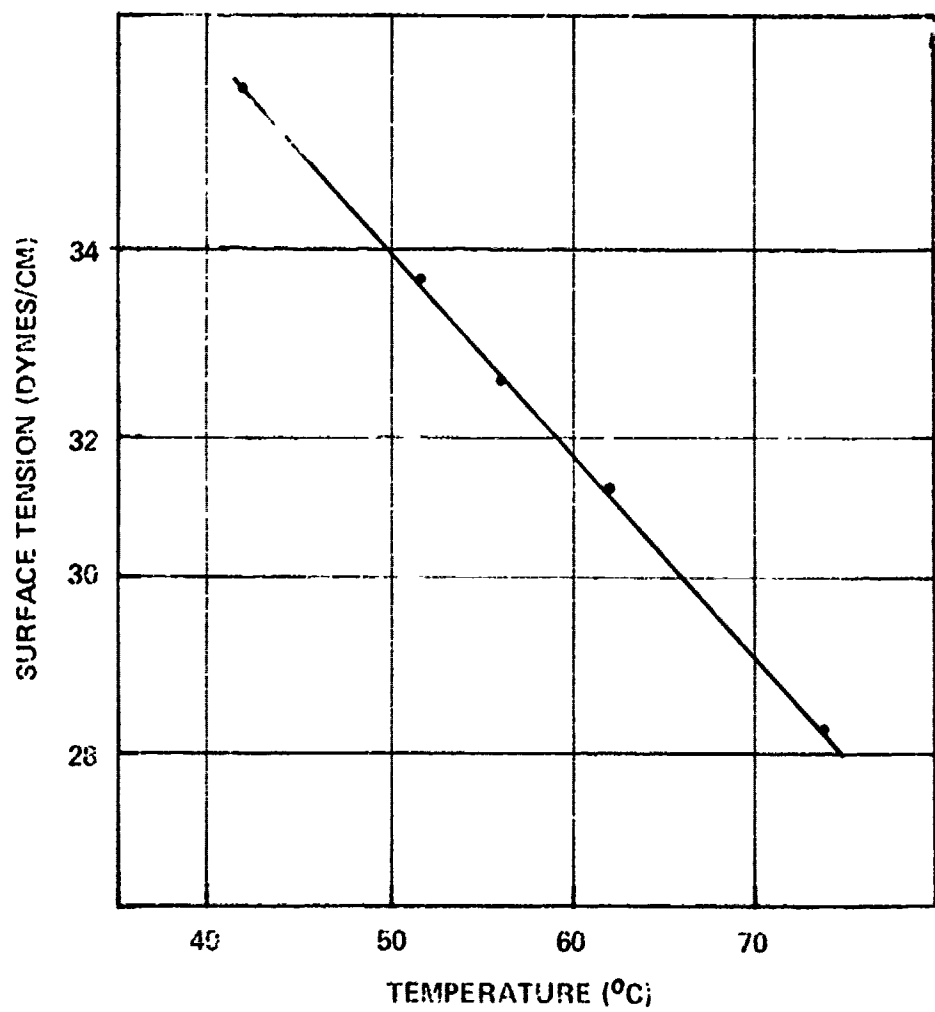


Figure 4. Surface Tension of Liquid Dicyanofuroxan (DCFO)

Thermal Stability: DCFO was observed to form bubbles at temperatures that varied from one sample to another. Samples D1 and D2 were observed to bubble as low as 60°C in early density measurements. Whether this is due to decomposition or "outgassing" is not known for certain, but mass spectra of vapor DCFO (in glass) remain constant up to 180°C. Between 180°C and 205°C the relative intensities of the following ions are observed to increase:  $C_2N_2$ , HCN, CHNO,  $CO_2$ ,  $C_2N_2O$ ,  $C_4N_4O$  (76).

AVCO reported "outgassing" of DCFO at 110°C to extent of 4-11 percent over 24 hours in glass, stainless steel and brass (48). Brass produced a marked discoloration at 110°C after 24 hours. However, neither brass nor copper discolored DCFO at 95°C after two hours. AVCO goes on to report a self-ignition point of 310°C (590°F). The thermal stability of DCFO was determined by Rocketdyne (58) using the JANNAF thermal stability apparatus. In this test the sample is gradually heated in a pressure bomb until sufficient pressure is generated to rupture a disc. The point at which the sample temperature became equal to the bath temperature is known as the "adiabatic self heating" point and is usually considered the most meaningful test result. For DCFO this occurred at 234°C (452°F). The disc rupture occurred without evidence of detonation.

Toxicity:

Dermal: DCFO is a primary dermal irritant when applied to rabbits. After 24 hours, rabbits dosed with DCFO had a severe reaction characterized by edema and erythema. The area of application had the appearance of a large bruise, with red and blue hemoglobin pigments surrounding a large yellow area. Two out of six rabbits died after 26 hours (59).

Ocular: DCFO ocular dosing resulted in the complete and apparently irreversible blinding of 6 out of 6 rabbits after 24 hours (59).

Oral: DCFO has an oral  $LD_{50}$  in rate of 93 mg/kg with 95 percent confidence limits of 52-160 mg/kg (59).

Intraperitoneal Injection: The  $LD_{50}$  is in the range of 8-12 mg/kg body weight.  $LD_{100}$  is in the range of 25-30 mg/kg (60).

Flash Point: AVCO reports a flash point for DCFO of  $79.5^{\circ}\text{C}$  (48). A substantially higher value was measured at Rocketdyne (61). In two runs using a modified Cleveland open-cup flash test, the flash point was measured at  $131.5^{\circ}\text{C}$  and  $134^{\circ}\text{C}$ . The modifications to the standard Cleveland open-cup test (ASTM D-92) included a thermocouple for remote readout, an automatic flame wand, and a reduced sample size (10 cc). The reason for so large a discrepancy is not apparent. At  $79.5^{\circ}\text{C}$  the vapor pressure of DCFO is only 4 mmHg, making the air-vapor mixture decidedly lean by comparison with the stoichiometric pressure of 47 mm (which occurs at  $120^{\circ}\text{C}$ ). The Rocketdyne flash point corresponds to about 65 mm of DCFO vapor pressure. This may be reasonable in view of the concentration gradient between the sample and the flame wand.

Friction Sensitivity: Samples of DCFO ground between two polished plates with diamond grit gave no reaction. This is usually considered the most severe condition and shows that DCFO is not friction sensitive (49).

Impact Sensitivity: The sensitivity of liquid DCFO was measured with the CPIA drop-weight tester (JANNAF Liquid Propellants Test Methods, July 1969). At  $75^{\circ}\text{C}$  the sample gave negative results in five measurements at 250 kg-cm. It is concluded that DCFO is not sensitive to impact (49).

Detonation Propagation: The object of these tests is to determine whether a column of material in a tube propagates or damps a high order detonation wave impinged on one end. A positive test is indicated by perforation of a witness plate at the other end of the tube. The results are sensitive to the diameter of the tube, with greater damping in the smaller sizes. The largest diameter that will not propagate the detonation is thus a measure of the propagation tendencies of a material. This "critical diameter" bears on the feasibility of using detonation "traps" to reduce the hazard of a material. Detonation propagation tests on DCFO were conducted by Rocketdyne under Contract F04611-71-C-0035. These

tests showed that liquid or solid DCFO will propagate powerful detonations at 0.1" tube inside diameter, the smallest size tested. This result is a serious shortcoming in the compound and led to studies of mixtures of DCFO with other less energetic compounds, namely malononitrile and maleic anhydride. Malononitrile was added to DCFO at various concentrations (62) and the effect on the critical diameter was determined. The results are shown in Figure 5. It is seen that DCFO/malononitrile mixtures become progressively less detonable with increasing malononitrile, and become essentially non-detonable above about 50 percent malononitrile. At this concentration the carbon to hydrogen ratio is about 2.5 to one. Maleic anhydride was tested at the 47 weight percent level. The mixture was found not to propagate detonations in 3/8" tubes, but it did propagate at 1/2".

Card Gap Tests: Standard card gap tests were made for DCFO and a DCFO-malononitrile mixture. Neat DCFO required 75 cards to prevent explosion (70 or more cards indicates a class A explosive). When 44 weight percent malononitrile was added, values ranging from six to 25 cards were determined (63).

Hazardous Reactions: DCFO is relatively unreactive towards oxidizing materials, and has been mixed with  $\text{ClF}_5$  at  $50^\circ\text{C}$  and with  $\text{ClF}_3$  at  $10^\circ\text{C}$  without reaction (64). It is compatible with and fairly soluble with  $\text{N}_2\text{O}_4$  at  $25^\circ\text{C}$ . When near stoichiometric quantities of DCFO and  $\text{N}_2\text{O}_4$  were heated slowly at 750 psia, smooth, rapid pressure increases were observed at  $110\text{--}115^\circ\text{C}$ .

The oxygen in DCFO on the other hand, is relatively active, liberating iodine from iodide solution. Reactions with amines can be vigorous and explosive with hydrazines (65). A comparative study was run on the reactivity of DCFO, DCFA, "bottoms" ( $\text{C}_6\text{N}_6\text{O}_3$ ), and furazan dicarboxamide with various amines and hydrazines. A one tenth gram sample of each was placed in an aluminum dish, and amines or hydrazines were added dropwise until 0.1 gram had been added, or until the mixture ignited. The resulting test matrix is given in Table 5.

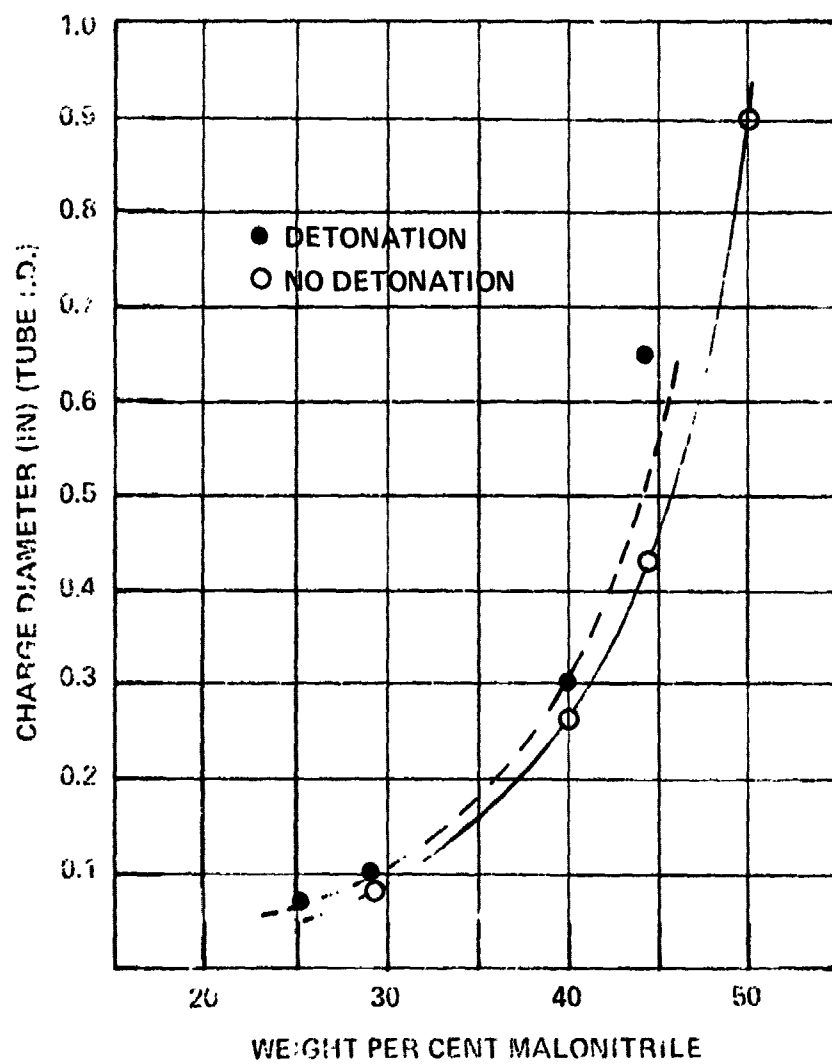


Figure 5. DCFO/Malonitrile Mixtures, Critical Diameter for Detonation

The table reveals that DCFO and "bottoms", which both contain the furoxan ring, are more reactive than DCFA and furazan dicarboxamide. "Bottoms", which contains both the furoxan ring structure and the furazan ring, appears to be even more reactive than DCFO.

DCFO was contacted with hydrazine at high pressures in another experiment. When 0.25 grams of DCFO was loaded into a 5" long, 3/8" id. 0.25" wall #347 stainless steel tube and contacted suddenly with  $N_2H_4$  at 750 psig, an immediate pressure spike to 1500 psig was observed. The DCFO was converted to soot and gases. With 2.5 grams of DCFO, the tube was violently ruptured, whether by a detonation or over-pressurization was not established.

DCFO Accidents: Some of the hazards tests detailed above were accomplished as part of a routine safety evaluation of a new reactant. Still others were done in the wake of two explosions involving DCFO, either by way of fixing the cause, or to learn the limits of operation with an increasingly sinister compound. The findings are summarized here for the benefit of potential users of this material.

The first explosion occurred at the AVCO Wilmington Plant. A tank containing ten pounds of DCFO blew up during preparations for a firing with  $N_2O_4$ . The tank was heated to melt the DCFO and was under the control of a thermostat set for  $75^{\circ}C$ . Unfortunately, the separation between the heater and the thermostat was shown by subsequent analysis to have been excessive leading to a locally overheated area. The accident was attributed to thermal ignition of the DCFO and subsequent over-pressurization of the run tank.

The second explosion occurred at AFRPL under a parallel project to obtain ballistic data on the  $N_2O_4$ -DCFO system at higher flow rates than were planned under this project. In the final minutes of the countdown for a firing, the tank, containing eight pounds of DCFO, detonated, severely damaging the cell. Subsequent investigation revealed the run line to be contaminated with a hydrazine blend from previous tests and water from an aspirator intended to clear the line. As was shown by

TABLE 5. REACTIVITY OF GDL FUELS

	DCFO	DCFA	$C_6N_6O_3$	Furazan Dicarboxamide
Hydrazine	H	RD	H	SD
MMH	H	RD	H	SD
UDMH	H	RD	H	SD
50/50	H	NT	H	NT
t-butyl amine	SD	SD	RD	NR
i-butyl amine	RD	SD	H	SD
di-n-hexyl amine	SD	SD	SD	SD
Pyridine	SD	NR	NR	SD
Diethyl amine	SD	SD	H	SD
Piperidine	H	RD	H	SD
Piperazine	RD*	NT	NT	NT

Legend: H = hypergolic; RD = rapid decomposition, no ignition; SD = slow decomposition; NR = no reaction; NT = not tested. MMH = monomethyl hydrazine; UDMH = unsymmetrical dimethyl hydrazine; 50/50 = a mixture of UDMH and  $N_2H_4$ .

\* Hypergolic if DCFO pre-melted.



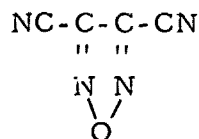
subsequent studies documented above, DCFO and hydrazines are violently incompatible, and the cause of the accident was attributed to a chemically initiated detonation.

The only actual firings with DCFO (2) were accomplished at AVCO Everett, and this work was abandoned when combustor "pops" damaged the injector. These were attributed to insufficient cooling of the DCFO elements which caused a pop during the run, and a delayed purge which caused a larger pop on shutdown. Again the limited thermal stability caused difficulty.

DCFO Evaluation: Although each of the above accidents involved some handling fault or oversight in design, and was thus preventable, DCFO appears as a very unforgiving compound. After considering the evidence, it was dropped from the project plan. This decision took account not only of the hazard to AFRPL personnel, but also the probable future resistance to placing such a compound in the AF inventory. The detonation propagation tests were a major factor in this decision, since they created doubts that the run tanks in either an experimental or operational system could practically be isolated from possible combustor malfunctions. The tendency of DCFO to detonate was, to be sure, found to be curable by heavy dilution with malononitrile. The decision not to pursue this approach was primarily an AFWL judgment based upon the relatively high hydrogen content (C/H 2.5) and concern over the loss of efficiency in the resulting laser medium.

#### Dicyanofurazan (DCFA)

This compound is structurally very similar to DCFO,



lacking only the oxygen datively bonded to one of the ring nitrogens. Its energetics and theoretical combustion products are very similar to DCFO.

Its main drawbacks relative to DCFO are its higher vapor pressure (20 times that of DCFO) and its poor synthesis. It was viewed throughout, most of the project as a possible back-up to DCFO and as a possible formulation partner with DCFO for melting point reduction. It was not characterized nearly so extensively and was not developed further after DCFO was dropped. Some of the pertinent properties measured at AFRPL are given below. The sample used was obtained from Rocketdyne and was synthesized by reduction of DCFO.

Melting Point: When first received, the DCFA sample melted at 38-40°C. During the density determination, a melting range of 34-40°C was recorded, and the liquid was noted to supercool as low as -12°C. These results suggest the presence of a contaminant, but its identity and origin are not known. This supercooling behavior was absent from a DCFA sample prepared in-house.

Vapor Pressure: The vapor pressure was measured (78) as a function of temperature using a 0-10 psia transducer, zeroed by cooling the sample to -15°C after pumping at 26°C for 2 minutes to remove any trapped gases. The data are plotted in Figure 6. They are represented by the equation

$$\log P(\text{mmHg}) = 8.568 - 2386/T(^{\circ}\text{K})$$

in the range of the liquid, and

$$\log P(\text{mmHg}) = 11.114 - 3180/T(^{\circ}\text{K})$$

in the range of the solid.

Heat of Vaporization: Calculated from the slope of the vapor pressure curve for the liquid to be 10.9  $\pm$  0.2 kcal/mole.

Heat of Sublimation: Calculated from the slope of the vapor pressure curve for the solid to be 14.6  $\pm$  0.5 kcal/mole.

Heat of Fusion: The heat of fusion was measured (55) by differential scanning calorimetry to be 30.7  $\pm$  0.7 cal/gram. A value in good agreement

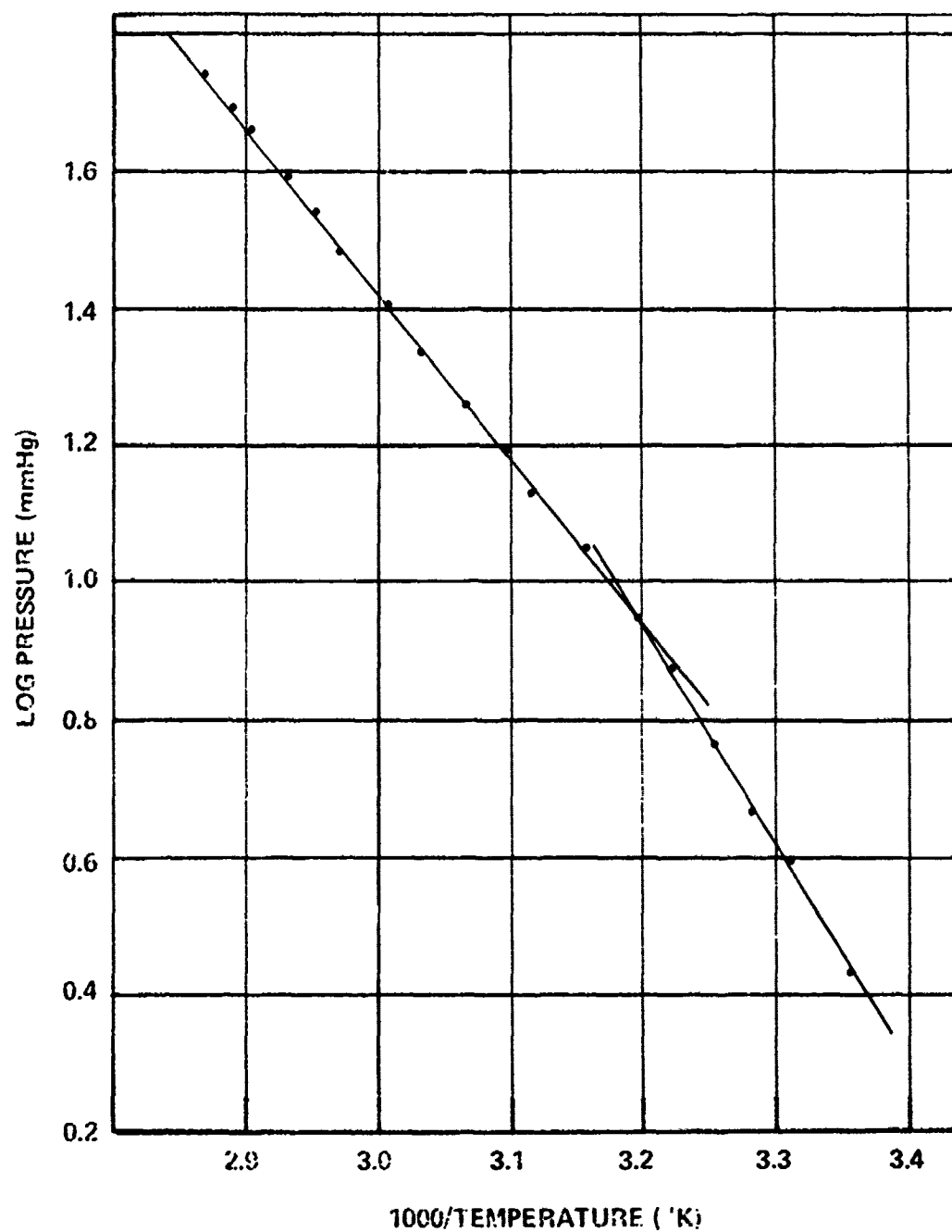


Figure 6. Vapor Pressure of Dicyanofurazan (DCFA)

with this, although less precise, is derivable from the difference between the heats of vaporization and sublimation.

Boiling Point: By extrapolation of the vapor pressure curve, the boiling point of DCFA is found to be  $146 \pm 2^{\circ}\text{C}$ .

Chemical Compatibility: Various polymers were immersed (79) in DCFA at  $48\text{-}50^{\circ}\text{C}$  for 12 days and the results are summarized below in terms of sample hardness and thickness before and after, and physical appearance of the DCFA afterwards.

TABLE 6. COMPATIBILITY OF POLYMERS WITH DCFA

<u>Polymer</u>	<u>Hardness (A Scale)</u>		<u>Thickness (cm)</u>		<u>DCFA Color</u>
	<u>Pre</u>	<u>Post</u>	<u>Pre</u>	<u>Post</u>	
Ethylene-Propylene	67	76.5	.1705	.1755	pale yellow
Neoprene	58.5	48	.340	.372	black
Viton	62	64	.342	.385	colorless
Silicone	54	64	.3455	.3450	colorless
Teflon	96	95	.3575	.3520	colorless
JM-76 (impregnated asbestos)	86	95	.1475	.1510	black
Asbestos	-	-	.2005	.1680	yellow

The most generally satisfactory results were obtained with teflon, and the other materials were marginal or unacceptable.

Chemical Reactivity: DCFA undergoes rapid decomposition with hydrazine and slow decomposition with many amines (see Table 5). Unlike DCFO it does not ignite, however.

Density: The density of DCFA was measured (78) by the dilatometer, and the results are shown in Figure 7.

#### "Bottoms"

The synthesis of DCFO produces a number of side products, including a less volatile residue, which on further work-up yields a white, free-flowing

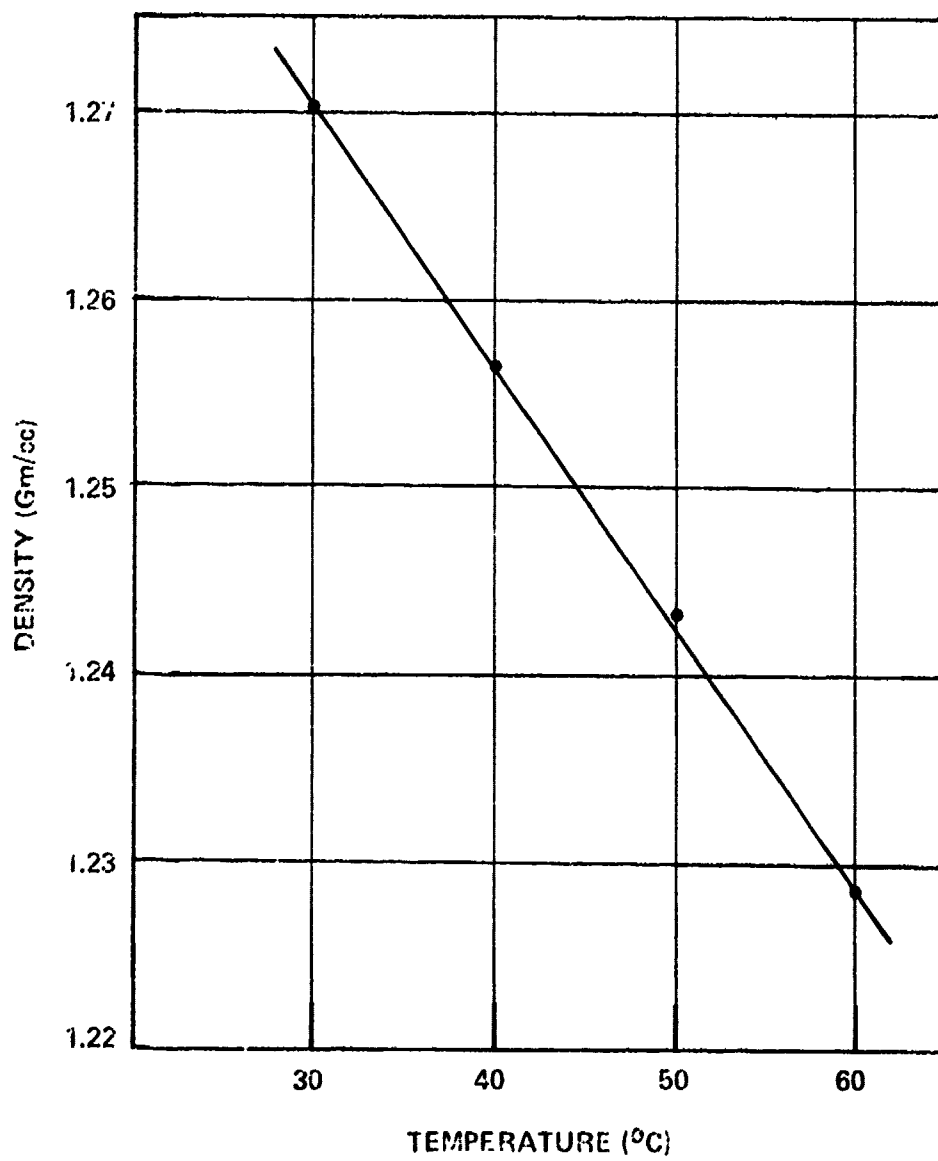
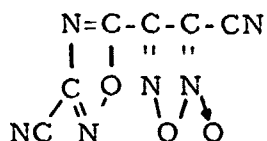


Figure 7. Density of Dicyanofurazan (DCFA)

powder which melts at 90°C and has a boiling point of 65°C at 0.5 mm Hg. Because of its origin, it was variously referred to as "DCFO pot residue" or simply "bottoms". The nature of the DCFO synthesis mechanism suggests the likelihood of the formation of a side product of structure:



The elemental analysis, mass spectrum, and nuclear magnetic resonance spectrum are consistent with this structure, which formally is 3- 5-(3 cyano-1, 2, 4-oxadiazolyl) -4 -cyanofuroxan. An infrared spectrum is shown in Figure 8.

Because of its relatively high melting point, the chief attraction was its possible use in mixtures. A limited amount of characterization was accomplished on the neat material.

Heat of Combustion: This was measured by oxygen bomb calorimetry (77) to be -3,422  $\pm$  5 cal/gram, which leads to -698.4 kcal/mole and a heat of formation of 134.1  $\pm$  1.0 kcal/mole, assuming a pure sample.

Detonation Propagation: The detonation propagation behavior is similar to that of DCFO. Samples melt loaded into the tubes were found to propagate detonations in the smallest tubes tested (62). A liquid mixture containing 40 W% bottoms, 34 W% DCFO, and 26 W% malononitrile propagated detonation in 3/8" tubes, but not in 1/4" tubes (61). This indicates somewhat better safety characteristics than DCFO, since 26 percent malononitrile with only DCFO will propagate in 0.1" tubes.

Hazardous Reactions: Bottoms undergo hazardous reactions with hydrazine and amines, as was shown in Table 5.

Heat of Fusion: An actual measurement of the heat of fusion was not accomplished. The value employed to estimate eutectic compositions

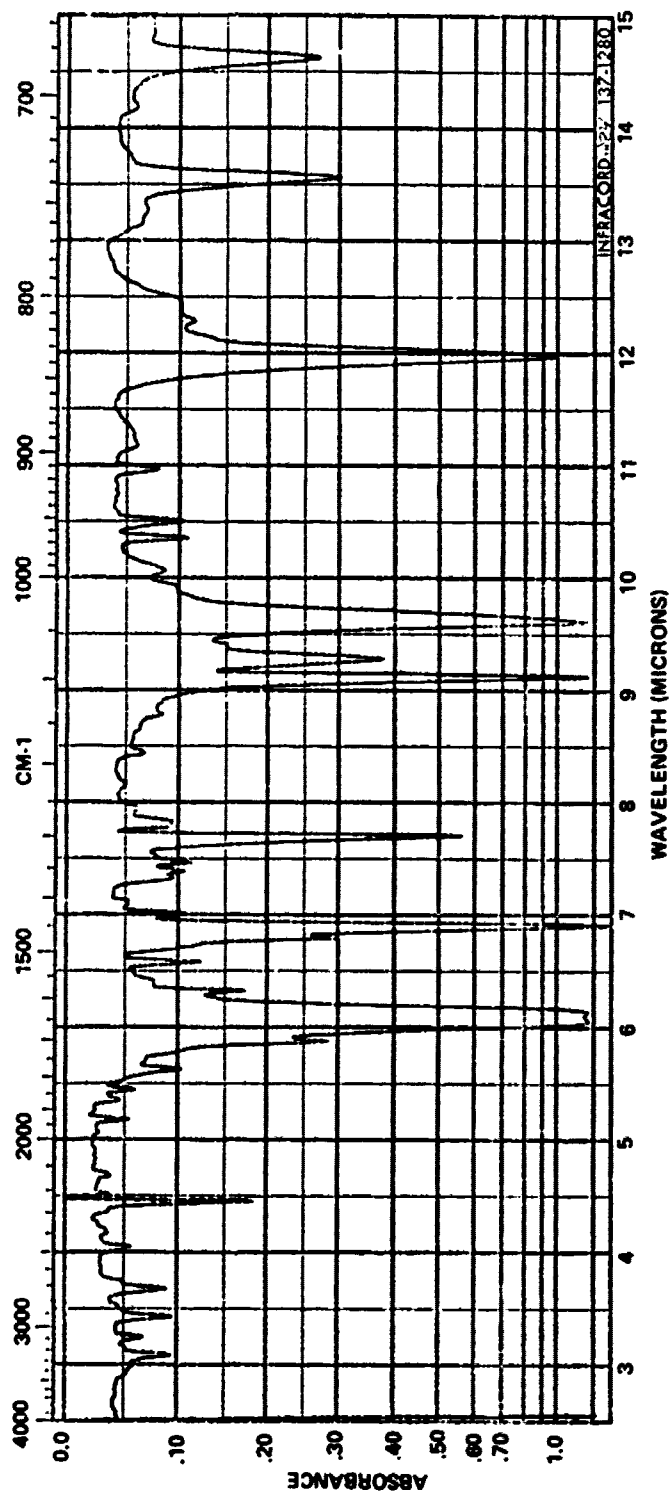


Figure 8. Infrared Spectrum of 3-[5-(3Cyano -1. 2, 4-Oxadiazoly 1)]-4-Cyanofuroxan ("Bottoms")

reported below was in turn estimated from a measurement of the temperature at which bottoms crystallized out of mixture with DCFO.

### Mixtures

The main emphasis of this effort was to find low melting combinations based on the depression in melting point which usually occurs when one compound is contaminated with another. The possibilities in this direction are almost limitless, since the eutectic temperature ordinarily continues to drop as more compounds are included in the mixture. Practical limits are set by the potential for accumulating the undesirable qualities of the various constituents, by cost and availability considerations, and by the onset of diminishing returns as higher melting compounds are added to the set. Furthermore, the higher melting compounds tend to add viscosity to the melt at temperatures much above the point where they actually crystallize out.

Compounds studied in this connection were DCFO, DCFA, malononitrile (MN), and the side product of the DCFO synthesis which came to be called "bottoms" ( $C_6N_6O_3$ ). All combinations of these four compounds were investigated theoretically, and several experimentally.

The freezing point depression may be calculated from a knowledge of the heat and temperature of fusion via the thermodynamic relation,

$$\Delta T = T - T_{fus} = \frac{-RT_{fus}^2 \ln x}{\Delta H_{fus}} ;$$

where  $T_{fus}$ ,  $\Delta H_{fus}$ , and  $x$  are the temperature of fusion, heat of fusion, and mole fraction in the liquid phase, respectively, of the compound in question. It is assumed that the liquid phase represents an ideal solution, that the heat of fusion is independent of temperature, and that the solid phases are pure. This equation may be rearranged as follows:

$$x_i = \exp (\Delta H_{fus} / R(T_{fus} - T)) ;$$



where  $x_i$  is the concentration at which the  $i$  th specie first crystallizes from solution at temperature  $T$ . The eutectic temperature is the temperature for which the mole fractions so calculated satisfy the relations  $\sum x_i = 1$ ; and it is conveniently found graphically by plotting  $\sum x_i$  versus  $T$ .

Experimentally, the eutectic temperature may be located by examining the Differential Thermogram of a mixture for the extrapolated onset of the first endotherm.

Table 7 gives the theoretical eutectic composition and temperature for the various binary, ternary, and quaternary mixtures and also gives several experimental eutectic temperatures.

TABLE 7. EUTECTIC MIXTURES OF LOW HYDROGEN FUELS

<u>DCFO</u>	<u>Mole Fraction</u>			<u>Eutectic Temperature (<math>^{\circ}\text{C}</math>)</u>	
	<u>DCFA</u>	<u>BOTTOMS</u>	<u>MN</u>	<u>CALC</u>	<u>EXP</u>
.272	.255	.047	.426	-33	-
.286	.270	-	.443	-30	-9
-	.372	.078	.550	-14	-
.378	-	.076	.546	-14	-
.415	-	-	.585	-9	1
-	.415	-	.585	-9	4
.453	.449	.098	-	-4	-
.500	.500	-	-	2	2
-	-	.169	.831	18	-
-	.795	.205	-	26	-
.783	-	.217	-	28	28

The following data was used in deriving the eutectic points:

		<u>DCFO</u>	<u>DCFA</u>	<u>BOTTOMS</u>	<u>MN</u>
$H_{\text{fusion}}$ (cal/mole)	:	3414	3684	6487	2422
$T_{\text{fusion}}$ ( $^{\circ}\text{C}$ )	:	42	38	89.5	32

The theoretical promise of ternary mixtures is evident, as is the favorable theoretical effect of malononitrile. Experimentally the predicted eutectic temperature of DCFO/DCFA was realized, whereas all mixtures involving malononitrile fell short, especially the ternary mixture DCFO/DCFA/MN. The full quarternary mixture was not attempted, but the additional effect of adding bottoms would apparently be minor.

#### Carbonyl Diisocyanate

This compound has resemblances to the other compounds discussed previously as GDL fuels, mainly in its lack of hydrogen. However, it has unique characteristics, which potentially suit it to a larger role in GDL technology. In particular, it is considered not in the context of a storable GDL fuel, but rather a storable replacement for the nitrogen diluent. The basis for this potential use is developed below, along with an introduction to the problem of devising a storable diluent.

At the outset of the project it was recognized that the successful development of a storable fuel would still leave an important need unanswered. Most of the bulk of the reactants lies in the nitrogen, which forms 85 to 95 percent by weight of the laser medium. Stored as a high pressure gas, it is extremely bulky and heavy. Stored as a liquid it is more packageable, but still requires special tankage and insulation, and creates operational problems in storage, transfer and transportation as well as complicating start-up procedures.

In principle the need for nitrogen might be met in non-cryogenic fashion by using an organic fuel with a high nitrogen to carbon ratio. In fact, one compound (66) was encountered in the literature,  $\text{C}_2\text{N}_{14}$ , with

a sufficiently large N/C ratio to be useful in this context. Two main drawbacks exist to this compound, and any other might be similar to it. It is a highly substituted organic azide, making for hazardous handling, and excessive flame temperatures.

Another approach considered was to attach the nitrogen chemically to something other than carbon--necessarily something that can be removed from the medium, or which has no unfavorable effect on it. Sodium azide is a natural choice, since it is quite stable, yet can be decomposed in a controllable fashion. Prior work existed (67, 68) in which sodium azide was burned under very cool, fuel-rich conditions, under which most of the sodium was converted to liquid sodium which could be filtered from the products. Neither of the referenced programs, however, demonstrated a filtration procedure which would be suitable at high flow rates. Another offsetting disadvantage is the large mass of inert material incorporated into the propellant.

The use of air as an oxidizer can supply much of the nitrogen needed and is conceptually an attractive way of reducing the reactant problem. However, the mass and bulk of the needed compression machinery is considerable, and outweighs the savings in reactants for the short missions of interest to AFWL.

Within the existing limitations, it appears most difficult to propose a non-cryogenic diluent source. To a certain extent the problem may be artificial, since the limitations arise from stringent gas composition requirements that may be too narrow. In particular, the  $N_2$  molecule satisfies a specialized role due to kinetic properties which are not wholly unique to it. These properties include primarily a long lifetime in its vibrationally excited state, and a rapid exchange of vibrational quanta with the asymmetric stretch mode of carbon dioxide. Early in the project the similarity of carbon monoxide to nitrogen in these respects was noted, and the possibilities for capitalizing on the resemblance were explored.

To be sure, carbon monoxide is also a hard cryogen, with no detectable advantage over nitrogen. The interest, however, derives from the possibility of forming carbon monoxide as a combustion product of a storable fuel and oxidizer combination. The prescription for the fuel in this combination has distinct differences from that of the GDL fuels that use  $N_2$  diluent. Namely, the carbon to hydrogen ratio must be higher, and the energy must be lower. Compounds such as DCFO and DCFA have no hydrogen, and they may in principle be burnt fuel rich to carbon monoxide. However, their flame temperatures are about double the range of interest. Nearly all the hydrogen-free compounds turned up by the literature search, in fact, have grossly excessive flame temperatures. The only exceptions found are those containing carbon in a substantially oxidized condition, such as the anhydride, carbonyl, and isocyanate groups. Only a few compounds are known which meet the requirements for both extremely low (or no) hydrogen and low energy. Among the solid materials are mellitic anhydride,  $C_{12}O_9$ , quinone-tetracarboxylic acid anhydride,  $C_{10}O_8$ , and pyrazinetetracarboxylic acid anhydride,  $C_8N_2O_6$ . Among ambient liquid compounds the only candidate is carbonyl diisocyanate,  $C_3O_3N_2$ .

The suitability of carbonyl diisocyanate (CDI) for this application hinges on a number of questions. The major question is, of course, the starting premise that carbon monoxide is indeed substitutable for nitrogen in the GDL medium. Another question is whether its heat of formation is acceptable. Estimates ranged from -25 to -100 kcal/mol, based on different model compounds. The former is too energetic, and the latter is too negative. Further, its combustion with a suitable oxidizer, say  $N_2O_4$  and  $N_2O$ , should be efficient at low oxidation ratios. And finally, its handling qualities should be better than those of liquid nitrogen.

On most of these counts the prognosis was favorable. A reasonable accounting of CO kinetics had been published by AVCO workers (69, 70), and indeed it was their conclusion on the tolerance of GDL's for CO which first stirred our interest in this approach. Through AFWL assistance,

the use of the AVCO computer code was made available and the gain and lasable flux for high CO content GDL mixtures was calculated (2). These calculations showed that the substitution was not exact. Gain was found to be reduced with increasing CO substitution. On the other hand, lasable flux was increased by the substitution. Although the net effect of these contrasting effects was not predicted, the results were taken to be generally encouraging.

The desired heat of formation of CDI was near the middle of the estimated range. The expected combustion efficiency was strictly conjecture, but it was noted that the molecule was already internally balanced to CO and had little more to do than break down thermally to CO and N<sub>2</sub>. The handling convenience associated with CDI was a moot point, since it was reported to polymerize on standing at room temperature. Its reported depolymerization at 150°C was an offsetting feature which indicated that at worst CDI could be viewed as a moderately high melting solid, usable with special techniques.

The use of CDI is thus a high risk approach with high potential payoff. The final decision to pursue its study was made amidst growing disenchantment with DCFO, DCFA, "Bottoms", and similar materials with their poor or questionable safety characteristics.

CDI is not commercially available, and its purchase was a lengthy enterprise, due largely to unexpected technical difficulties in the scale up. Two pounds were eventually received from Allied Chemical Company under Contract F04611-72-C-0065. During part of this period the project was essentially inactive due to a decision to do no further work on the storable fuels. The receipt of the CDI reactivated the characterization phase, although full restoration was withheld until CDI passed its safety tests and until its heat of formation was measured. The key results are described below:

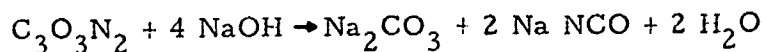
Detonation Propagation: The same technique described previously for DCFO was applied to CDI, again under Contract F04611-71-C-0035

with Rocketdyne. Using 50 grams of "Composition C" booster with a DuPont E-83 blasting cap, "critical diameter" deformation propagation tests were run in 3/8", 1/2", and 1" tubing at ambient temperature (20°C) (26, 71). All tests were negative, indicating that CDI is non-explosive.

Thermal Stability: The adiabatic self heating point for CDI was measured in the JANNAF thermal stability apparatus (71). Mild exotherms were encountered at 345°C (650°F) in one sample and 357°C (675°F) in another.

Flashpoint: The modified Cleveland open cup apparatus was used to determine the flash point (71). The sample reached the boiling point 105°C (220°F) and evaporated without igniting. The flame was observed to flare a little, but the liquid did not ignite. After the test a heavy rime was noted on the top rim of the cup.

Heat of Formation: The heat of reaction of CDI with aqueous sodium hydroxide was accomplished (72) according to the assumed stoichiometry:



No analysis of products was performed, but this reaction is reported to be quantitative (8). The average reaction heat for two runs is  $-62.7 \pm 0.5$  kcal/mole. Combining this with the heats of formation for water and aqueous  $\text{Na}_2\text{CO}_3$  and  $\text{NaNCO}$  yields a heat of formation for CDI of  $-83.3$  kcal/mole. A probable uncertainty of  $\pm 5$  kcal/mole is attached to this number due mainly to the effect of an impurity which survived the purification procedure.

The effect of this heat of formation is shown in Figure 9 in terms of the flame temperatures versus  $\text{CO}_2$  content. In the calculations for this figure, liquid  $\text{N}_2\text{O}$  was assumed as oxidizer and CDI was used as both fuel and diluent; that is, a portion was oxidized to  $\text{CO}_2$  and the remainder simply pyrolyzed to  $\text{CO}$  and  $\text{N}_2$ . Enough water was added to form one percent in the product gases, although the "water gas" reaction.

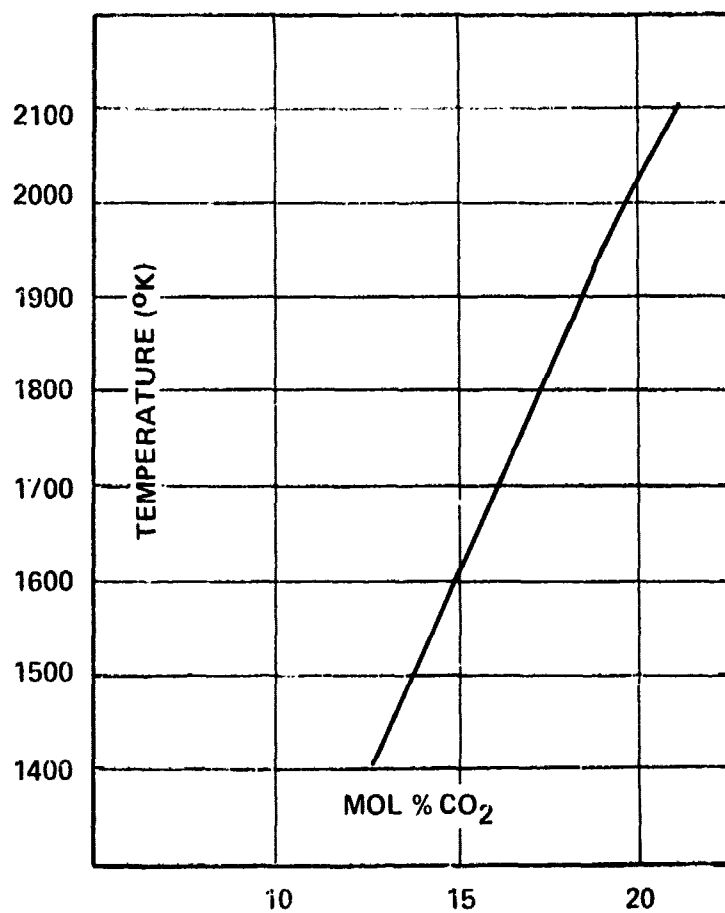


Figure 9. Flame Temperature Versus CO<sub>2</sub> In The System  
CDI + N<sub>2</sub>O(L) + 1% H<sub>2</sub>O<sub>2</sub>



reduced the water to about a half percent and formed elemental hydrogen. The CO level was nominally 50 percent ( $\pm 5\%$ ) in the range plotted, and  $\text{N}_2$  formed the balance.

The calculation shows that CDI has some utility as a combined fuel and diluent, alleviating the need for a distinct fuel stream and simplifying the hardware. However, in this context the flame temperatures admittedly cover only the low range of interest when  $\text{CO}_2$  content is held below 15 percent. Since  $\text{CO}_2$  levels around 10 percent are desirable for many cases, the energetics of the simple CDI- $\text{N}_2\text{O}$  system are definitely marginal at a CDI heat of formation of -83.3 kcal/mole. Furthermore, the calculations are slightly optimistic, since more water is needed in the propellant to assure an equilibrated one percent in the products.

Fortunately, the low energy is easy to cure if one is willing to forego the simplicity of a combined fuel-diluent. If the needed water is assumed to be formed from a combustion reaction, as is the usual case anyway, then temperatures may be raised to any reasonable level desired. The proper fuel to accomplish this is not critical, but the usual patterns and trends are evident; the higher the carbon to hydrogen ratio, the less water is needed for a given temperature. Additional calculations showed that there was little reason to seek C/H ratios much above 1 or 1.5. After a brief search it was concluded that commercially available benzonitrile ( $\text{C}_7\text{H}_5\text{N}$ , m.p. =  $-13^\circ\text{C}$ , b.p. =  $191^\circ\text{C}$ , C/H = 1.4) was representative of the type of fuel needed to derive maximum benefit from CDI. A plot of flame temperature versus  $\text{CO}_2$  content is given in Figure 10 for the system CDI + benzonitrile +  $\text{N}_2\text{O}$  (L). The water content is, of course, derived from benzonitrile combustion and an iterative procedure was used to adjust total reactant ratios for a water level of one percent in the products with due consideration for the "water-gas" reaction.



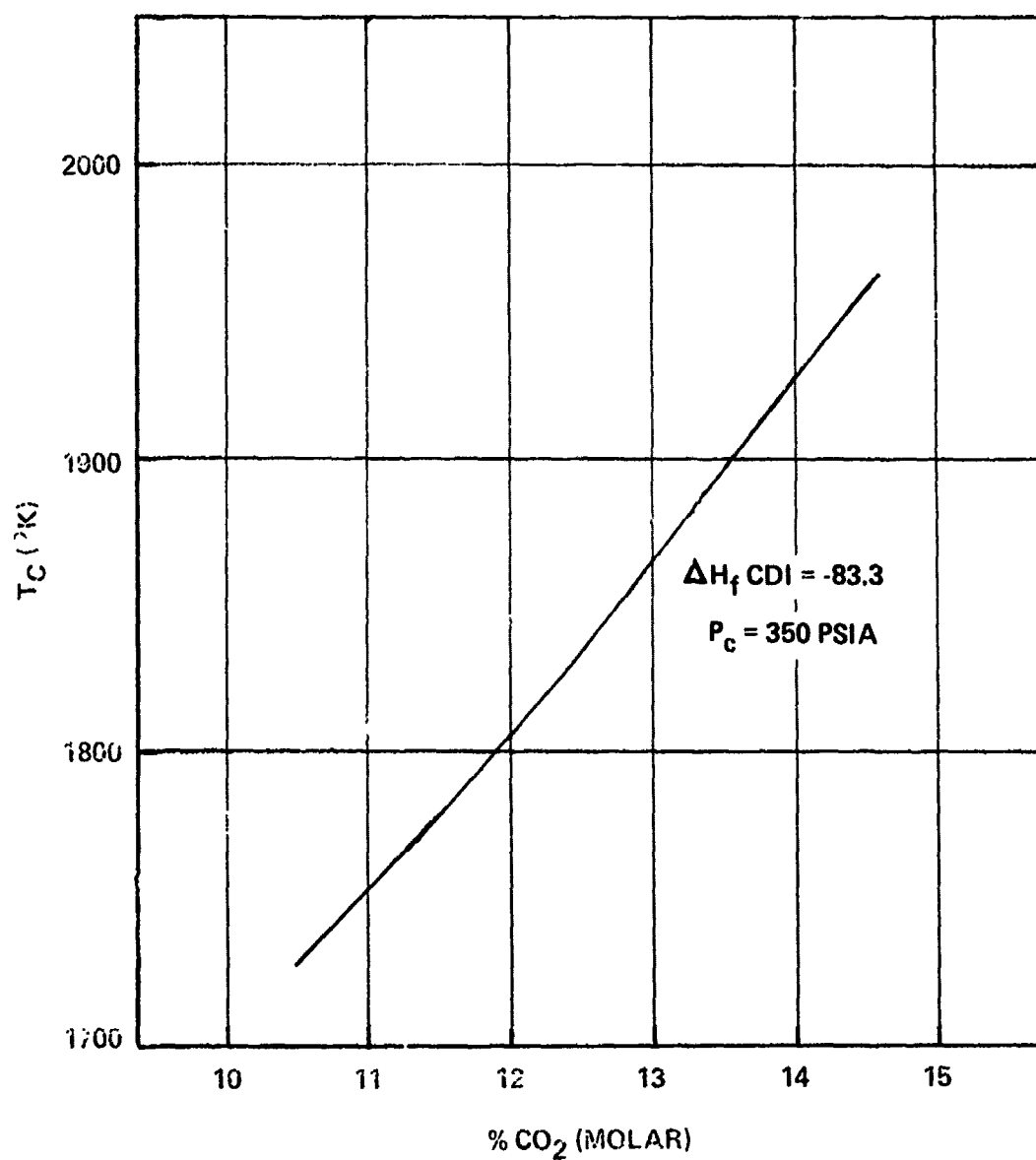


Figure 10. Flame Temperature Versus CO<sub>2</sub> at 1 Percent H<sub>2</sub>O; CDI + Benzonitrile + N<sub>2</sub>O (L)

The available temperatures and CO<sub>2</sub> content at one percent water are very attractive in themselves. Furthermore, if still higher temperatures are desired, only a modest increase in water content is needed to obtain them.

These theoretical results, derived from a reliable heat of formation for CDI, along with the favorable results from the safety tests, encouraged a continuation of the project to further characterize the material. Of chief concern was its stability towards polymerization. Because of this tendency, the CDI was shipped to AFRPL packed in dry ice, and was stored thereafter in a dry ice chest. Samples were withdrawn from cold storage periodically and subjected to tests at ambient temperatures. The three main objectives of the tests were 1) to measure the rate of polymerization and how it is affected by temperature and container materials, 2) to determine if polymerization could be slowed or halted by chemical stabilizers, or perhaps by storage in the dark, and 3) to verify the reported thermal depolymerization and determine the conditions needed to cause this behavior.

Two types of measurements of the rate of polymerization were conducted. The rate of viscosity increase with time was measured at the AFRPL, and the rate of formation of "non-volatile residue" was measured at Rocketdyne under Contract F04611-71-C-0035.

Viscosity: For these tests the CDI was distilled immediately before use. A capillary viscometer, tube size 50, of the Cannon type was used. The results are kinematic viscosity (centistokes) and were calculated by multiplying the viscometer constant by the time in seconds for the CDI to flow through a fixed volume by gravity. The constant was obtained with double distilled water as the reference liquid. Measurements of viscosity were taken (73) at 10°C, 20°C, 30°C, 40°C, and 50°C over a period of several hours. The increase in viscosity with time, shown in Figure 11, is taken as a qualitative measure of the rate of polymerization of CDI, and is a practical tool in evaluating the time available for

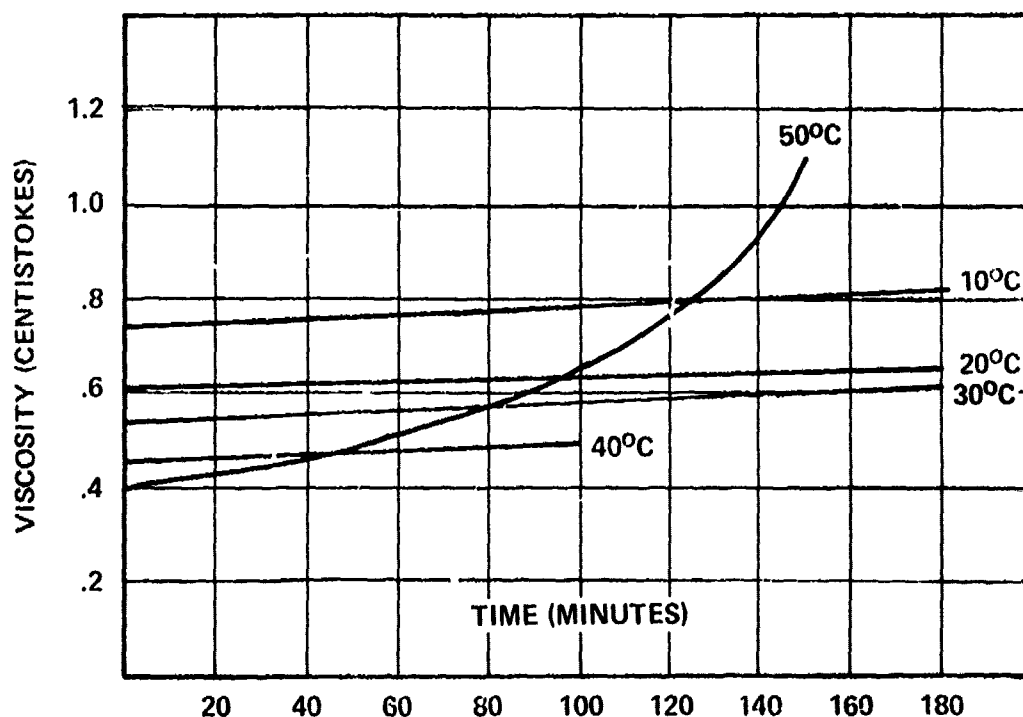


Figure 11. Rate of Viscosity Change of CDI

countdown procedures and other ambient temperature operations. Although the results are reported as viscosity increases, presumably from growth of dissolved polymer, the possibility cannot be eliminated that the capillary bore was simply being clogged by particulate matter. Plugging was indeed observed in some runs; and the best evidence that real changes in viscosity were being observed is that such plugging led to abrupt and obvious changes in flow time and was accompanied by visible particulates. Shown in Figure 12 is the viscosity at time zero for the different temperatures, which is assumed to be the viscosity of pure monomer.

Non-Volatile Residue (NVR) Tests: These tests also measure the rate of polymerization. The name NVR refers to the method of analysis, which consists of post test distillation of CDI, and collection and weighing of the non-volatile residue. The test consists of sealing freshly distilled

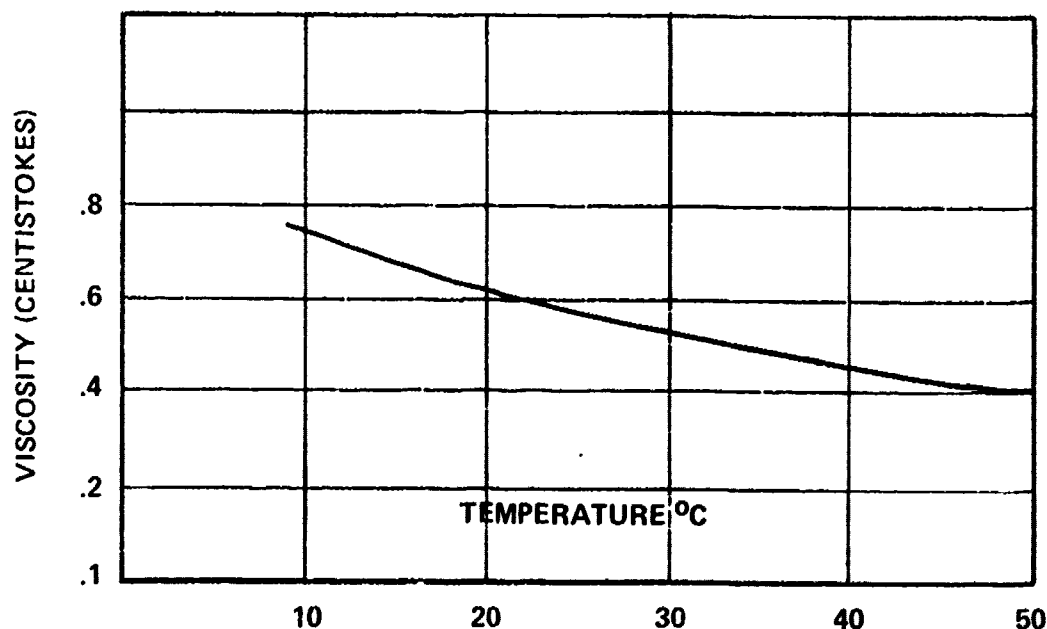


Figure 12. Initial Viscosity of CDI Versus Temperature

CDI in glass ampoules and holding the samples in a constant temperature bath for varying lengths of time. After the waiting period the sample is removed from the bath and the NVR is determined, and reported as a percent of the initial sample. All of the tests were done in glass ampoules, into which specimens of other materials were introduced to determine their effect. The surface to volume ratio ( $S/V$ ) was maintained constant at about  $12 \text{ inch}^{-1}$ , including the wetted surface of the ampoule. For the all glass cases a glass rod was introduced to maintain the  $S/V = 12 \text{ inch}^{-1}$  condition. Specimens included 347 stainless steel, copper, chrome, and apiezon L grease. For these comparative tests, the temperature was maintained at  $30^\circ\text{C}$ . The results are shown in Figure 13. Allowance was made for the NVR formed during operations before and after each test, using an iterative procedure. The results show that after this correction is made the NVR still does not pass through zero at zero time, except with glass (pyrex). This indicates either an initial reaction

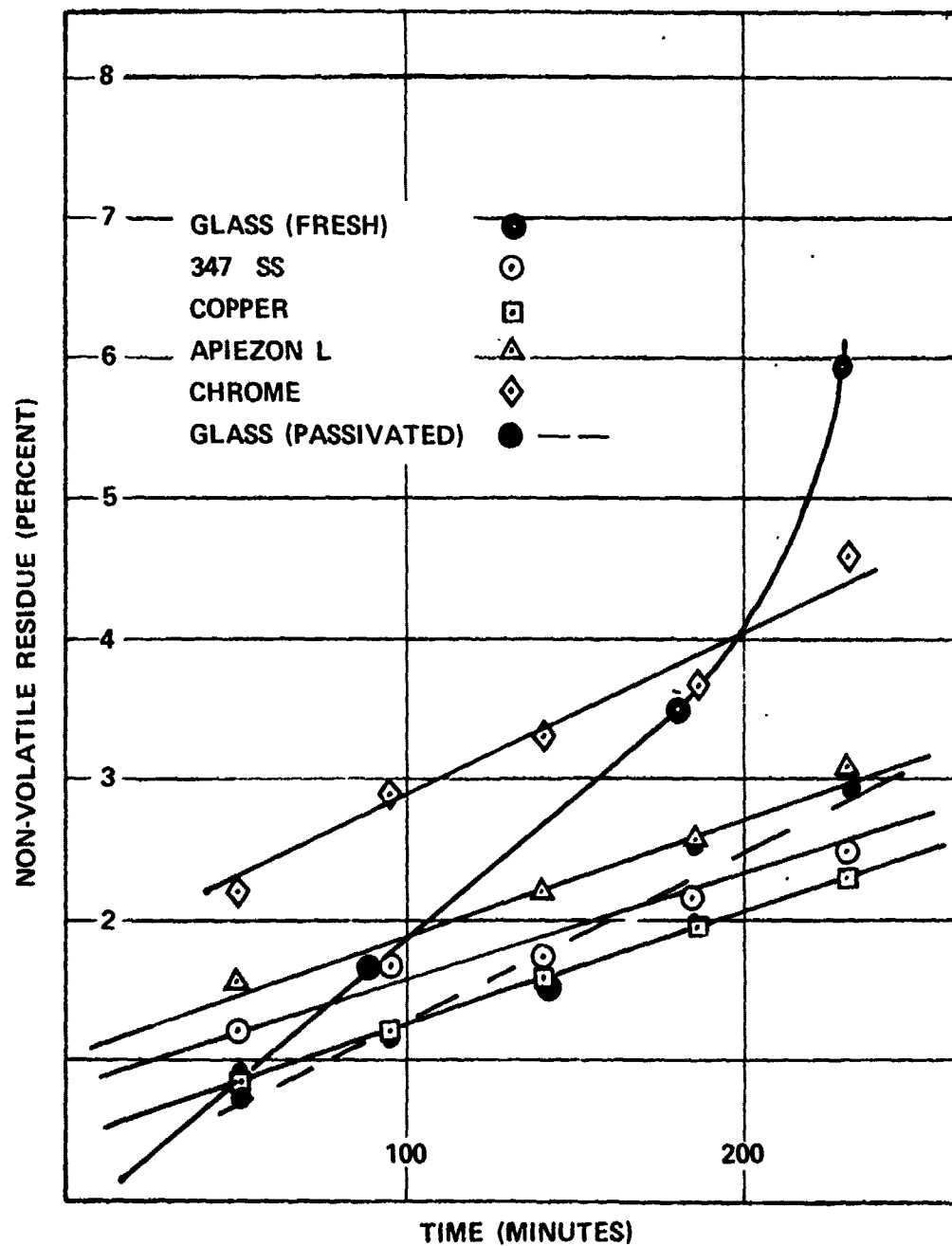


Figure 13. Effect of Materials On Polymerization of CDI ; -30°C

with (and consumption of) surface contaminants, or else an initial rapid reaction catalyzed by the surface, followed by surface passivation. Furthermore, the slopes of the plots after the initial reaction are very similar for all the specimens except glass, which is three times as high. This result is quite surprising, since the wetted area of the glass ampoule, present in all tests, was well over a third of the total glass area. Subsequently the test with the glass rod was rerun. In the second test the glass was pre-passivated with CDI prior to the test. Although there was some scatter, the data appear to be more similar in slope to the other materials than was the original run with glass. The difference has not been explained. For the most part the slopes are constant, with only the final point with fresh glass suggesting a rapid, perhaps self-catalyzed runaway. The specimen surfaces themselves were not visibly affected by contact with CDI. In the apiezon L case, the grease was smeared on a glass rod and appeared intact. However, there were a few waxy floating particles in the CDI. The appearance of the non-volatile residue varied, including powder, crystals, and glasses, either clear or milky; and no consistent pattern to these variations was evident.

Additional NVR rates were measured at 20°C and 40°C in glass only; and extended studies were done at -10°C, the final sample being removed after 1388 hours.

The rates for all the temperatures were correlated against temperature using an Arrhenius relation for temperature dependence, and were fitted remarkably well by the equation,

$$r = 9.19 \times 10^{11} \exp (-8524/T) ;$$

where  $r$  is the rate of NVR buildup in weight percent per hour, and  $T$  is temperature in degrees Kelvin. If this rate is extrapolated to the freezing point of CDI (-50°C), it indicates that the material can be stored at that temperature five years for each percent of NVR formed. The details of the above tests are given in Reference 74.

CDI Stabilizers: A number of chemicals were tested for possible reduction of the rate of polymerization. Unstabilized, CDI converts to a solid generally overnight, even in the dark, if left at ambient temperatures. No improvements were obtained over this behavior with any of the chemicals tested (73, 75). These include sebacyl chloride, a known stabilizer for some diisocyanates, and barium oxide, a non-acidic de-hydrating agent (on the theory that moisture was a factor). Since acetone is a good solvent for CDI polymer, other similar compounds were investigated for possible use as a CDI additive on the theory that a solvent for the solids mixed with CDI itself would afford a compatible and stable solution. All of the compounds tested as a solvent for CDI solids, however, were found to be ineffective. They include methyl ethyl ketone, 2-methyl cyclohexanone, 2-octanone, acetophenone, and glyme.

Several other compounds were tested with CDI, not specifically as stabilizers, but to see if a high carbon to hydrogen compound could be found which would add energy to the CDI system without accelerating its polymerization. Toluene diisocyanate was found to be compatible at 2 percent, lasting 39 hours at room temperature. At 4 percent, however, it drastically accelerated the solidification (5 hours at R. T.). Toluene, nitrobenzene, benzonitrile, and pyridine accelerated solidification, with pyridine causing almost immediate solidification.

Regeneration of CDI from its polymer: One of the surprising and potentially useful aspects of the CDI polymerization is its reversibility. We have observed (75), that heating of the solid to  $114^{\circ}\text{C}$  causes it to melt, and that recooling causes a hard glass to form. The infrared spectra of the glass and of the original solid are identical.

When the solid is warmed to  $150\text{--}160^{\circ}\text{C}$  the glass becomes extremely fluid and remains fluid after the material is cooled to room temperature. The infrared spectrum of the fluid is identical to that of pure CDI liquid, and the peaks for the solid are absent. The newly formed liquid, however, converts to glass much more readily in a glass capillary than CDI normally

does (10-15 minutes). CDI may be regenerated also by bulb to bulb distillation, and such CDI is "normal" in all respects.

A summary of the thermal behavior is given below:

160°C	Solid regenerates CDI monomer
114°C	Solid melts
90°C	CDI solidifies rapidly
25°C	CDI solidifies overnight
0°C	CDI remains liquid 1-2 weeks in polyethylene flask
-50°C	CDI freezes (as monomer). Stable for years.

The melting of CDI polymer is a complex phenomenon, producing a liquid that is partially CDI monomer. It might be regarded as a eutectic mixture of monomer and polymer. With increasing temperature the concentration of monomer grows, until at 150 to 160°C the polymer is essentially zero. In support of this claim, it is noted that the 114° "melting point" is not observed unless the sample is sealed. This is probably due to the vaporization of the monomer in unsealed vessels, carrying away its solvent power. In unsealed vessels, in fact, no melting or reaction is observed to 290°C.

Reaction With Water: CDI is very hygroscopic, and it absorbs moisture from the atmosphere and probably moisture bound to metal surfaces. When several aluminum tubes were filled with CDI prior to elemental analysis, and sealed so that no weight loss by evaporation was observed on the microbalance, a steady increase in hydrogen was observed (75) from the first sample analyzed to the last. In one case hydrogen increased from 0.10 percent to 0.18 percent in about one hour. According to Nachbaur (8), the reaction product of CDI with water is 90 percent 2, 4, 6 -trioxotetrahydro - 1, 3, 5, oxodiazine and 10 percent urea plus carbon dioxide.



Infrared Spectra: The infrared spectrum of CDI has four peaks at  $2240\text{ cm}^{-1}$ ,  $1775\text{ cm}^{-1}$ , and  $1075\text{ cm}^{-1}$  (75). These agree with the spectra reported by Nachbaur (8). Additional small unassigned peaks existed at  $1750\text{ cm}^{-1}$ ,  $1740\text{ cm}^{-1}$ ,  $1405\text{ cm}^{-1}$ ,  $1230\text{ cm}^{-1}$ ,  $990\text{ cm}^{-1}$ ,  $830\text{ cm}^{-1}$ ,  $730\text{ cm}^{-1}$ , and  $1610\text{ cm}^{-1}$ .

Mass Spectra: Satisfactory mass spectra were not obtained for CDI. Several of the peaks remained constant, but others showed large variations (75). The results of four runs are shown in Table 8. The presence of hydrogen in several of the variable intensity peaks suggests a possible reaction with moisture from the walls of the mass spectrometer inlet. It is notable that the  $\text{CO}_2^+$  peak is largest when these hydrogen peaks are highest.  $\text{CO}_2$  is one of the known reaction products with water.

Vapor Pressure: The vapor pressure of CDI was measured (78) by techniques described previously, and the results are given in Figure 14. The data may be represented by the equation,

$$\text{Log PmmHg} = 7.651 - \frac{1770}{T} ,$$

from which the extrapolated boiling point is  $105^\circ\text{C}$ .

Heat of Vaporization: From the above equation, the heat of vaporization is calculated to be  $8.1\text{ kcal/mole}$ .

Entropy of Vaporization: The corresponding entropy of vaporization is  $21.4\text{ cal/degree-mole}$ .

Density: The density of CDI versus temperature as determined (78) using the dilatometer technique is shown in Figure 15.

TABLE 8. MASS SPECTRA OF CDI

<u>Peak Intensity</u>					
<u>Mass Assignment</u>	<u>Mass Number</u>	<u>Run #7</u>	<u>Run #8</u>	<u>Run #9</u>	<u>Run #10</u>
Constant Intensity Peaks					
OCNCO <sup>+</sup>	70	100	100	100	100
OCN <sup>+</sup>	42	31	27	25	23
CO <sup>+</sup>	28	423	427	753	315
Variable Intensity Peaks					
OCNCONCO <sup>+</sup>	112	12	14	Chart Torn Off	0
OCNC <sup>+</sup>	54	9	2	1	3
CO <sub>2</sub> <sup>+</sup>	44	181	264	35	18
OCNH <sup>+</sup>	43	38	27	5	2
NCNH <sup>+</sup>	41	8	5	3	1
NCN <sup>+</sup>	40	0	0	1	1
O <sub>2</sub> <sup>+</sup>	32	15	23	2	1
NO <sup>+</sup>	30	8	6	1	2
HCO <sup>+</sup>	29	42	45	6	3

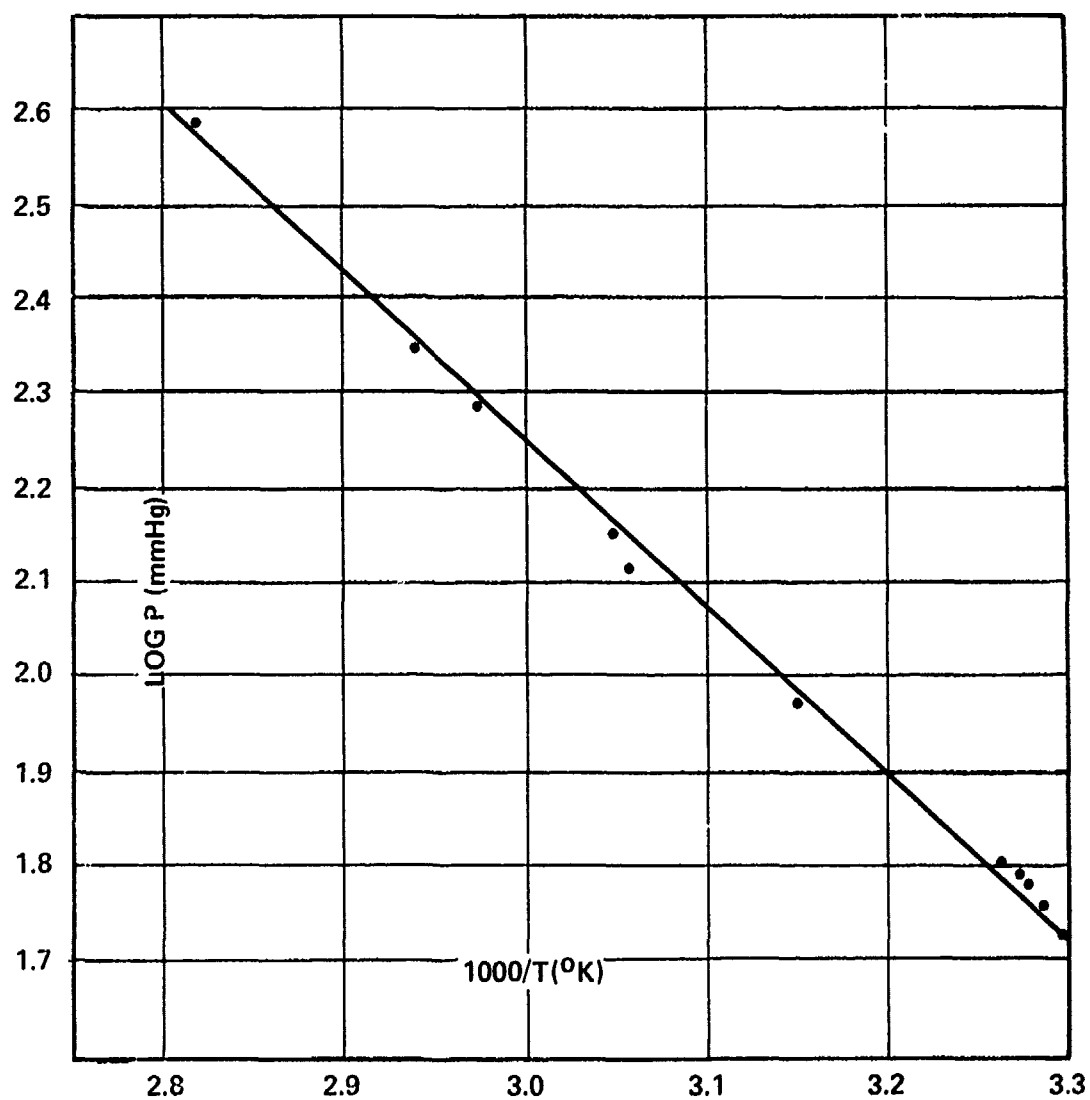


Figure 14. Vapor Pressure of CDI

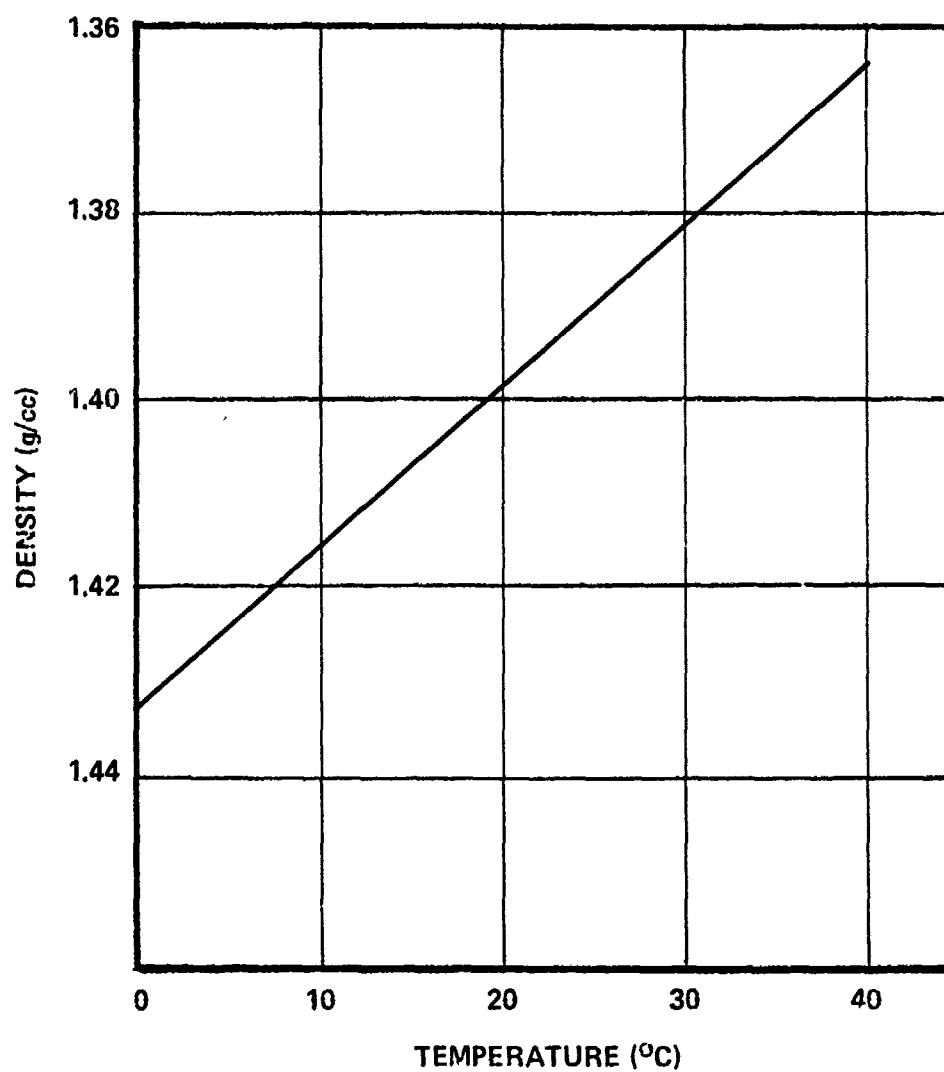


Figure 15. Density of CDI Versus Temperature

## SECTION V

### HARDWARE AND TEST FACILITY FOR COMBUSTION TESTS

The hardware to accomplish the CDI combustion tests was built to make maximum use of combustion hardware originally designed for studying storable GDL fuels. Thus it will be convenient to describe the original design philosophy and the resulting facility, and then trace the transformation of the device into a tool for characterizing diluents.

The peculiar characteristics sought in a GDL fuel have already been discussed. An unsought, but apparently unavoidable, characteristic of all the known candidates was a disposition towards rarity and unavailability. The facility was conceived and designed at a time when a several dozen compounds with theoretical utility were identified from the literature, most of which were poorly characterized, but had known flaws of some nature. It was considered that a final choice might entail combustion tests of up to half a dozen compounds, aside from any that might arise from the synthesis phase of the project and ignoring the multiplicative effects of mixture possibilities. Conventional approaches to a combustion evaluation facility were deemed economically infeasible for a broad comparative study of these laboratory curiosities. Accordingly, a major concern was to minimize flow rate. Very low flow rates can create problems in measurement and potentially bias the phenomena being studied; and some pains were taken to minimize factors which would compromise the data. Important considerations included control and measurement of flow rate; the injection process, and heat loss characteristics of small combustors.

#### Combustor Design

The general sizing of the combustor was set by the smallest flow rate of fuel which is feasible to inject. Fabrication tolerances in the

injector orifices suggested about five grams per second as a reasonable lower limit. Approximately an equal flow of oxidizer (assuming nitrogen tetroxide) is required; and a much larger flow of nitrogen diluent, typically about 40 grams per second, completes the system. At the large surface to volume ratios for small combustors, heat losses are severe and consume a large fraction of the total heat release for such small flow rates. A heat loss near 50 percent was projected for a chamber of this flow rate and having residence times commonly believed necessary for good combustion.

It is possible to make measurements of heat loss and apply corrections to the ballistic parameters. The weakness of this approach is that for very large heat losses a coupling is likely to occur between heat loss and combustion efficiency for which no correction can be made.

There is one characteristic of the GDL reactant scheme which offers an unusual possibility for sharply reducing heat loss, and that is the presence of an inert diluent as the preponderant flow. This stream can be used as a regenerative coolant prior to injection downstream of the main combustion zone. Ordinarily, regenerative cooling is not feasible in very small combustors because the large ratio of heat rejected to propellant injected creates destructive temperatures in the propellant used as the coolant. However, in this case, the nitrogen is stable to very high temperatures. Furthermore since it contributes cooling without contributing to the heat release, the thermal burden on the walls themselves becomes tolerable, at least for certain refractory materials of construction. What is implied by these remarks is a hot refractory liner bounding the combustion zone, with a back flow of nitrogen. At some point the nitrogen is injected into the chamber, bearing with it much of the heat which escaped from the combustion zone. A suitable additional mixing length allows the nitrogen to mix and equilibrate with the

combustion gases, after which a near adiabatic temperature may be assumed to exist for measurement purposes. In the design actually adopted, a double liner was employed, consisting of a pair of inner liner tubes made of a refractory material, and an outer liner tube made of stainless steel. This arrangement reduced heat loss even further by providing an additional path for the nitrogen to absorb heat and by creating an additional pair of boundary layers to impede the flow of heat from the chamber. The general arrangement is shown in the inset for Figure 16. A photograph of the combustor, unassembled is given in Figure 17.

The combustor consists of four basic parts, an injector, an upper chamber, a lower chamber referred to hereafter as the "instrumentation block", and a nozzle. Depending on the injector used, a fifth part, an igniter plate, may be inserted between the injector and the upper chamber.

Upper Chamber and Liners The upper chamber is fabricated of oxygen-free copper. It is 12 inches long and 4 inches in outside diameter. The diameter is widened through a  $30^\circ$  fairing section to a 5.25 inch diameter mating flange at the upper, or injector end. The upper end is tap drilled for four stainless steel thread inserts, and the lower end is tapped for five inserts for joining to the injector and instrumentation block, respectively. "O"-ring seals are provided between the chamber and the injector and instrumentation block. The chamber bore is 0.98 inches, leaving a 1.5 inch thick wall. The thick wall is for thermal mass since the chamber is uncooled. A 0.1 inch counterbore at the top is provided for the liner flanges described below. The diluent is brought in through a pair of 0.25 inch drill holes whose center-lines graze opposite sides of the chamber bore 0.4 inches above the bottom. The holes enter from opposite directions, imparting a swirl to the flow.

The two inner liners are identical with one another, and each consists of a tube 5.91 inches long with an inside diameter of 0.6 inches and a

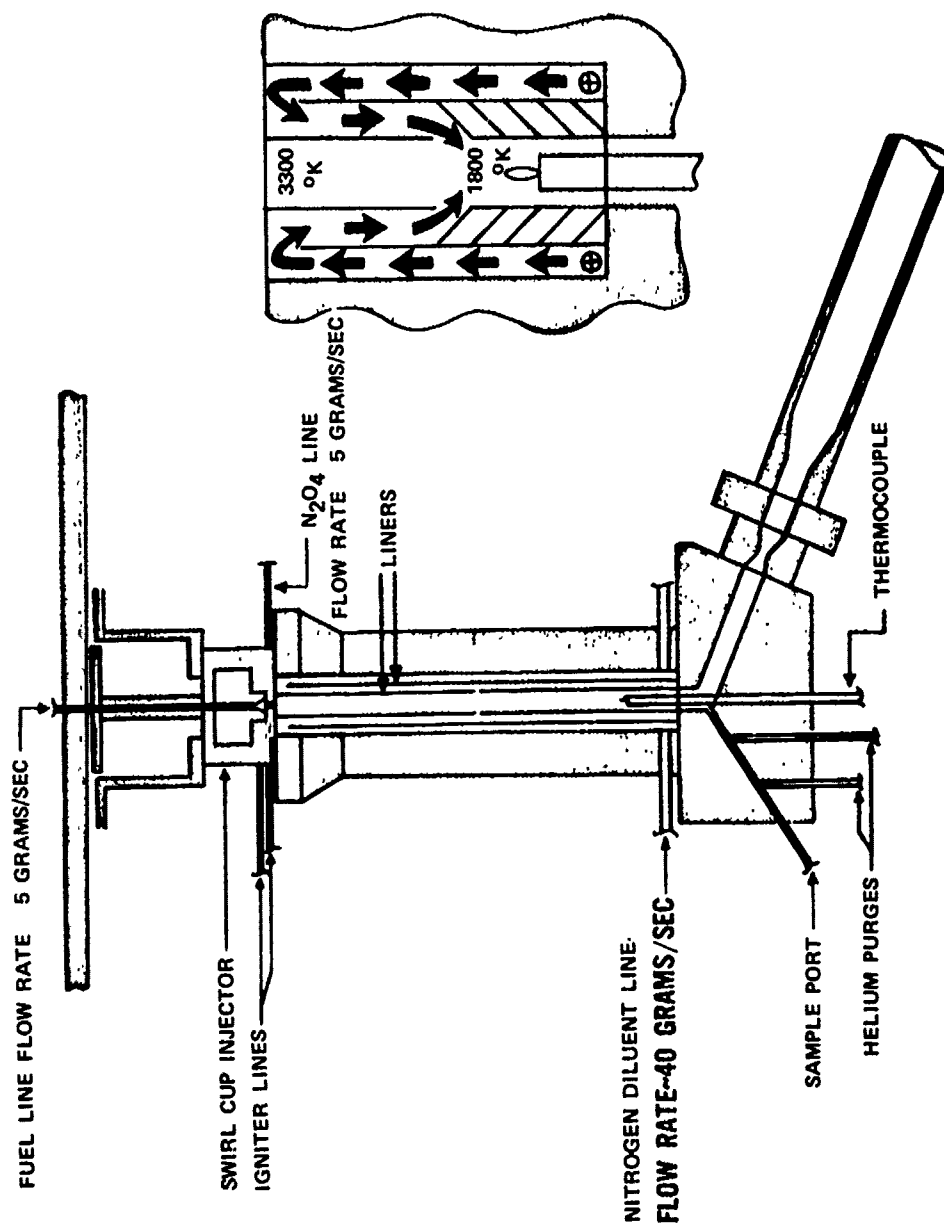


Figure 16. Mini-Combustor Fuel Configuration



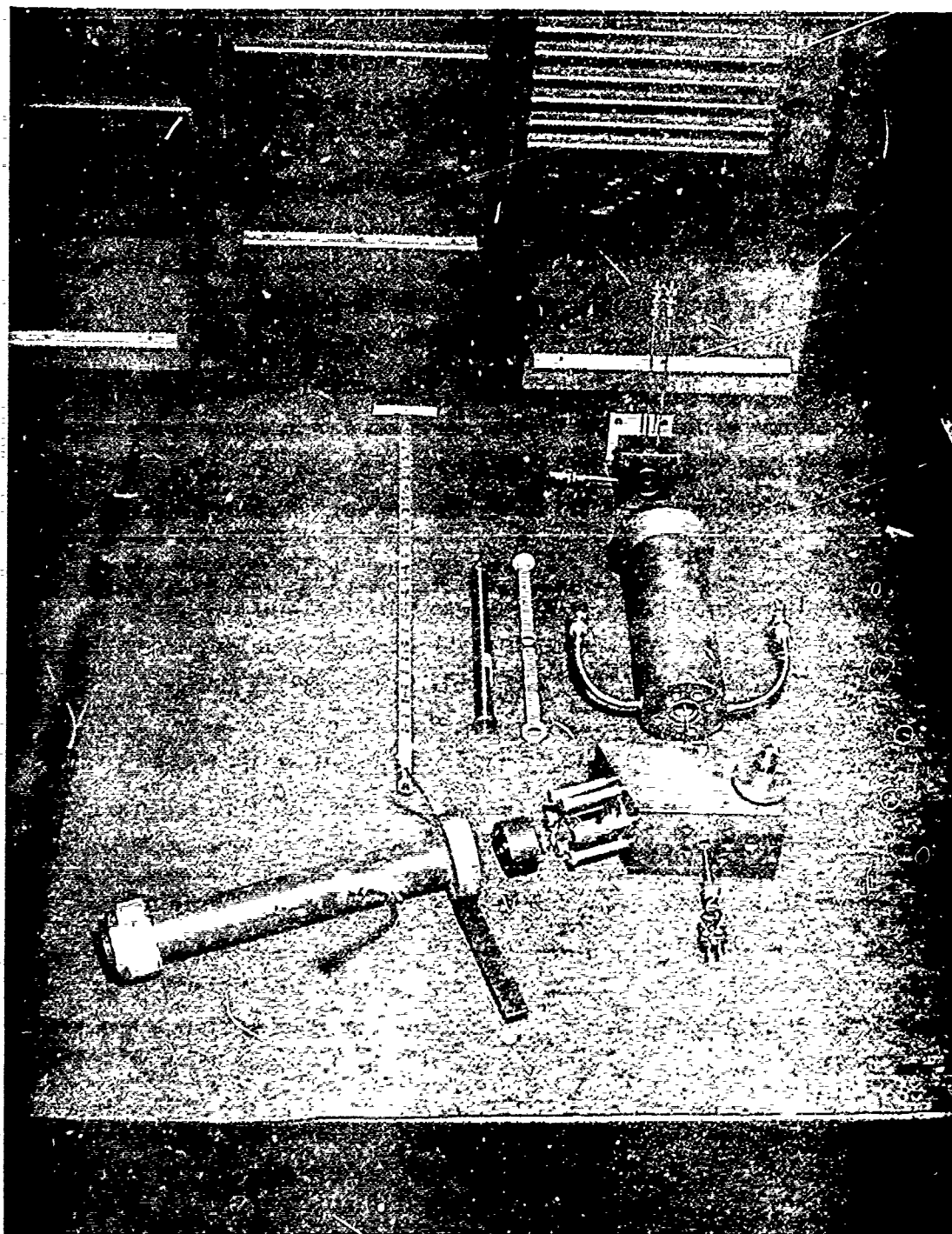


Figure 17. Mini Combustor Disassembled

wall thickness of 0.020 inches. There is a mounting flange at one end of the liner and three positioning clips at the other which help to center the inner liners within the outer liner. The liners are fabricated from a refractory tantalum base alloy, WC-222, available from the Wah Chang Albany Corporation. The alloy is 90 percent tantalum and 10 percent tungsten and was chosen for its high temperature strength and good machining and welding qualities. It retains acceptable tensile strength above 3400°F. The entire surface of the liner is coated with a 2 to 4 mil thickness of hafnium silicide for resistance to oxidative attack by oxygen itself, carbon dioxide, or even nitrogen. This coating was applied with a slurry technique by the Vac-Hyde Corporation and had been previously successfully employed in oxidizing atmospheres to 3400°F. The coating brings the wall thickness to 0.024 to 0.028 inches. A photograph of one of the liners is given in Figure 18.

The outer liner is subject to much lower temperatures and is constructed of 304 stainless steel. It is 11.65 inches in length, has a 0.875 outside diameter and 0.049 inch wall. A mounting flange is welded to one end and positioning clips at the other end to help center the tube in the bore of the chamber. The inner wall of the liner is gold coated to present a highly reflective surface to the radiation from the inner liners.

The upper inner liner is mounted flange upward, by clamping the flange between the chamber and the injector in a close fitting counterbore in the body of the chamber. The lower inner liner is mounted flange downward, by clamping the flange between the outer liner flange and the "instrumentation block". The outer liner is also mounted flange downward and is clamped in place between the flange of the lower liner and the chamber body.

The chamber bore itself is 0.98 inches in diameter. Thus an annular space of about 0.062 inches exists between the body of the chamber and the outside of the outer liner; and a second annular space exists between

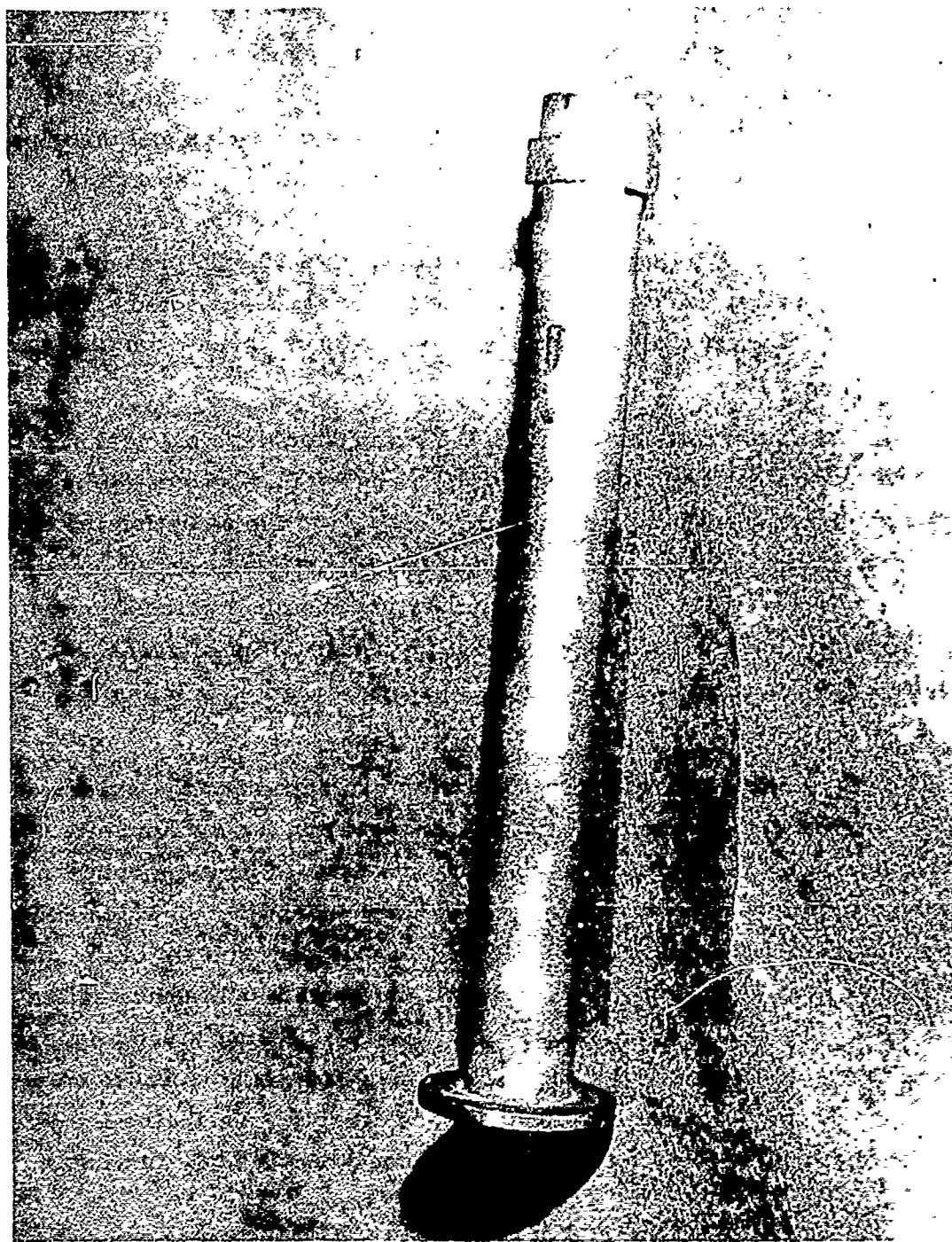


Figure 18. Inner Refractory Liner

the outer liner and the inner liner with a width of 0.062 inches. Through these annular spaces the nitrogen must pass in a folded path before injection into the combustion chamber. It is brought in near the bottom of the chamber, flows upward through the outer annulus to the top, turns  $180^\circ$  and flows downward half way through the inner annulus and then flows into the combustion zone by passing through the gap between the upper and lower liners. The width of this gap is a function of the temperature of the liners and was sized for about a 50 psia pressure drop between the annulus and chamber with the liners at the expected equilibrium temperature. The annular space outside the lower inner liner contains stagnant gas.

Heat transfer characteristics for the combustor were calculated using standard models for turbulent flow in pipes and annular spaces (80). Terms were included for gas radiation by  $\text{CO}_2$ , and the radiation in enclosures between partially reflective walls (81). Transport properties for the gases were calculated from equilibrium chemical calculations of gas composition along with the transport properties of pure gases tabulated by Svehla (82) and the semi-empirical equation of Wilke (83) for deriving transport properties of mixtures.

The calculations are of interest from the standpoint of the expected heat losses from the chamber, and also in revealing the maximum temperatures the hardware might see in combustion tests. The main concern over high temperature, of course, involves the inner liners, which are next to hot combustion gases. The lower liner is downstream of the diluent injection, where gas temperatures are within the safe operating regime of the liners. The desire in this case is for the liner temperature to approach closely the temperature of the gas. The upper liner is adjacent to combustion gases the temperature of which considerably exceeds the limits of the liner materials, and its temperature must be reduced by flowing

the diluent past the outer surface. The temperature of the liner varies with the thickness of the annulus, due to the effect on coolant velocity; and the annular thickness was designed to give wall temperature in the vicinity of  $1800^{\circ}\text{K}$ .

Some of the thermal balances for a nominal case involving a DCFO/ $\text{N}_2\text{O}_4$  combustion are as follows: For a stoichiometric mixture of DCFO and  $\text{N}_2\text{O}_4$  totaling 10 grams per second and a  $\text{N}_2$  diluent flow of 40 grams per second, the heat generated by the reaction is 70 BTU/sec. Of this total, about 12 BTU/second flows to the inner liner by convection and radiation, most of which is passed on to the innermost  $\text{N}_2$  path. About .18 BTU/sec is radiated to the outer liner, assuming its emissivity to be .04 and that of the inner liner to be 1.0. Of the heat picked up by the nitrogen, about 87 percent is retained, and 13 percent passes on to the outer liner. Of this heat, about 80 percent is passed into the outer  $\text{N}_2$  stream and 20 percent deposited on the outer wall of the chamber as total heat loss. Thus, about .3 BTU/sec, or about one half of one percent of the total heat released, is lost to the outer wall. By comparison, the expected heat loss for this section without the liners would be about 20-25 percent of the total heat released.

The lower liner section has similar heat losses. It has lower gas temperature (after mixing) and a stagnant gas between the inner and outer liners. However, there is one less regenerative flow path for the heat to cross and a longer flow path next to the cold outer wall of the chamber. About .5 BTU/sec passes through the walls by free convection and radiation, and only about half of this is returned in the  $\text{N}_2$ . Thus another half of a percent of the total energy is lost in the lower liner section. In the absence of liners, the loss is calculated to be about 18 percent in this lower section.

The figures given above for the various heat loss terms are regarded as very approximate, since they involve a number of idealizations.

However, if they are accurate only to an order of magnitude, they demonstrate sharply reduced heat losses with the refractory liner arrangement. Unfortunately, no combustion tests were accomplished with the configuration for which these calculations were made, due to a realignment of program objectives.

However, a configuration similar in most respects was employed in the combustion experiments with CDI, and this configuration will be discussed next. A schematic of the CDI configuration is shown in Figure 19. The main difference concerns the mid-chamber injection of the CDI. The CDI injector at this point may be thought of as a section of 1/4" tubing, mounted transverse to the combustor axis. A way had to be devised of passing the injector through the liners. Since the inner liners have a gap between them at mid chamber anyway, all that was needed was to widen it by lowering the lower liner. The counterbore in the instrumentation block was deepened, the liner was lowered into it, and a shim was inserted over the flange to restore the clamping action which holds the liner. The outer liner had to be cut into two sections, which were supported independently with a gap between them for the CDI injector. The support for the lower outer liner was unchanged. A mid-chamber "shelf" for the upper liner was provided by counterboring the chamber to the diameter of the liner flange. The liner was lowered onto the shelf and a copper sleeve was lowered onto the top of the flange to clamp the liner into place.

One feature of the arrangement described above is that the upper liners are reversible. That is, either liner may be mounted on the shelf, with the other liner mounted flange upward. This flexibility was deliberate. It permitted a choice between bringing the diluent into the chamber near the middle, as was the case in the original design, or near the injector. Two new diluent channels through the body of the chamber were also

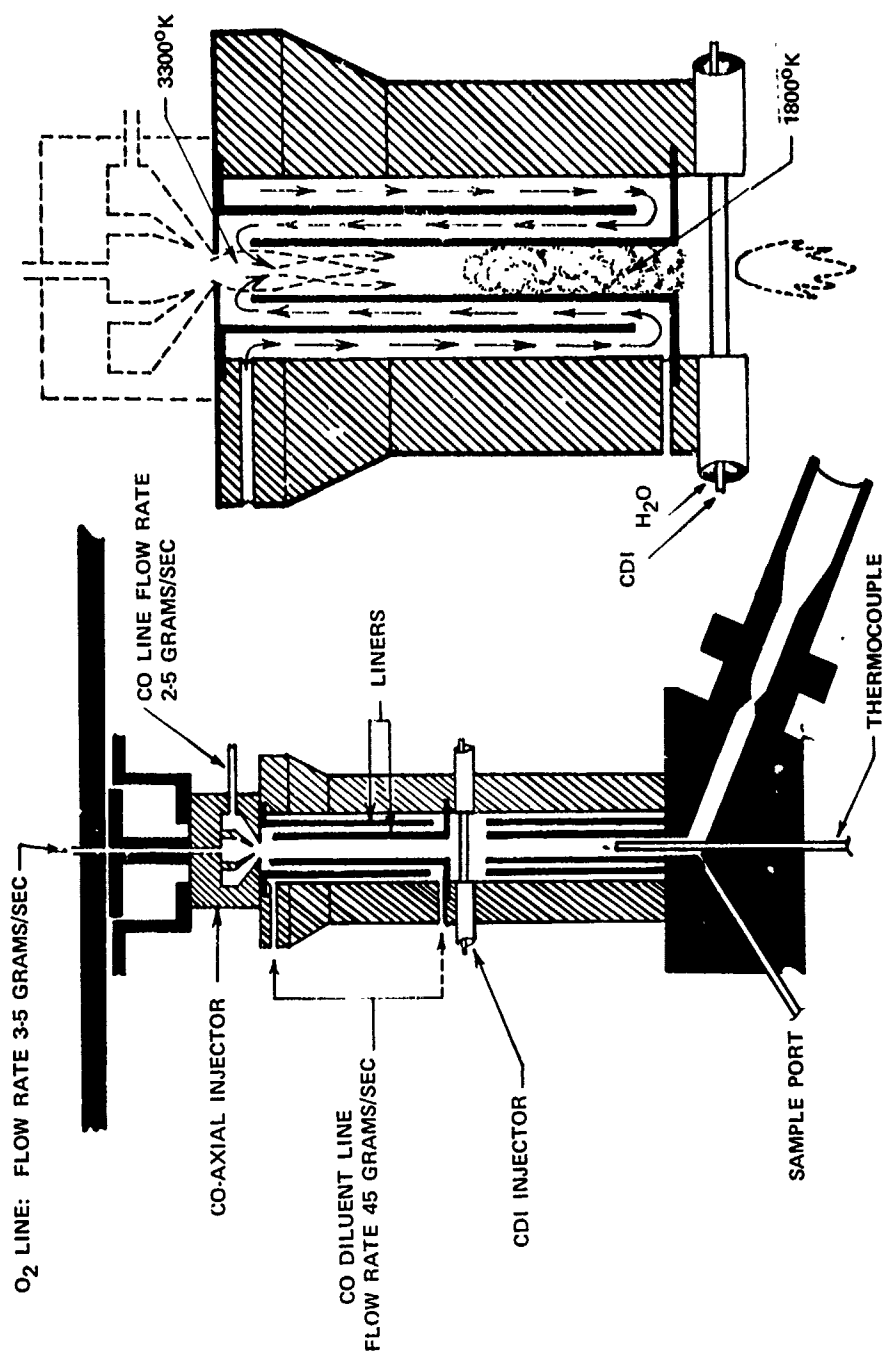


Figure 19. Mini-Combustor CDI - Configuration

provided, one near the middle and one near the tip. The two choices obviously represent drastically different combustor arrangements, each with advantages and disadvantages. The advantage of mid chamber injector is that it avoids deluging the main combustion zone with diluent, which might impede or even quench combustion. The advantage of top injection is that a greater length for mixing is available, and the CDI is thus injected into a more uniform medium. Since there were initially no concrete grounds for a selection, the hardware was built for either mode. Early check-out tests with gaseous  $O_2/CO$  reactants showed that ignition could not be accomplished when the diluent was injected at the top of the chamber. Subsequently this was overcome, and the test program included firing with both configurations.

From a heat transfer standpoint the major difference is that there is no regenerative flow of diluent behind the lower liners (mid chamber injection). An analysis of the heat transfer aspects of the CDI configurations was also accomplished. In this analysis the fuel-oxidizer combination was again  $CO$  and  $O_2$ , the reactants chosen for the CDI pyrolysis studies. The gaseous diluent shown in Figure 19 was included partly to conserve CDI but primarily to cool the liners. As such it was still the major stream. The calculations may be summarized by noting that the heat losses calculated for the entire liner area were between 0.5 and 1.0 percent of the total heat release.

Injectors Two injectors were required for the CDI combustion tests: (a) a gas-gas injector, burning  $CO$  and  $O_2$  to establish the main combustion zone, and (b) a liquid injector for mid-chamber injection of the CDI.  $CO/O_2$  INJECTOR: The project had already built a gas-gas injector for baselining (check-out) the original combustor, and this injector was



modified for use in the CDI series. The design operating conditions were as follows:

$$\dot{W}_{CO} = 2.5 \text{ gm/sec}$$

$$\dot{W}_{O_2} = 5.0 \text{ to } 7.0 \text{ gm/sec}$$

$$P_c = 300 \text{ psia}$$

The configuration used during these experiments is shown in Figure 20. The gaseous  $O_2$  was injected through the control orifice as a high velocity, sonic stream. The gaseous CO was injected at low velocity through an annulus surrounding the central  $O_2$  jet.

The modifications made to the injector were based on the data in Ref. 86 which gives turbulent mixing data for an axisymmetric jet injected into a secondary stream with a differing velocity but equal temperature and density. Because the molecular weights of CO &  $O_2$  are 28 and 32, respectively, it was assumed that the equal density assumption was a valid approximation. Data from the reference show that mixing is dependent upon the velocity ratio of the two jets. Because the prior configuration made it impossible to modify the  $O_2$  orifice diameter without extensive and timely machining, the original  $O_2$  orifice was maintained. The original .029 inch orifice diameter resulted in the  $O_2$  having a sonic injection velocity of 1100 ft/sec, assuming an inlet temperature of  $100^\circ\text{F}$ . Figure 21 shows the predicted inlet pressure as a function of  $O_2$  flowrate assuming sonic flow. It can be seen that this assumption is valid for  $O_2$  flowrates greater than approximately 4.2 gm/sec for the design chamber pressure of 300 psia.

Since the  $O_2$  injection velocity was fixed, the degree of mixing, and hence combustion efficiency, was controlled by the CO injection velocity.

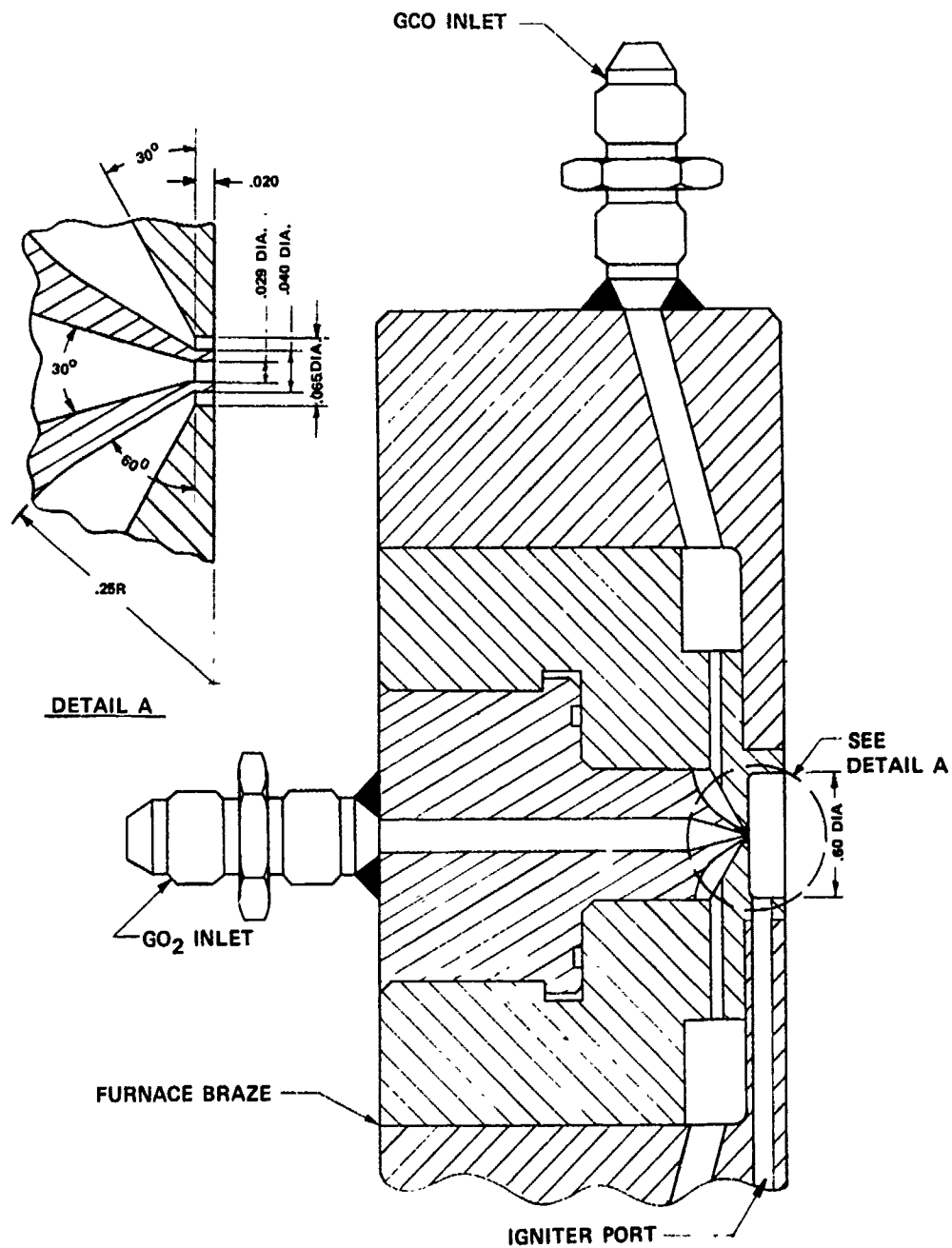


Figure 20. Gaseous  $O_2/CO$  Coaxial Injector  
84

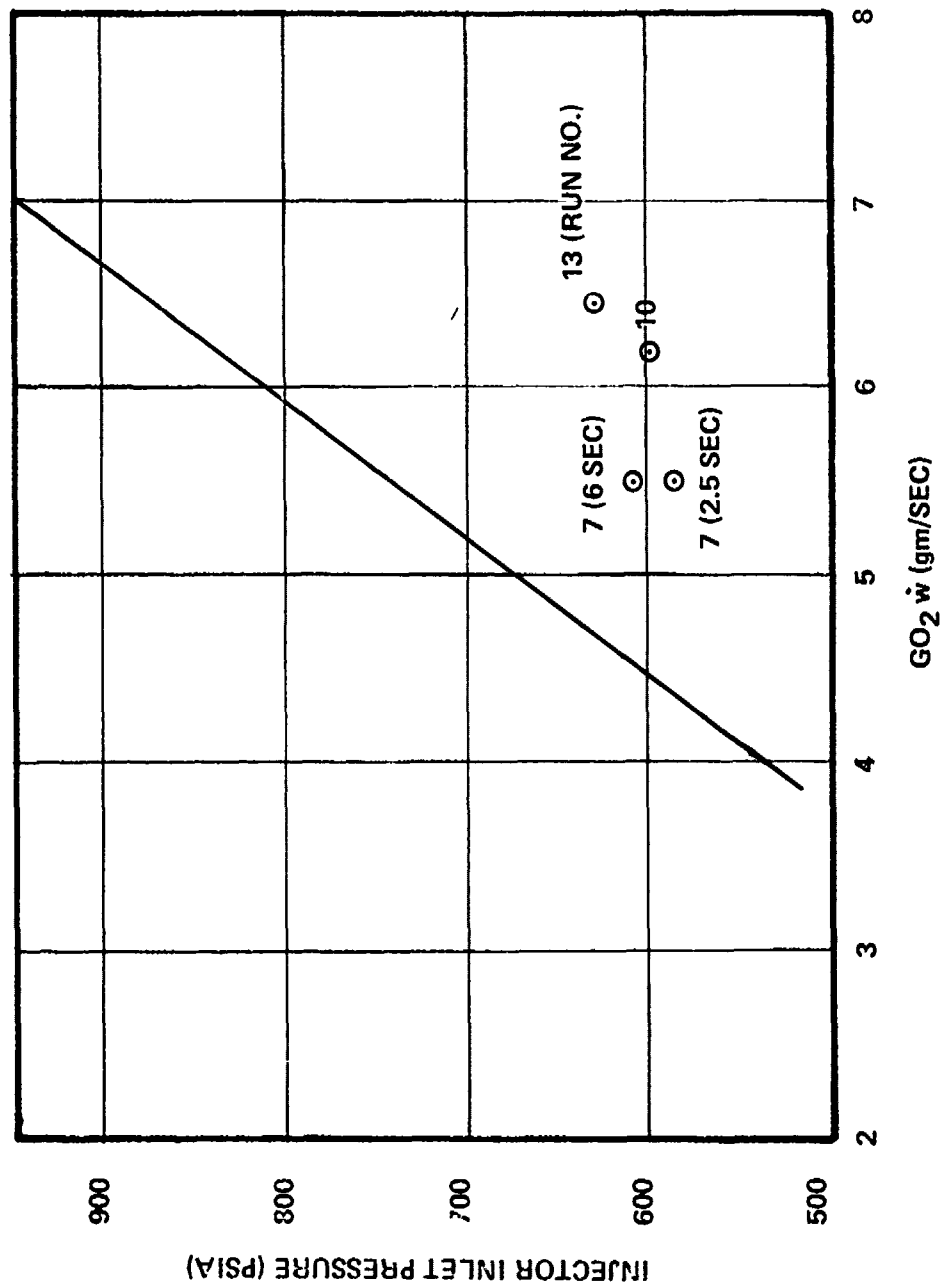


Figure 21.  $\text{GO}_2$  Inlet Pressure vs. Flowrate

Because it was anticipated that the large CO diluent flowrate injected at mid chamber, which dropped the combustion temperature from approximately 2800°K to approximately 1800°K, could effectively quench the CO/O<sub>2</sub> reaction, it was desirable for the mixing to be complete as possible within six inches even though the total chamber length to the thermocouples and gas sample ports was twelve inches. For an additional safety factor, a design goal of complete mixing by three inches was selected. Figure 22 shows the calculated centerline O<sub>2</sub> concentration at both three and six inches as a function of CO injection velocity. As can be seen, the centerline concentration is relatively insensitive to CO velocity but does decrease with lower CO injection velocities.

The injector was modified by enlarging the CO annulus to decrease the CO injection velocity as much as possible. Figure 23 shows the injector inlet pressure as a function of the CO annulus outer diameter for the design chamber pressure of 300 psia, as well as several other pressures which are representative of the actual chamber pressures without and with CDI injection. Even though the CO flowrate is controlled by a sonic nozzle flowmeter and therefore is not sensitive to injector pressure drop, it was desirable to maintain feed system stiffness downstream of the sonic nozzle. A rather arbitrary but commonly selected value of 10 percent of chamber pressure was selected for the CO injection pressure drop. This resulted in an outer diameter of .065 inches for the design chamber pressure. The corresponding injection velocity is approximately 400 ft/sec which gave a calculated centerline O<sub>2</sub> concentration of 68.6 and 67.2 percent at three and six inches, respectively, compared to a fully mixed value of 65.8 percent.

Figures 21 and 23 also show the actual injector inlet pressures measured during the tests. The lower than calculated values for the O<sub>2</sub> and the higher values for the CO gave strong evidence that the injector

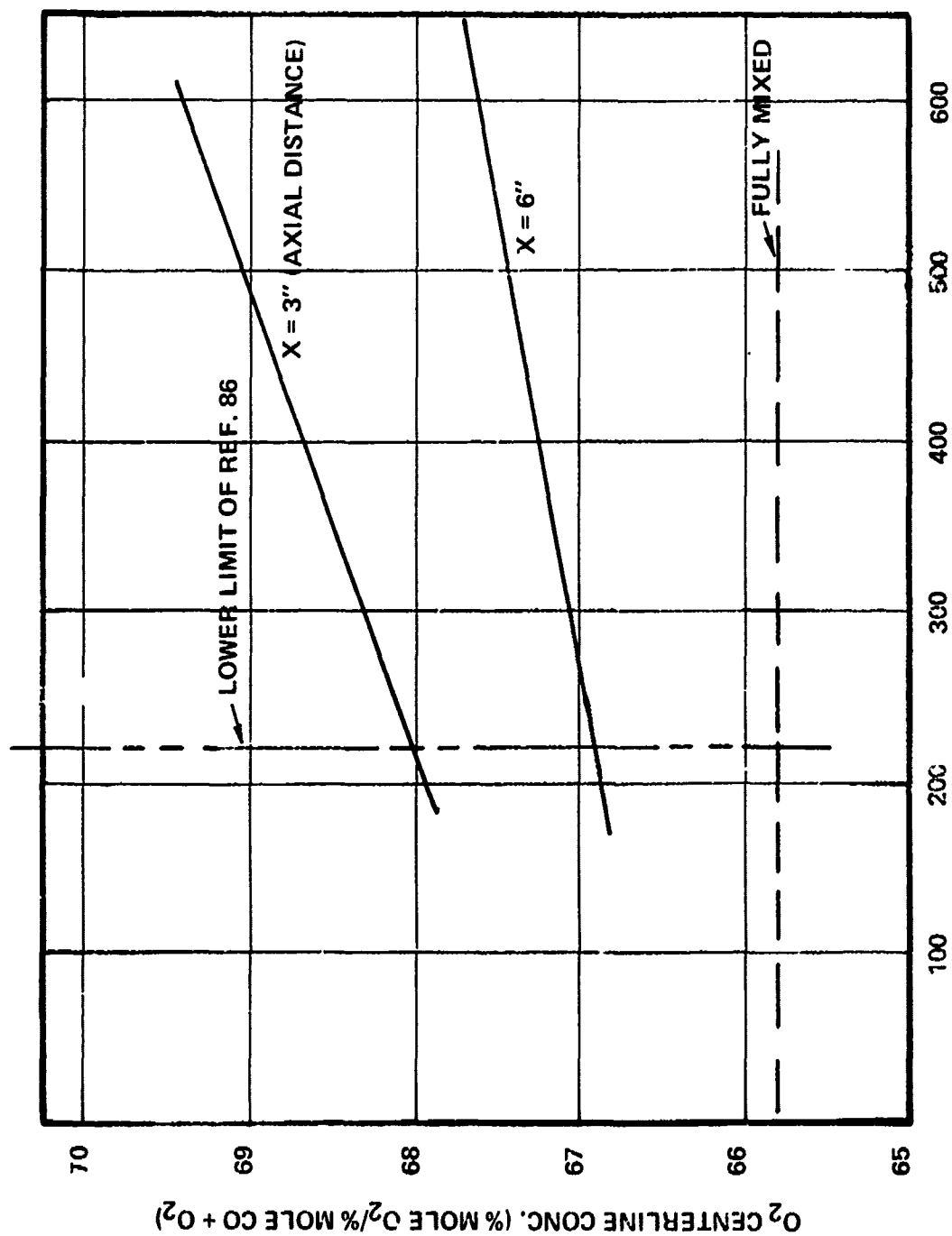


Figure 22. O<sub>2</sub> Concentration vs Injection Velocity

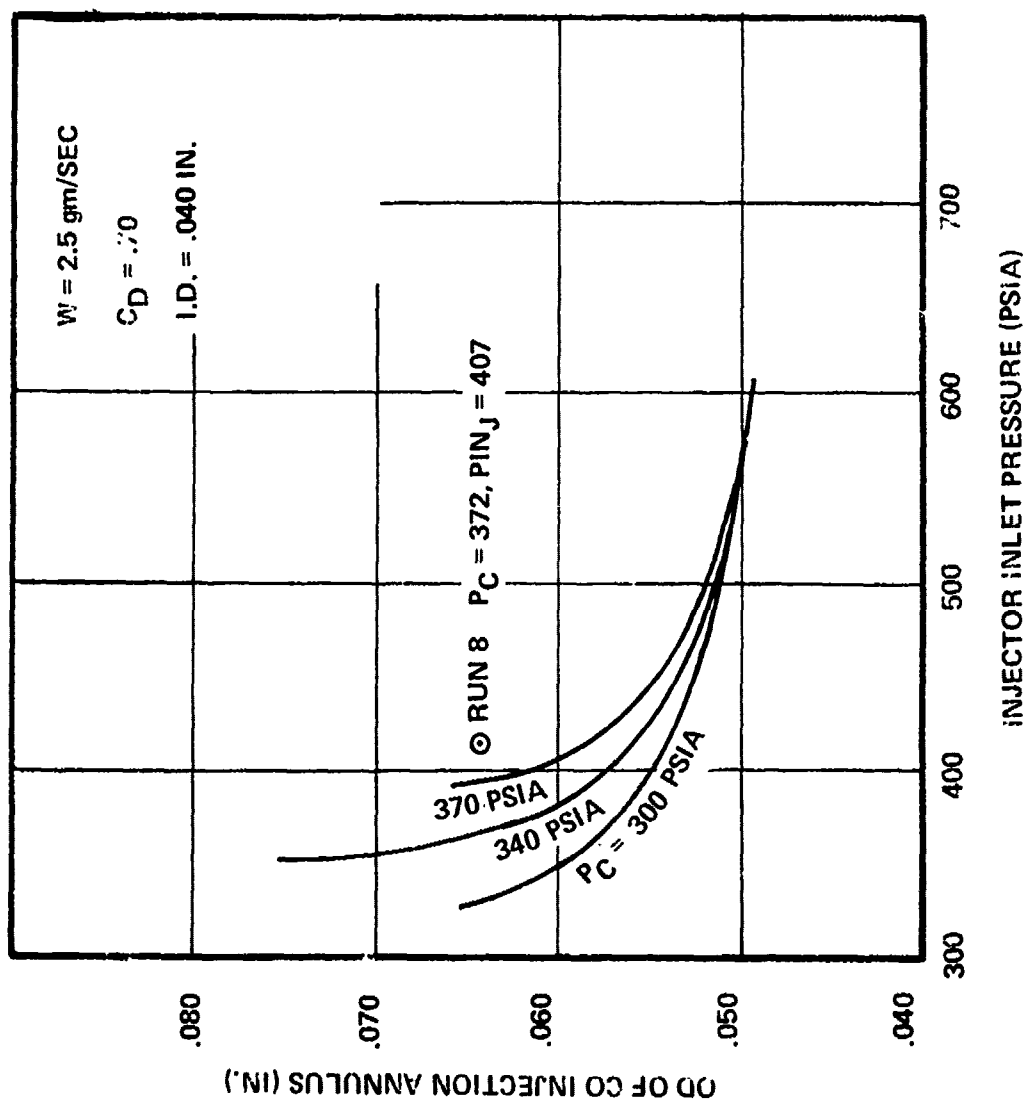


Figure 23. CO Injection Annulus O.D. vs Inlet Pressure

had been damaged internally. The injector was therefore disassembled. Figure 24 shows the burnt  $O_2$  pintle that resulted in an enlarged  $O_2$  orifice diameter which is reflected in the low inlet pressure. Apparently, the higher than calculated CO inlet pressures were caused by an unknown percent of the  $O_2$  being injected laterally into the fuel upstream of the CO annulus. Because of uncertainties in the amount of  $O_2$ , the CO annulus area, and the density of mixed and partially combusted gas mixture, it is impossible to quantitatively calculate the detrimental effect that the burnt  $O_2$  pintle had on mixing. However, these effects should have resulted in some deterioration in injector performance.

CDI Injector: The CDI was injected at mid-chamber into what was ideally a completely mixed and reacted hot gas stream. The purpose of the CDI injector was only to provide a uniform mass flux spray field with very small droplet diameters, the small droplet diameter being desirable to insure complete CDI vaporization and decomposition prior to obtaining gas sampling and temperature measurements. Again the small flowrate, the design flowrate being 10 gm/sec, made the problem more difficult. The design approach selected was a single spray cone located on the chamber centerline. The spray cone design was advantageous both because it increased the orifice diameter by decreasing the effective discharge coefficient and maximized the circumferential mass uniformity. Because of the low flowrate no mechanical swirlers were readily available, therefore a hydraulic swirl cup was used to form the hollow cone spray. The high gas stream temperatures, 1800-2800°K, required the whole injector to be water cooled. Figure 25 shows a sketch of the injector. The swirl cup and its 1/8" copper tubing feedlines were located inside thin walled 1/4" stainless steel tubing and welded in place. The annulus between the 1/8-inch and 1/4-inch tubing providing the water cooling circuit. The tubing was inserted through the chamber walls and located so that the swirl cup outlet nozzle was located on the chamber centerline. A photograph of the injector is shown in Figure 26.



Figure 24. O<sub>2</sub> Pintile; Post Firing



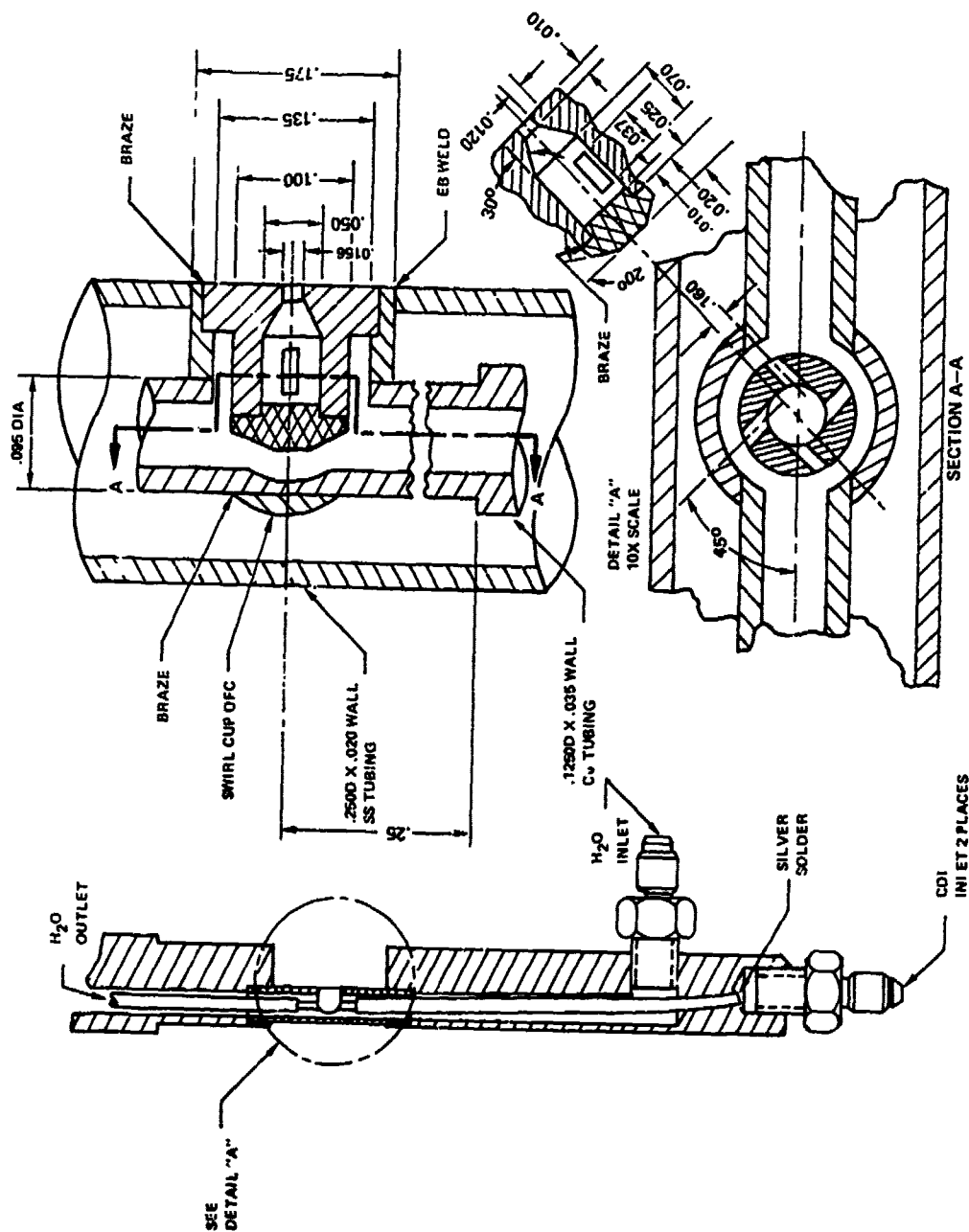


Figure 25. Section Drawing of CDI Injector

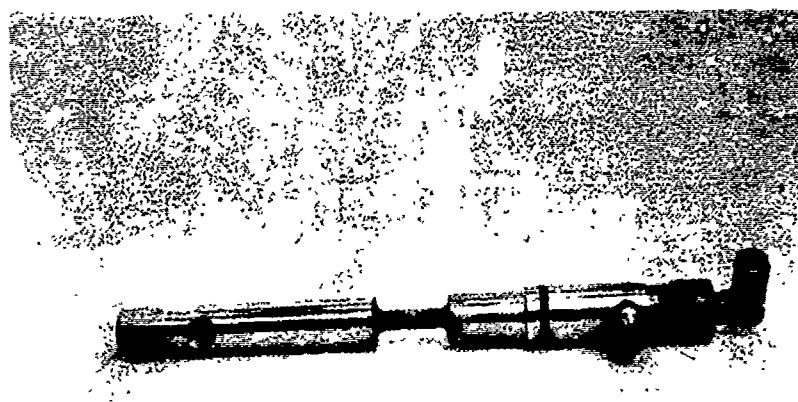


Figure 26. CDI Injector Assembly

The swirl cup design was based upon empirical correlations that the Russians developed during their research into this type of injector. A computer program discussed in Ref 85 was used to design the swirl cup. This program calculates the swirl cup's physical dimensions and maximum droplet size based upon the flowrate and desired pressure drop, the swirl chamber to nozzle diameter ratio, desired cone angle, and the propellant physical properties. The desirability of small droplet diameters require large swirl cup pressure drops which in turn result in small swirl cup dimensions. Figure 27 shows these relationships. A pressure drop of 600 psia at the design flowrate was finally selected. A spray cone angle of  $30^\circ$  included angle was chosen because it provides approximately 1.1 inches axial distance before the spray impinges on the chamber wall, and the maximum droplet size is slightly smaller than for larger angles. For spray angles much below this value, the spray cone becomes ill defined and non-uniform. Four rectangular inlet orifices were also selected to maximize uniformity of the small spray cone and to minimize the swirl chamber diameter. Figure 28 shows the water flow characteristics of the two injectors used during the testing. Figure 29 shows a typical spray cone during water flows.

A detailed heat transfer analysis was conducted of the injector water cooling circuit. Data from Ref 80 gave an average gas side film coefficient of  $.0015 \text{ BTU/in}^2\text{-sec } ^\circ\text{F}$ . Using this value, a water outlet and gas side wall temperatures of  $82^\circ\text{F}$  and  $600^\circ\text{F}$ , respectively, were calculated for a water flowrate of  $.2 \text{ lb/sec}$ . A hydraulic analysis of the cooling circuit gave a pressure drop of 30 psid for the same flowrate. Figure 30 shows the coolant circuit calibration for one of the two injectors. Since the coolant outlet temperature was not recorded during the tests, no quantitative measure of the thermal environment was obtained, but the excellent condition of the injector following the tests proved the adequacy of the water cooling.

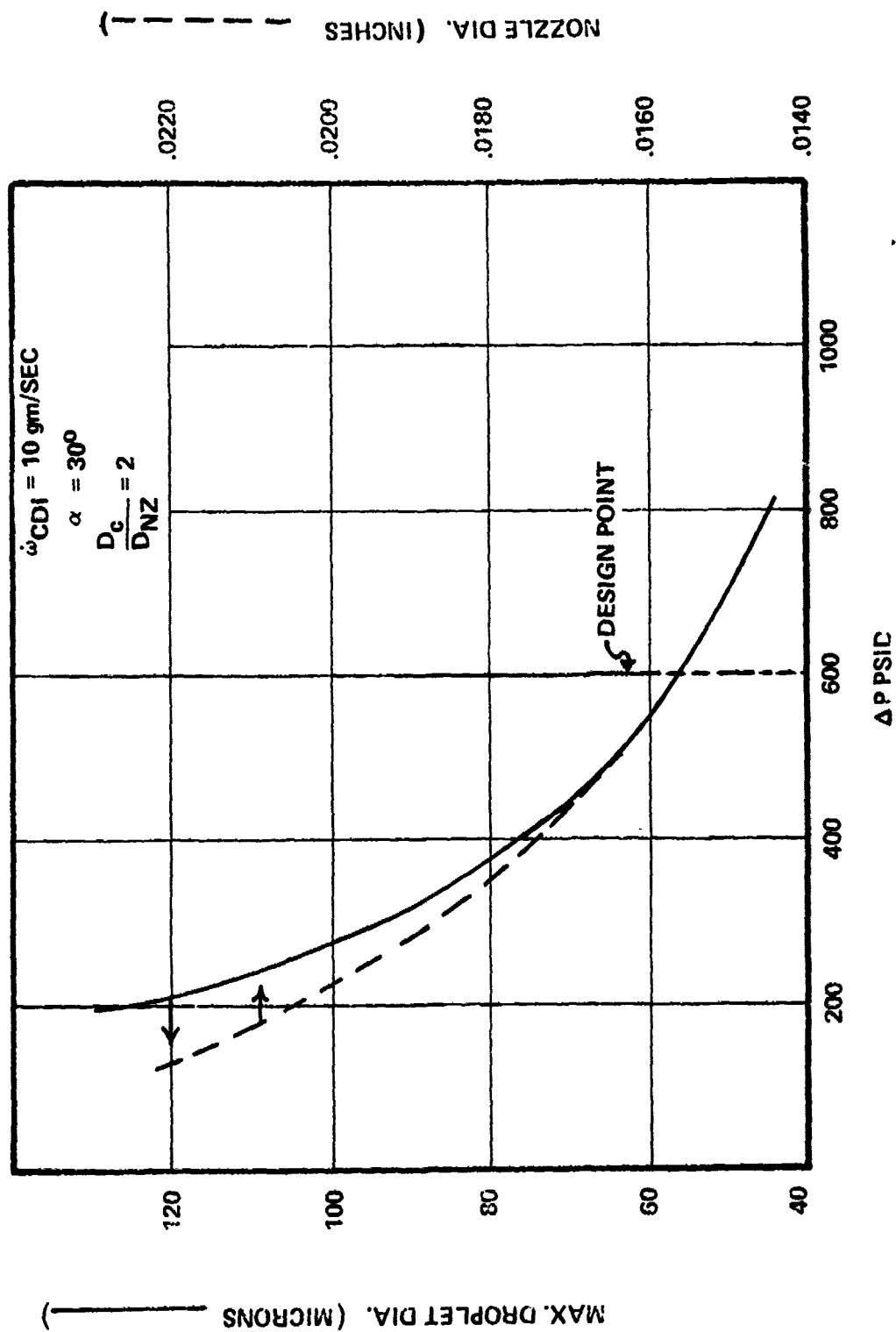


Figure 27. Droplet Size & Nozzle Diameter vs DP, CDI Injector

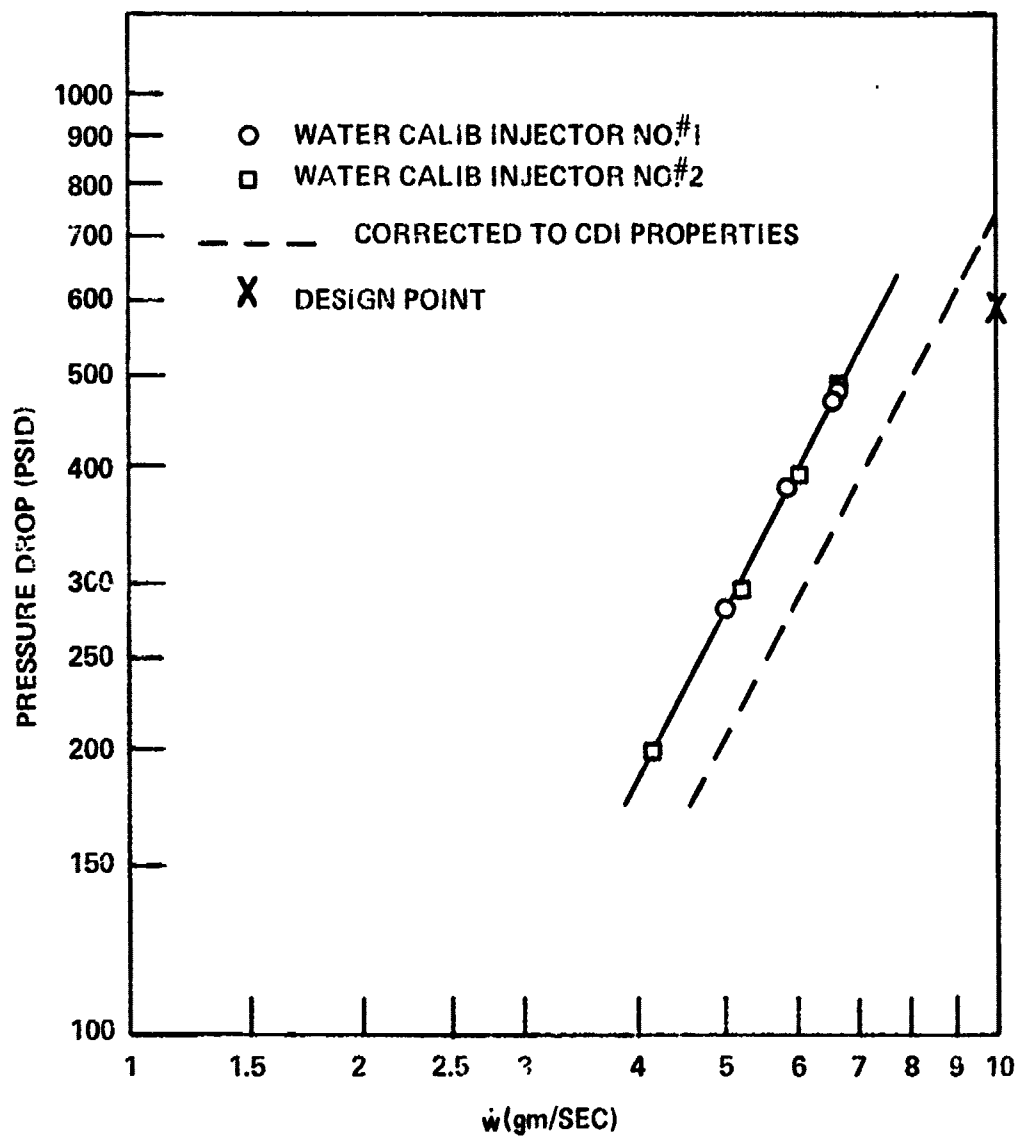


Figure 28. Water Flow Pressure Drop  
vs  
Flowrate CDI Injector



Figure 29. Water Spray From CDI Injector ( $\Delta P = 700$  psid)

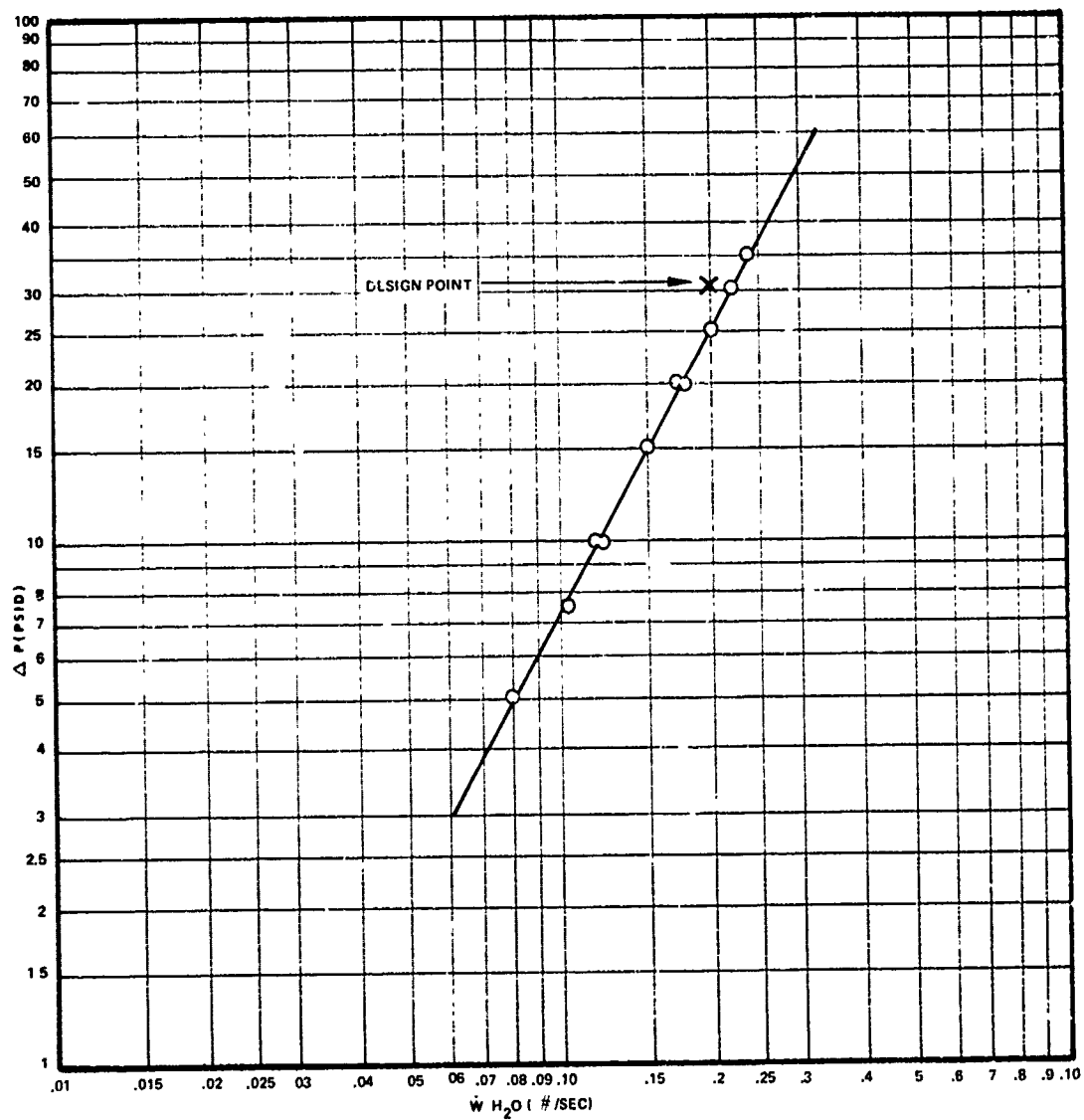


Figure 30. Pressure Drop Through Water Coolant Circuits, CDI Injector

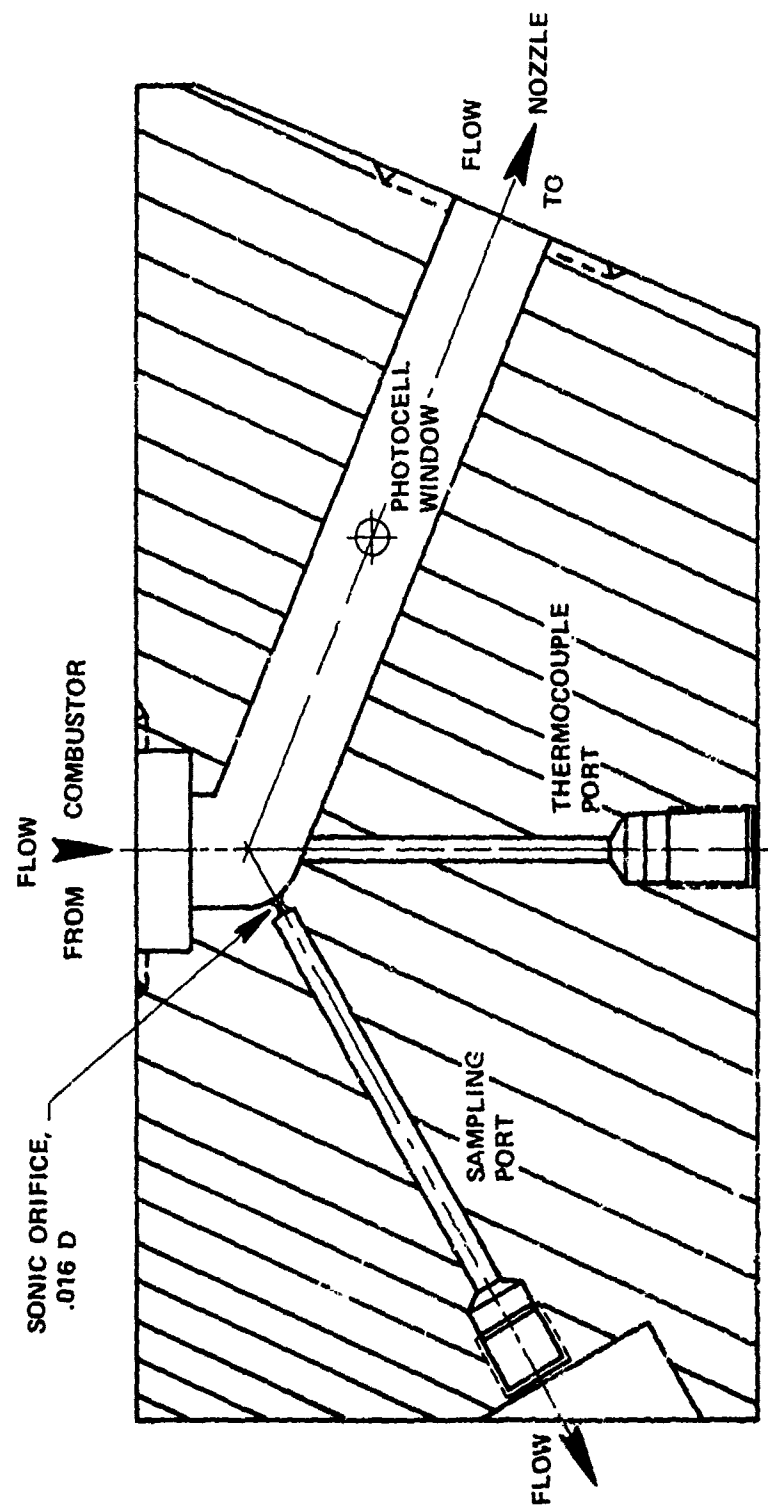
Instrumentation Block The combustion and mixing are intended to occur in the upper chamber. The instrumentation block is an extension of the chamber, uncrowded by refractory liners, where various instrumentation and sampling parts may be conveniently located. These include a thermocouple, a pressure transducer, a window for the photocell, and a gas sampling orifice. Each of these will be described in detail in later sections, and only general comments will be given here. The instrumentation block is constructed of oxygen-free copper and operates as a heat sink during firing. A spray of cooling water is directed onto the outside of the block during and after firings, to allow multiple firings without accumulating excessive heat and also to carry away heat before it can soak into the heat sink blocks that the photocell is mounted on. Approximately 15-20 percent of the heat of the reaction is calculated to be transferred to the instrumentation block, which will raise its temperature about 5 degrees Fahrenheit per second of firing. A schematic of the instrumentation blocks is given in Figure 31, and a photograph showing the chamber and instrumentation blocks installed is given in Figure 32.

Nozzle An exchangeable set of nozzles with various throat areas was fabricated. Nozzles were machined from copper bar and operated as a heat sink. The throat diameters available were 0.111, 0.172, 0.188, 0.203, and 0.208 inches, although only the last two were actually employed. The total nozzle area also included a small contribution from the sampling orifice of .0002 square inches.

#### Catch Tank

Downstream of the nozzle was a duct containing an internal cooling spray of water, discharging into a 500 gallon catch tank. The tank was capable of capturing the contents of a full firing in the event unfavorable winds prevented a direct discharge to the atmosphere. The nature of the exhaust was unknown, but was assumed to be potentially toxic.





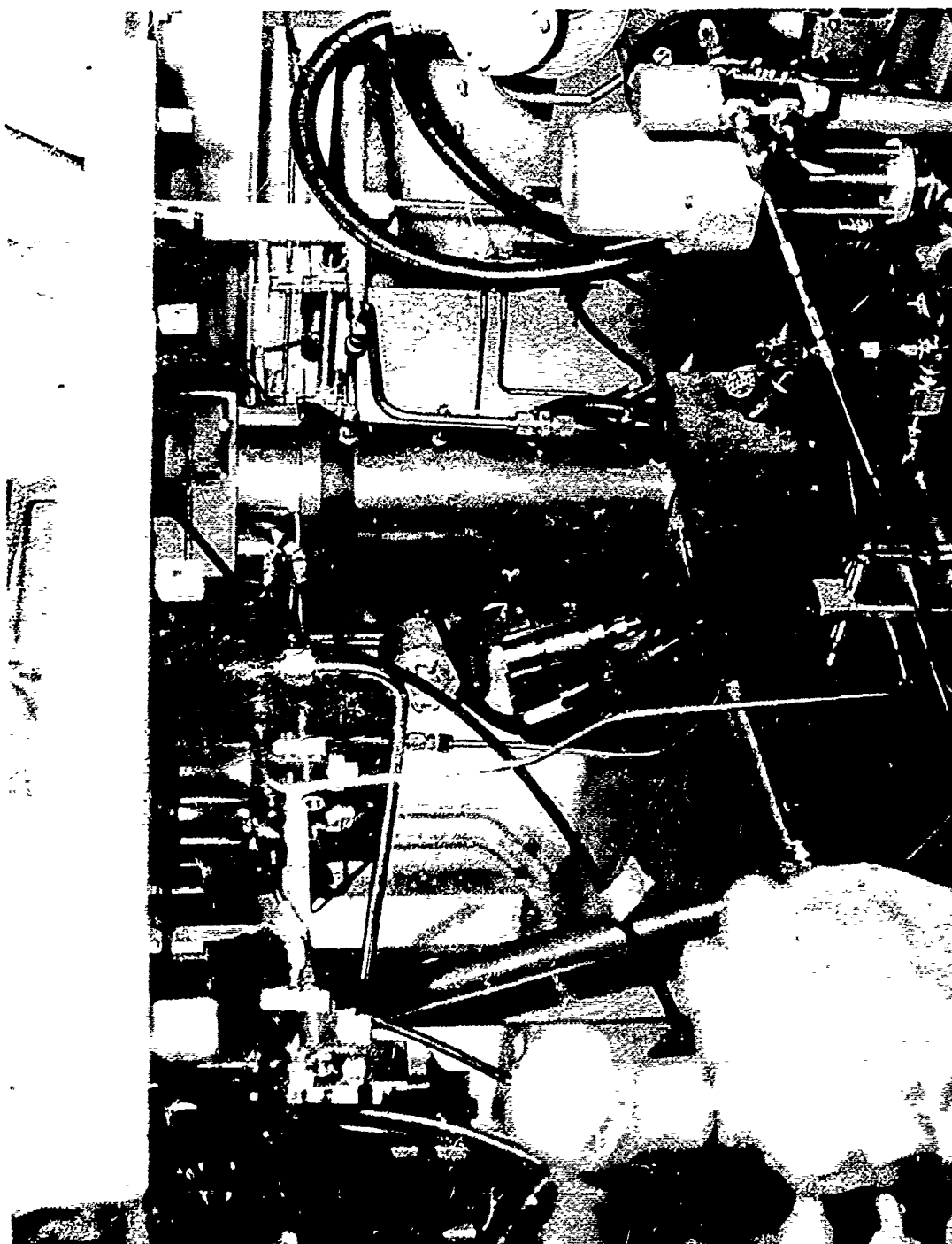


Figure 32. Chamber and Instrumentation Block Installed.

### Liquid Feed System

The design of the feed system was originally for fuels studies and was influenced by two main considerations. One was the fact that most of the fuels of interest were not ambient liquids, but low melting solids. The other was the low flow rates decided upon. Since the fuels were to be used in a liquid injection scheme, the feed system had to be heated above their melting points. This was accomplished by immersing portions of the feed system in a thermostated water bath. This included the fuel storage tank, run cylinder, transfer lines and valves, run line, and prop valve. The injector itself was outside the bath, but in the case of DCFO, had channels which circulated temperature conditioned water from the bath via concentric tubes around the fuel line. Since the only material tested in the facility, CDI, is an ambient liquid, this capability was never employed.

The most commonly employed device for controlling and measuring liquid flow rates in rocket engines is perhaps the cavitating venturi. Over a wide range of conditions the flow rate through a cavitating venturi is independent of the downstream pressure, as a consequence of the throat pressure remaining fixed at the vapor pressure of the fluid. For very low vapor pressure fluids it is difficult to assure cavitation, and if cavitation occurs it is less certain to be due to vapor pressure and may be due to release of dissolved gases. To this problem we may add the low flow rates of the present application, which would require a throat diameter of 0.002 - 0.003 inches. This was not deemed a promising approach, in view of the extreme machining tolerance and the potential for plugging.

The method adopted was a piston-cylinder positive expulsion device. Like the cavitating venturi, positive expulsion offers a way of both controlling and measuring flow rate and can be made very insensitive to

back pressure. Furthermore, there is no need for pre-knowledge of vapor pressure, making it a more general tool. And of course there is no need for a small restriction in the line. There is a disadvantage in mechanical complexity, however.

A schematic of the system is shown in Figure 33. The device is powered by an induction motor developing  $3/4$  HP at a full load speed of 1725 R.P.M. The motor operates through a gear box with an 8.75/1 ratio and a clutch-brake assembly turning a precision  $3/4$  inch ball screw with a 0.250 inch lead. The ball screw is pre-loaded for zero back-lash and is accurate to 0.0005 inch/ft. Since the motor is a constant speed device and the gear box and lead screw provide a constant ratio, an additional element must be included to allow variation of piston speed. This provided by an adjustable ramp which bears against a roller mounted at one end of a 2 inch push rod. The ramp is mounted in journals on a carriage that slides in two parallel 2 inch support shafts at right angles to the axis of the piston. The ramp angle is adjusted with positioning nuts on a threaded shaft connected between the ramp tip and the carriage, and the ramp angle is measured with a vernier protractor. The carriage is translated at about 51 inches per minute by the ball screw. Allowance is made for about 0.5 percent slip in the motor at the expected loading for a typical run, and the probable uncertainty in the slip is less than this, typically around 0.25 percent.

The expulsion cylinder is chrome plated 304 stainless steel with a 1.000 inch bore. The piston rod is also chrome plated stainless steel with a 0.937 inch diameter. The sealing member is a teflon cap snapped over a retaining groove at the bottom of the piston. The bottom of the piston is concave upward to collect any trapped bubbles at the center of the piston, where a  $1/16$ " bore rises through the piston rod to an outlet to aid in their expulsion. This concern over bubbles, and where their bouyancy

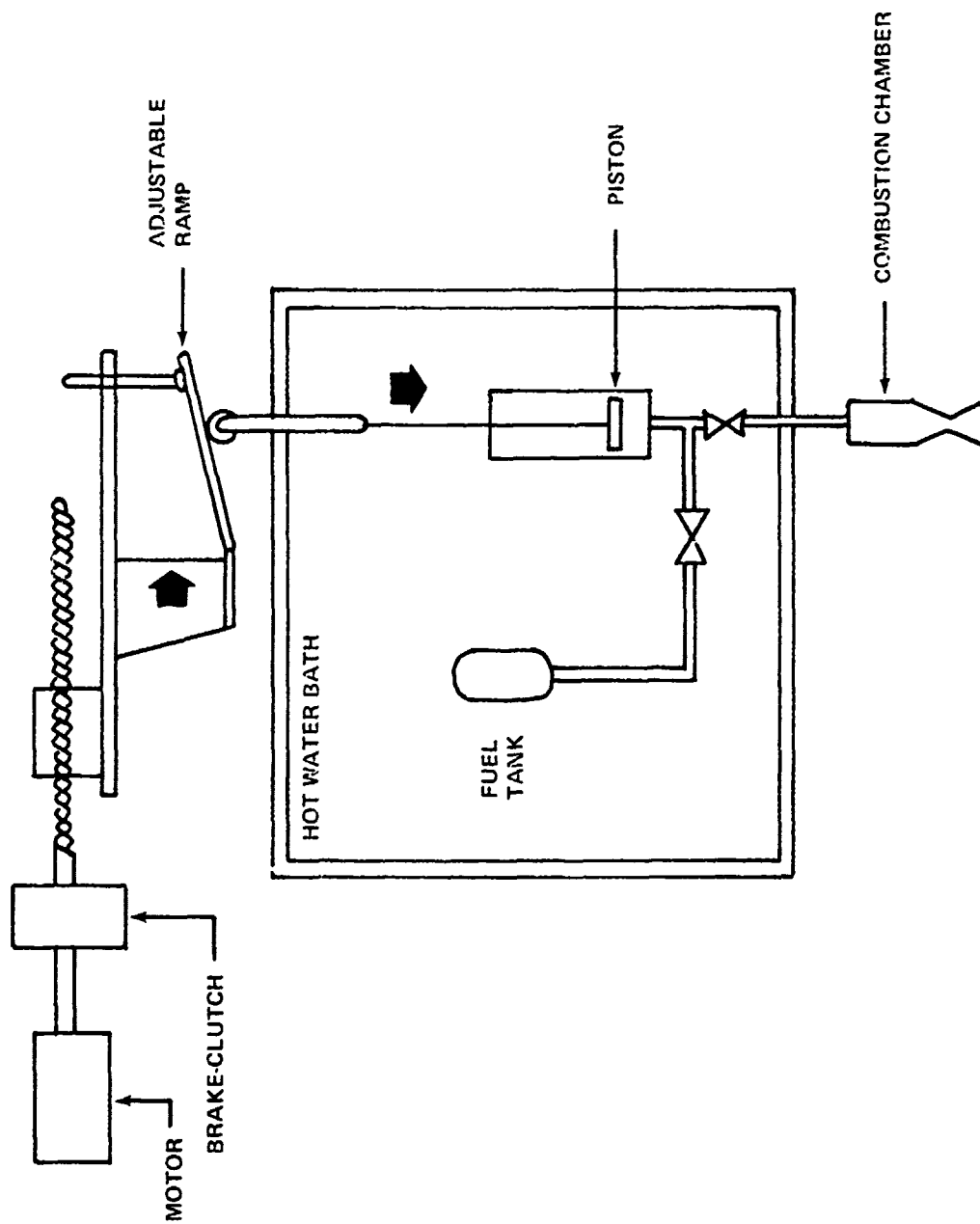


Figure 33. Positive Feed Mechanism

might trap them, was prompted by the assumption that a "soft" piston would not yield accurate flow rates.

The flow rate for a given run is calculated from the cylinder area, the piston speed, and a knowledge of propellant density. The piston velocity may be calculated from the motor speed and the various mechanical ratios. In addition it is measured directly by a linear voltage differential transformer (LVDT) position sensor actuated from the push rod.

The system was built for bipropellant operation and includes two pistons and cylinders mounted on opposite sides of a steel plate that forms the back wall of the fuel bath. The carriage is provided with a pair of independently adjustable ramps, and it is useful to note that the mixture ratio is a function of the two ramp settings and is independent of carriage speed.

The original intent was to fill the run cylinder with fuel or oxidizer directly. When the program was aligned to study CDI, the oxidizer cylinder became superfluous and was not used. Filling the fuel cylinder with CDI was regarded as risky, since only a small amount of CDI polymer might cement the piston and cylinder together. A revised procedure was devised in which the cylinder was filled with mineral oil, and this was used to displace the CDI from a specially designed tank, and into the combustor.

The CDI tank was designed to hold 27 cc of CDI (38 grams), or enough for only a single firing. The CDI was loaded into the tank from storage in a dry ice chest immediately before a firing. It was necessary to face both the inlet and the outlet of the CDI tank upwards. The inlet needed to face upwards since the mineral oil is lighter than CDI, and would rise through it if brought in through the bottom. The outlet needed to face upwards, since an ullage was needed to allow for CDI expansion during warmup. It was desired that this ullage not be on the inlet side since it would constitute an air "cushion" throughout the firing and compromise the flow

rate measurement. The tank design which best met these requirements was simply a section of tubing bent into a "U" and with an isolation valve at each end. Actually two sets of tubing were used, half inch for the main tank and 1/8" for the outlet leg. This minimized the volume in the section where an inversion of mineral oil and CDI might occur during the last stages of expulsion. This possibility arises because the mineral oil becomes the bottom layer after it reaches the bottom of the tube and starts around the "U". The condition of the final cc of CDI is thus not known.

The loading of the CDI tank was accomplished under dry nitrogen in a hood. One feature of the tank design and the loading procedure which helped assure a uniform charge was that the outlet valve was located above the inlet fitting. The CDI was funneled into the inlet fitting until it almost overflowed. Then the inlet valve was closed and the excess was poured back into the container from the fitting of the inlet valve. This assured both that no gas was on the inlet side and that an ullage existed in the outlet leg above the inlet fitting. With the position of the ullage thus controlled, it was possible to evacuate the ullage without fear of pressure in the inlet leg forcing the CDI out.

The CDI circuit included a flush system by which a mixture of acetone and methylene chloride is used to purge the tank lines filter and injector after a run.

#### Gaseous Reactant Feed System

For the CDI studies carbon monoxide and oxygen are used to establish a flame into which the CDI is injected. The flame is cooled to typical GDL temperatures with a diluent consisting of carbon monoxide and 3.5 percent hydrogen. The method employed for measurement and control of these gaseous reactants is conventional. The reactants are stored in the size 1A cylinders in which they were delivered. A hand loaded pressure regulator controls the pressure upstream of a sonic orifice. The prop valve is immediately downstream of the control orifice and is a two way remotely controlled valve which passes reactant to the chamber when in one

position and passes a purge gas to the chamber when in the other position. The fuel and oxidizer flow rates are low enough to be supplied by a single bottle of each reactant. The diluent flow rate is much larger, and three storage bottles are ganged together. The sonic orifices are mounted in special fittings and have flow straightening sections upstream and downstream. Orifice discharge coefficients were measured in these standard sections as a function of Reynolds number under a contract to the National Bureau of Standards.

### Igniter

The igniter consisted of a bit of solid propellant "igniter paste" smeared on a loop of fine (#20) nichrome wire strung through a 1/16 inch double bore alumina insulator tube. The outer end of the tube was sealed with RTV rubber cement. The tube was inserted into the chamber through a small hole in the injector and held in place with a compression fitting. Each tube was good for a single ignition, but the tubes were easily fabricated, inserted, and removed. A thin (1/4 inch) igniter plate was fabricated for use with injectors for which no separate provision for igniter insertion was made. The external igniter circuit consisted of a DC power supply with up to 30 volts output and a "Silicon Controlled Rectifier" (SCR) actuator for remote operation.

### Instrumentation

Gas Sampling and Temperature Probe. Early in the CDI firing series the sampling system underwent a change in probe location. Originally the sampling orifice consisted of a 0.016 inch diameter contoured nozzle machined into the sidewall of the bend in the flow field (see Figure 31). The degree to which this location represented the average flow condition was called into question by the results of the first two CDI firings, and a new arrangement was devised which combined the gas sampling and temperature probes. The thermocouple originally used had a 1/8" inch



sheath and projected from the instrumentation block and into the upper chamber along the centerline (see Figure 31). The bend in the flow in the instrumentation block was, in fact, done to permit a centerline probe without bending the thermocouple or bringing it in through the nozzle. For the combined gas sampling and temperature probe, the drill hole through the instrumentation block was widened to accept a 1/4 inch probe. A schematic representation of this probe is shown in Figure 34. The proportions of the drawing are greatly distorted for pictorial clarity. The copper rod is 0.25 inches in outside diameter and contains three 0.066 inch drill holes equally spaced around the tube axis. Two of the holes are drilled through and conduct two 1/16 inch diameter thermocouples into the chamber. The third hole is drilled to within 0.1 inches of the chamber end, and completed with a 0.016 inch hole which serves as the orifice for the gas sampling probe. The thermocouples and sampling line are silver soldered to the copper rod at the outside end. The chamber end of the copper rod has a step reduction in diameter for the last 0.5 inches to accept a thin wall (0.010 inch) 0.25 inch O.D. platinum tube. Only the platinum tube and the thermocouples project past the chamber wall into the combustion gases, to a distance that carries the thermocouple tip about 0.75 inch into the region of the refractory liner, and brings the platinum tube to about 0.50 inches inside. The entire probe is six inches long and is held in place by a compression fitting screwed into the wall. The double thermocouple allows a measurement of both centerline temperature and temperature near the wall. The exact tip positions are undoubtedly affected to some extent by flutter, due to the small diameter of the thermocouples, and part of the function of the platinum tube was to help confine their movement. The main function of the platinum tube, however, is to conduct a gas sample from the vicinity of the thermocouple to the sampling orifice. One notable characteristic of this type of sampling arrangement is the long residence time of the gas at chamber conditions.

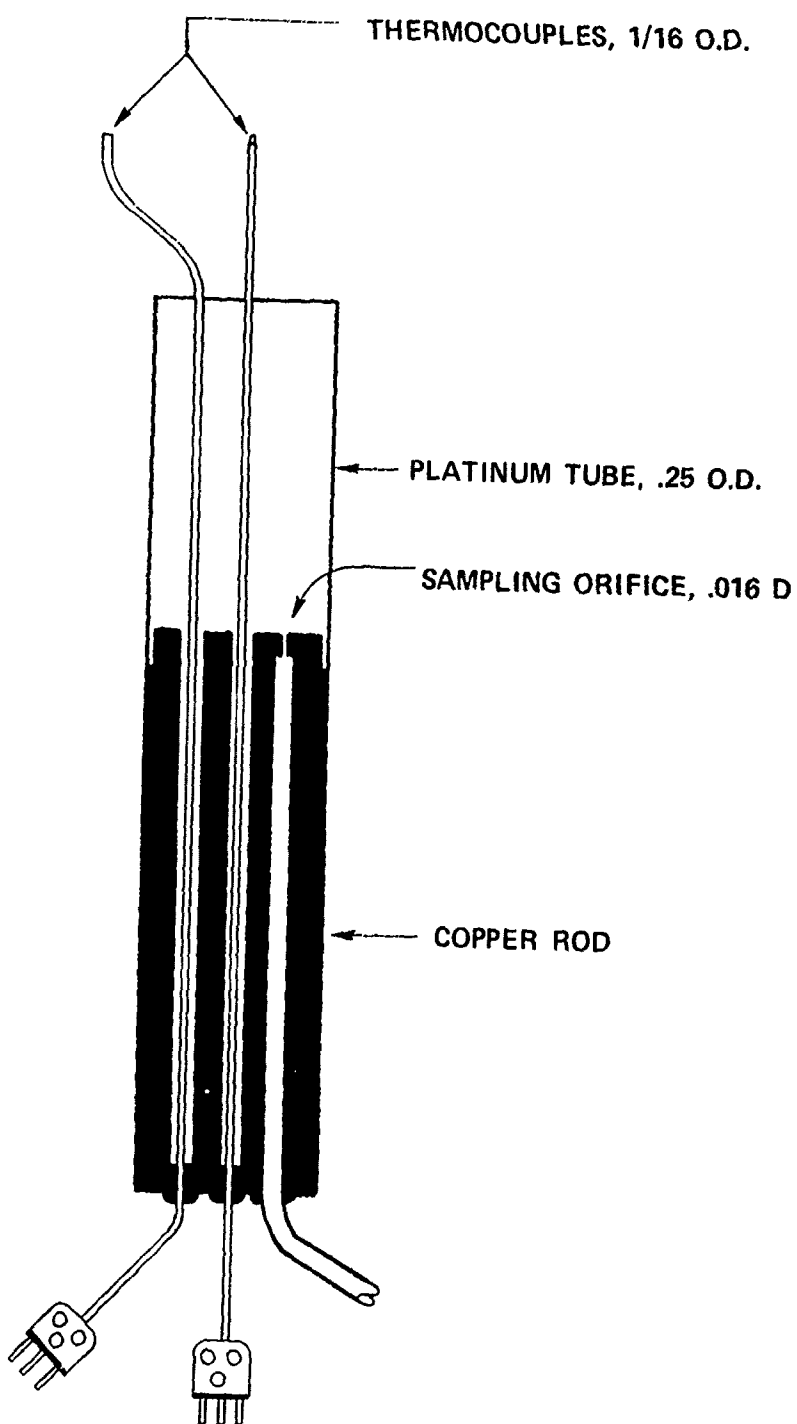


Figure 34. Sampling/Thermocouple Probe Schematic

Due to the high contraction ratio between the inside diameter of the platinum tube and the diameter of the sampling orifice, the gas travels at only about 6 feet per second down the tube. It is effectively at chamber temperature and pressure during this transit, which occupies about 27 milliseconds. Such a comparatively long residence time allows more opportunity for complete combustion, making the sample not entirely comparable with the conditions measured by the thermocouple. However, the modified probe was installed at a time when the extra residence time was welcome, since some evidence of a non-equilibrium specie (HCN) was being obtained. The long residence time is not incompatible with a practical size GDL combustor.

The samples are conducted from the probe to pre-evacuated sample collection cylinders. Two 3 liter stainless steel cylinders are employed, since there are two distinct periods in a CDI run from which samples are needed. Since a single orifice and line are common to both bottles, this line is purged between samples by forcing a flow of helium back into the chamber. This helium stream flows at all times that a sample is not being taken and thus also excludes the combustion gases from the sampling system during start-up and shut-down transients.

Photocell The purpose of the photocell was to give a record of the light emission from the chamber as a qualitative indicator of the presence or absence of particulate matter in the combustion gases. The detector consisted of an npn junction Planar Silicon Phototransistor, Texas Instrument Company model TIL 615. No filter or dispersive element was used, and the output was an integration of the output spectrum of the flame and the spectral response of the detector. The spectral response curve for the photocell is given in Figure 35. It is a broad curve roughly spanning the visible spectrum, but with its peak in the near infrared around 0.9 microns, followed by a sharp drop to zero at around 1.1 microns.

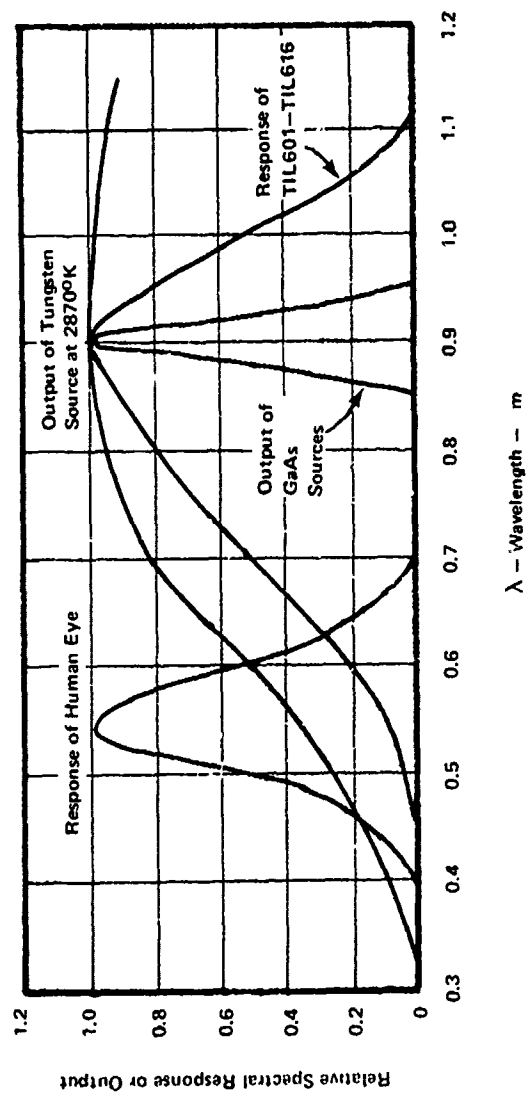


Figure 35. Spectral Response Curve of Photocell

Gaseous emissions expected in this region consist primarily of third and higher order overtones of the vibrational frequencies of CO, CO<sub>2</sub> and H<sub>2</sub>O, and should be relatively minor compared with potential black body radiation from particulates. The photocell experiment was qualitative and consisted of comparing the radiation from a CO/O<sub>2</sub> flame before and after injection of CDI.

Thermocouples Measurements were taken for the temperatures of the gaseous reactants immediately upstream of the sonic control orifice, of the CDI in the run tank, and of the chamber gases in either one or two chamber locations. The reactant temperatures were measured with iron-constant and junction thermocouples, and the chamber temperature was obtained with platinum/platinum - 13% rhodium junctions. The reference junction was maintained at 150°F in all cases. Narrow diameter sheaths were employed in the chamber thermocouple to reduce rise time and stem losses. The early CDI tests were run with a 1/8" sheath, reduced in two steps to a 0.040 inch tip for the last half inch. These were specially fabricated by the Thermoelectric Corporation. Subsequent tests with the combined gas sampling and temperature probe used standard 1/16" constant diameter sheaths. The manufacturers calibration curves were used to convert the thermocouple output to temperature. Check points were run at two points using the melting points of copper and aluminum as reference. At these two temperatures, agreement with the manufacturer's curves was to about 3 degrees fahrenheit.

Pressure Transducers Remote pressure measurements were taken of the three gaseous reactant streams upstream and downstream of the control orifices, the CDI expulsion cylinder, the combustion chamber, the exhaust catch tank, and the pressurization gases used for purging the sampling lines and reactant streams. All transducers were of the temperature compensated strain gage type. A calibration curve was determined for each transducer prior to installation on an automatic calibration

machine using a precision pressure balance standard, the calibration of which is traceable to the National Bureau of Standards.

#### Data Acquisition and Control System

The test program was conducted in area 1-30, Propellant Evaluation Facility, which has one main instrumentation and control room supporting nine test pads. A general description of the data acquisition and control capabilities of this area is given below. The system contains both analog and digital capability.

The analog system includes a 48 trace oscillograph and a 36 trace oscillograph (CSC 5-119) with a frequency response of 0 to 5000 Hz and an accuracy of  $\pm 3$  percent of full scale. There are 26 strip chart recorders with various ranges from 1 to 100 mv, accuracy  $\pm 0.25$  percent of full scale, and frequency response of DC to 1Hz. Forty channels of amplification are available (NEFF Instrumentation Corporation type 122) with step frequency response from DC to 100 KHZ.

The digital acquisition and control system is built around a dedicated computer (Systems Engineering Laboratory 810 A computer). Inputs are scanned with a 100 channel SEL multiplexer with a sampling rate of 15 KHZ. Signals are digitized also at 15 HZ with an accuracy of  $\pm 0.2$  percent of full scale and transmitted to the 810 A computer. This computer has a core memory of 16,884, 16 bit words, and a basic cycle time of 1.75 microseconds. Its main purposes are to mediate the storage of data to the output tape, to serve as a timer and controller during the firing sequence, and to provide a "quick look" printout of key parameters in engineering units after a firing. To accomplish these tasks, it has access to an interval timer with frequency sources to 572 KHZ, a SEL output control with unit 100 SCR switches, a SEL tape control unit with up to 8 tape decks, a SEL CRT display, a SEL Nixie display, a Teletype Corp. ASR-35 teletype, a Franklin line printer, a Versatec Corp Printer plotter, and paper tape

input and output units. It also has an input channel for accepting pulse signals from up to 8 turbine type flowmeters.

Signal conditioning available to both digital and analog systems include 48 channels of strain gage conditioning (B&F Instruments Inc. 1-401); 48 channels of thermocouple conditioning (Analex Instruments TC-8); 6 channels of linear voltage differential transformer conditioning (Schaevitz Engineering); and 8 channels of high response pressure conditioning (Kistler Instruments Model 566M100).

## SECTION VI

### COMBUSTION TESTS

The problem addressed in these tests is whether or not CDI injected into a characteristic high temperature environment will decompose to equilibrium products of carbon monoxide and nitrogen. A secondary problem is the production and characterization of the environment into which the CDI is injected. Each test was conducted in two parts and consisted of a nominal five second period in which carbon monoxide was burned with oxygen followed by a nominal 5 second period during which CDI was also injected. Thus each CDI firing established its own baseline without CDI flow. Ballistic measurements and gas samples were collected during both portions of each run. A back flow of gaseous diluent, which was injected into the chamber as a major portion of the flow, was maintained behind the upper liners during both periods. The diluent was predominately carbon monoxide with various amounts of hydrogen added to simulate the hydrogen which an actual GDL pre-combustor would be expected to supply. The choice of carbon monoxide as diluent rather than nitrogen was made on practical grounds. By avoiding nitrogen elsewhere, any nitrogen collected in the second portion of the run would arise only from the CDI and could be used as a gage of CDI pyrolysis. In some of the later runs, small amounts of neon and krypton were added to the fuel and diluent, respectively, in order to determine the local mixture ratio at the sampling part and allow an assessment of mixing in the combustor. A summary of the reactants used is given in Table 9, and a key to their usage in the various tests is given in Table 10.

#### Procedures

The countdown for a CDI combustion test typically would begin on the day preceding the test. The CDI was stored inside a dry ice chest in plastic containers also inside a plastic bag containing dessicant. On the day before a test, a sample of CDI was removed from storage, distilled



Component	<u>Reactant</u> (Mole Fraction)						
	1	2	3	4	5	6	7
O <sub>2</sub>	.9977	-	-	-	-	-	-
CO	-	1.0	0.953	0.937	0.959	0.909	-
H <sub>2</sub>	-	-	0.047	-	0.037	0.0305	-
Ar	.0023	-	-	-	-	-	-
Kr	-	-	-	-	.004	-	-
Ne	-	-	-	.063	-	0.061	-
CDI	-	-	-	-	-	-	1.0

TABLE 10. IDENTITY OF REACTANTS USED IN VARIOUS RUNS

<u>Run</u> <u>Number</u>	<u>Reactants*</u>			
	<u>OX</u>	<u>FUEL</u>	<u>DIL-1</u>	<u>DIL-2</u>
3	1	2	3	7
5	1	2	3	7
6	1	2	3	7
7	1	2	3	7
8	1	4	5	7
9	1	4	5	7
10	1	4	5	7
11	1	4	3	7
12	1	5	6	7
13	1	5	6	7

\*See Table 9 for reactant composition.

and returned to storage. Meanwhile, the CDI run tank was cleaned with solvent and dried with dry nitrogen. About 30 minutes before run time, loading the CDI into the tank was started. The details of the loading procedure were described in the hardware section for continuity reasons and will not be repeated here. It should be recalled that care was exercised to avoid capturing an air bubble over the CDI, which would cause an error in the flow measurement. Similar precautions were taken on the test stand in loading the run cylinder with the mineral oil expulsion fluid. The piston was raised to full height, drawing mineral oil into the cylinder, and all connecting lines were bled out until no springiness remained in the piston movement. All these precautions did not prevent a compressible gas cushion from existing downstream of the CDI tank; but it was reasoned that springiness there would not be harmful, since flow-rate measurement was not important until this gas was expelled and CDI filled the injector. Subsequently, it was decided that the downstream line filling would be much cleaner if the line were evacuated prior to CDI flow, and beginning with run 7, a vacuum line was added between the tank and the prop valve. To avoid polymerization problems, installation of the CDI tank was one of the last items in the countdown. The final procedure after opening the CDI isolation valve and filling the line down to the prop valve was to translate the carriage ramp and drive down the piston to the initial run position. Since the prop valve was still closed, this resulted in opening the relief valve and expelling excess mineral oil into the atmosphere. The remaining volume of oil under the piston was just equal to the run requirements and was calculated to equal the volume included between the top valve of the CDI tank and the prop valve. A few extra cubic centimeters were included to assure voiding the CDI, and this resulted in the injection of a small amount of mineral oil during the purge.

Other procedures in the countdown were the manual setting of pressure regulators for the helium and nitrogen stations and for the fuel, oxygen, and diluent. To assure an accurate setting, the regulators were "read up" to pressure with the same transducers and data channels used in recording the data during the run.

The two gas sample bottles were installed and evacuated, typically until about 0.05mm was measured with a McCleod gage, and this pressure was checked periodically to guard against leaks.

The igniter wire was installed, and finally a flow of water which flows through the annulus around the CDI injector and sprays out onto the outside of the combustor was turned on.

The earliest acts in the countdown are the loading of the control program into the computer and the performance of electrical calibration of the transducers. The final human act before a firing is to return control to the computer. The computer starts the oscillographs, the recording tapes, controls the opening and closing of the propellant valves, the energizing of the igniter circuit, the sequencing of the sample valves, and the starting of the drive piston. It digitizes the data, mediates its storage onto tape, and monitors the data for potential abort conditions. In the event of an abort, the computer initiates and sequences the shut-down operations. After a test the computer converts the data to engineering units and prints out a "quick-look" summary of the important parameters collected during the firing, such as chamber temperature and pressure, and the propellant temperatures and pressures. In much of its operation, the computer is little more than an elaborate timer and limit switch; but its accuracy is high, and it is very convenient to key in new timing sequences.

#### Performance of the Hardware and Instrumentation

Before presenting the detailed results of the combustion tests, it will be useful to record some observations on the performance of the hardware and instrumentation.

CDI Feed System. In general the positive expulsion system performed well. The only failure directly chargeable to the drive and piston-cylinder systems occurred when a key slipped out of its keyway in the joint between the clutch shaft and the lead screw, halting the CDI flow during a test. A more chronic problem arose from plugging of the filter installed ahead of

the CDI prop valve. The filter was selected for minimum free volume due to the small quantities of propellant involved in a run. This reduced filter area and invited plugging problems. The CDI tank, inlet and outlet valves, and filter were cleaned with a methylene chloride-acetone solvent between runs, and the CDI itself was always freshly distilled prior to a run. Nevertheless, fine particulates had been seen to form when CDI is stored in glass, and the NVR tests reported earlier suggest an initial reaction when CDI is first exposed to a fresh metal surface. The positive expulsion system yields a flow which is insensitive to back pressure up to a point. However, the system contains a relief valve, whose set pressure was frequently exceeded because of plugging. When this occurred, the CDI drive pressure became regulated at the set pressure, and a portion of the piston movement simply expelled mineral oil through the relief valve. The CDI flow rate during such incidents was unknown, being dependent on the relief pressure and the unhindered area of the filter.

Calculation of the CDI flow rate during unhindered periods can be accomplished by either of two methods. The first is to assume the constancy of the speed of the drive motor, and figure the piston speed from the various known mechanical ratios, such as the gear box, the lead screw angle, and the adjustable ramp angle. The second is to monitor the piston position with the LVDT position sensor and take its derivative with respect to time. The latter technique has the potential for measuring instantaneous flow rate, or at least the average flow rate over a short period of time. In practice this potential was not realized, since derivative techniques are very sensitive to noise. The noise in question was only about 0.1 percent of the full range of the LVDT, and a few tenths of a percent of the signal change during a run. However, the noise was an appreciable part of the signal change over the sampling interval of two milliseconds.

A spectrum analysis of the signal revealed a strong component near 60 hertz. Averaging samples for a short period substantially reduced the amplitude of the noise, but the technique was not notably successful. Due to the regularity in the noise, a beat frequency developed between it and

the frequency represented by the averaging interval. These showed up as low frequency oscillations in flow rate, of an amplitude that depended on the averaging interval. The nominal 60 cycle noise was not exactly 60 cycles, nor exactly constant, discouraging attempts to compensate for it. Thus "instantaneous" flow rate was not obtained. However, it seemed more important to show that the noise was really noise, and not rapid excursions in flow rate. The best evidence on this point is the pressure drop between the CDI tank and the combustion chamber. Since this pressure drop would vary as the square of flow rate, any actual changes in flow rate would generate enormous high frequency pressure drop fluctuations. None were ever found.

The average piston speed over a run, as determined by the LVDT, agreed reasonably well with the set value. The ramp angle was set with a vernier protractor and was held at  $26.5^{\circ}$  for all runs. This angle may also be calculated from the ratio of the piston travel to carriage travel, since both were instrumented with LVDT's. Ramp angles calculated from LVDT information were about  $26.35^{\circ}$ .

In summary, the instantaneous flow rate of the CDI is believed to be accurately reflected by the time averaged flow rate and to be as good or better than 1 percent.

Refractory Liners. The survivability of the liners was a central question in early check-out tests. The upper liner was a particular question mark, since its operating temperature depends on the balance between heat flowing from the combustion gases and heat flowing into the back flow of diluent. The analysis indicated a safety factor of 2-4 but was considered to be optimistic, since it assumed a fully developed boundary layer. A thin boundary layer, or stagnation point at or downstream of the main zone of heat release, could result in failure. The liners survived the first  $O_2/CO$  check-out tests, but the upper inside liner showed evidence of incipient melting of the oxidation resistant coating. For this reason it was decided to run the upper chamber off the stoichiometric mixture ratio to cool the combustion down. The oxygen flow was held at the original value.

but the carbon monoxide flow was reduced so that the calculated flame temperature in the upper chamber was about  $2800^{\circ}\text{K}$ . The reduced carbon monoxide flow from the injector was made up by increasing the diluent (CO) flow. After injection of the diluent, the mixture ratio was decidedly fuel rich, in accord with the expected situation in an actual CDI gas generator (laser) device. Temperatures in the lower region were in the range  $1600\text{-}1900^{\circ}\text{K}$ , easily withstood by the liners. The oxygen rich environment was maintained in the upper chamber during most of the CDI firing program, and no further problems were experienced with the inner liners. The outer liners showed little effect from the firings, except in the quality of the reflective gold coating. This coating gradually deteriorated through the firing series and was probably ineffective towards the end. A photograph of the liners after the CDI series is shown in Figure 36.

Species - Temperature Sampling Probe. After the first two firings with CDI, analysis of the gas samples failed to show the presence of nitrogen, and it was feared that a severe mixing problem existed. The CDI is injected along the centerline, and the sampling port was in the wall. Although the lack of nitrogen was subsequently found to be an artifact of the chemical analysis, as discussed later, the incident set in motion a redesign of the sampling probe. This led to the second probe (platinum tube) described in the section on hardware and to the decision to incorporate labeling gases of krypton and neon into the diluent and fuel. The oxygen already contained argon as a manufacturing impurity which served as a label. The platinum extension tube which formed the basis for the new probe appears to have survived well until run 10, after which it was found to have sagged. In addition to its major role in collecting a sample from a point near the thermocouple, it provided support for the thermocouple. In fact this permitted a smaller diameter thermocouple to be used, which in turn allowed a second thermocouple to be inserted for sampling temperatures near the chamber wall.

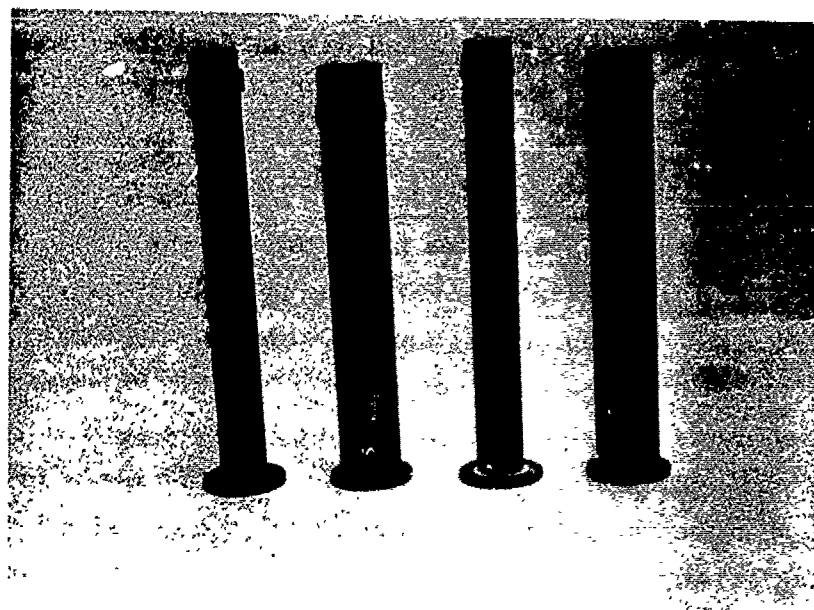


Figure 36. Refractory Liners After CDI Series  
122

CO/O<sub>2</sub> Injector. The injector was disassembled after the series, and it was found that the tip of the O<sub>2</sub> pintle was melted. Although only a small amount of material was lost, the enlargement of the orifice was a significant fraction of the small area of the original opening. Mixing was undoubtedly affected, but to what extent is not known.

### Results of the Firings

The permanent record of a firing resided primarily in the magnetic tape created by the control program at the time of firing. Parameters included are the chamber temperatures, the chamber pressure, the pressures of the gaseous reactants upstream and downstream of the control orifice, the pressure in the CDI run cylinder, the gaseous reactant temperatures immediately upstream of the control orifice, the CDI temperature, and the carriage and piston position. Also stored on the magnetic tape are the electrical calibration steps determined for each transducer during the "pre-cal" phase of the countdown. Auxiliary information available from the Instrumentation and Mechanical "Spec" sheet are the barometric pressure, throat area, reactant identification, and an identification of the various transducers used and their primary calibration date.

The voltage readings stored on the tape are converted to engineering units via a "General Engineering Units" program which has access to curve fits for calibration data on all the transducers employed. Flow rates for the gaseous reactants were determined with a special "Performance Program" from the reactant pressures and temperatures, from stored viscosity and equation of state data, and from stored data on discharge coefficient versus Reynolds number for the various sonic orifices, as determined by calibration studies performed by NBS. The CDI flow rate used was determined from the average rate of piston movement recorded by the LVDT and the density of CDI at the recorded fuel temperature.

Computer plotted traces were generated for chamber temperature and pressure.



A characteristic chamber temperature ( $T_c$ ) trace using the original thermocouple probe is shown in Figure 37. The trace is complex and close attention to the sequencing of various events (Table 11) is necessary for a proper interpretation. Several of these events are marked on the trace for convenience. Highest temperatures occurred during the period when only  $CO$ ,  $O_2$ , and gaseous diluent were flowing. The trace is depressed early in the run by a nitrogen purge being injected through the CDI injector orifice, and later in the run by the arrival of CDI. The original purpose of the nitrogen purge was post test clearing of the CDI injector and feed line, but in most of the firings it was turned on early to suppress temperatures during the ignition overshoot. Otherwise it was found that overshoot temperatures exceed the abort setting and terminated the firing. Since the purge came through one side of the two-way CDI prop valve, it was automatically shut off when the CDI began to flow. Note the long delay between energizing of the CDI prop valve and the actual arrival of the CDI at the combustion chamber. This delay was a convenience since it created a period when neither CDI or purge was flowing, and allowed determination of the baseline data ( $O_2/CO$ ).

Figure 38 shows a temperature trace using the revised thermocouple - gas sampling probe. Recall that this probe featured an off-center thermocouple (TC 2) in addition to the centerline thermocouple (TC 1). The pair of traces reveal in several ways that mixing is incomplete in the chamber. One way is the general disparity in temperature sensed. In addition the centerline thermocouple senses the ignition overshoot and the nitrogen purge, whereas this structure is missing from the off-center thermocouple trace. The CDI effect on temperature, however, is fairly evenly sensed by the two thermocouples indicating a good spray distribution in the chamber.

The traces discussed above were taken during firings in which the chamber liners were arranged so that the gaseous diluent entered at mid-chamber. Late in the firing series, the liner configuration was changed so that the gaseous diluent was injected near the  $CO/O_2$  injector

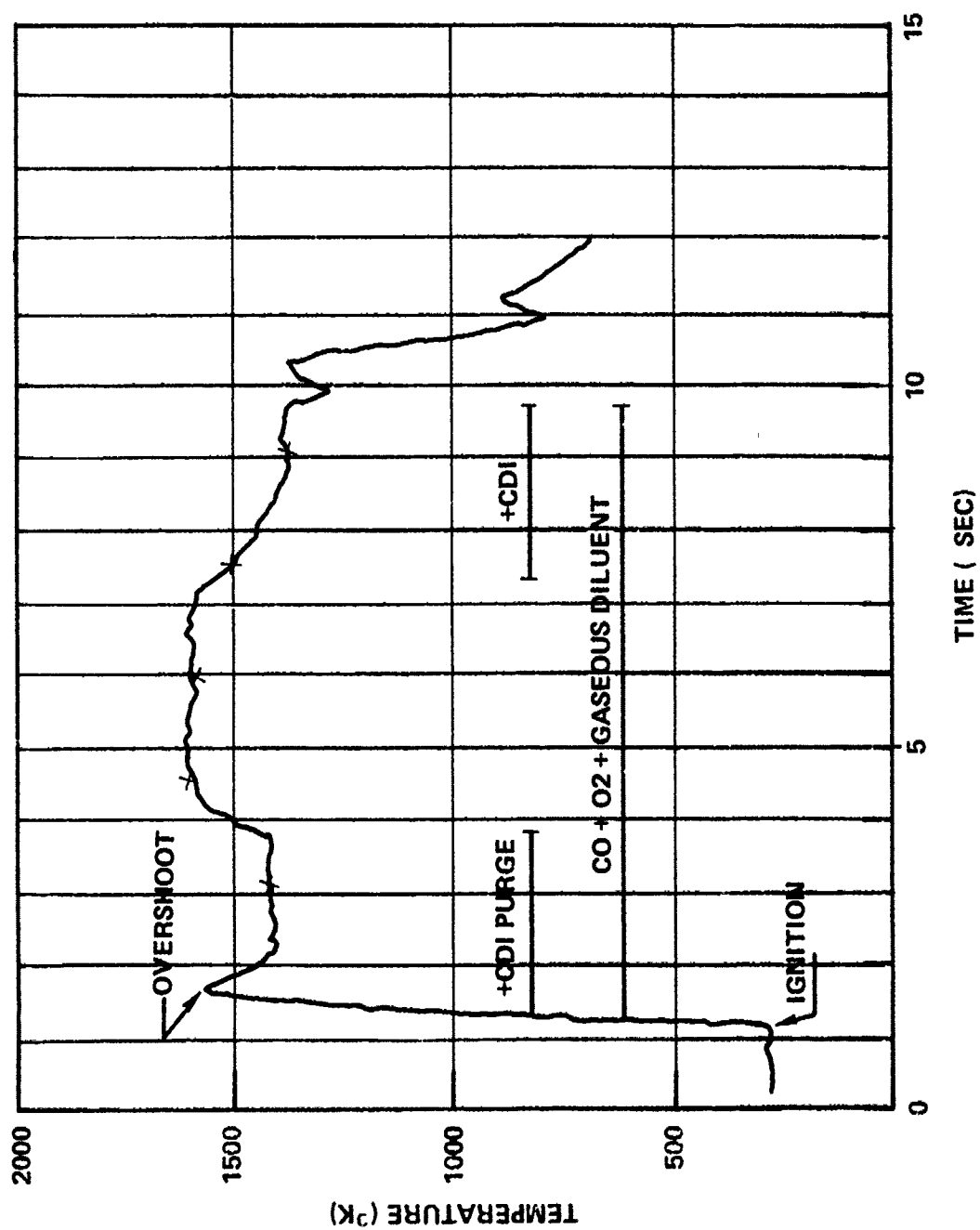


Figure 37. Chamber Temperature (°K) Run 3

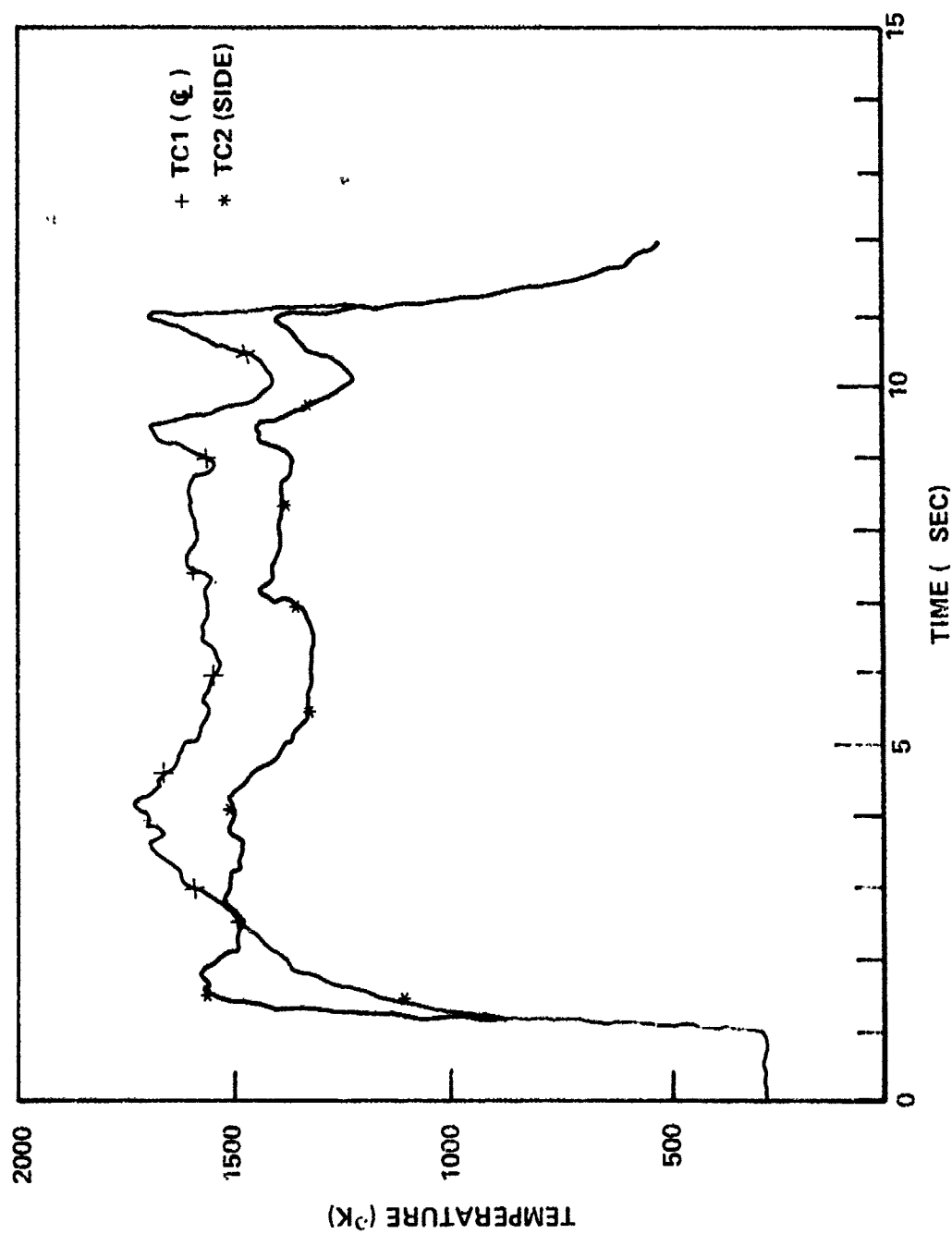


Figure 38. Chamber Temperature ( $^{\circ}$ K) Run 7

at the head of the combustion chamber. This extra mixing length had a decisive effect on the appearance of the temperature traces. The temperature difference between the two thermocouples dropped to about  $20^{\circ}\text{K}$ . Furthermore, the traces were much less noisy. It is probable that the thermocouples were oscillating in the flow-stream, and that the resulting translation through an inhomogeneous medium was responsible for the noise in the earlier firings. The trace for a firing with the liners in this configuration is shown in Figure 39. The trace is a calculated arithmetic average of TC 1 and TC 2.

A characteristic chamber pressure ( $P_c$ ) trace is shown in Figure 40. This trace is generally less noisy than the thermocouple trace, but has more structure. This extra structure is due to the fact that the pressure transducer also recorded the activity of the purge gas for the sampling probe (which was downstream of the thermocouple). Also, it recorded the entry sequence of the cold reactants prior to ignition. Note that the chamber pressure rises with the entry of the CDI, in contrast to the simultaneous fall in chamber temperature. Both of these effects are predicted theoretically.

The data for the firing series were summarized by selecting two points from each temperature and pressure trace, representing baseline and main firing periods. The selection of the points was closely constrained by the effects of the various purges. Suitable "windows" could be located with the aid of timing table (Table 11). Some additional constraints arose from inspection of the data itself. The arrival of CDI at the chamber was visible in the  $T_c$  and  $P_c$  traces, and could also be seen as a sudden rise in injection pressure. The "injection pressure" included pressure drops through the entire CDI feed system. Particularly significant was the drop through the filter, which is believed responsible for sudden increases in upstream pressure late in most of the runs. The data "window" was thus constrained to periods when injection pressure was satisfactory. The data summary is presented in Table 12. Data tabulated includes the reactant flow rates, chamber temperatures (TC 1 and TC 2) and their

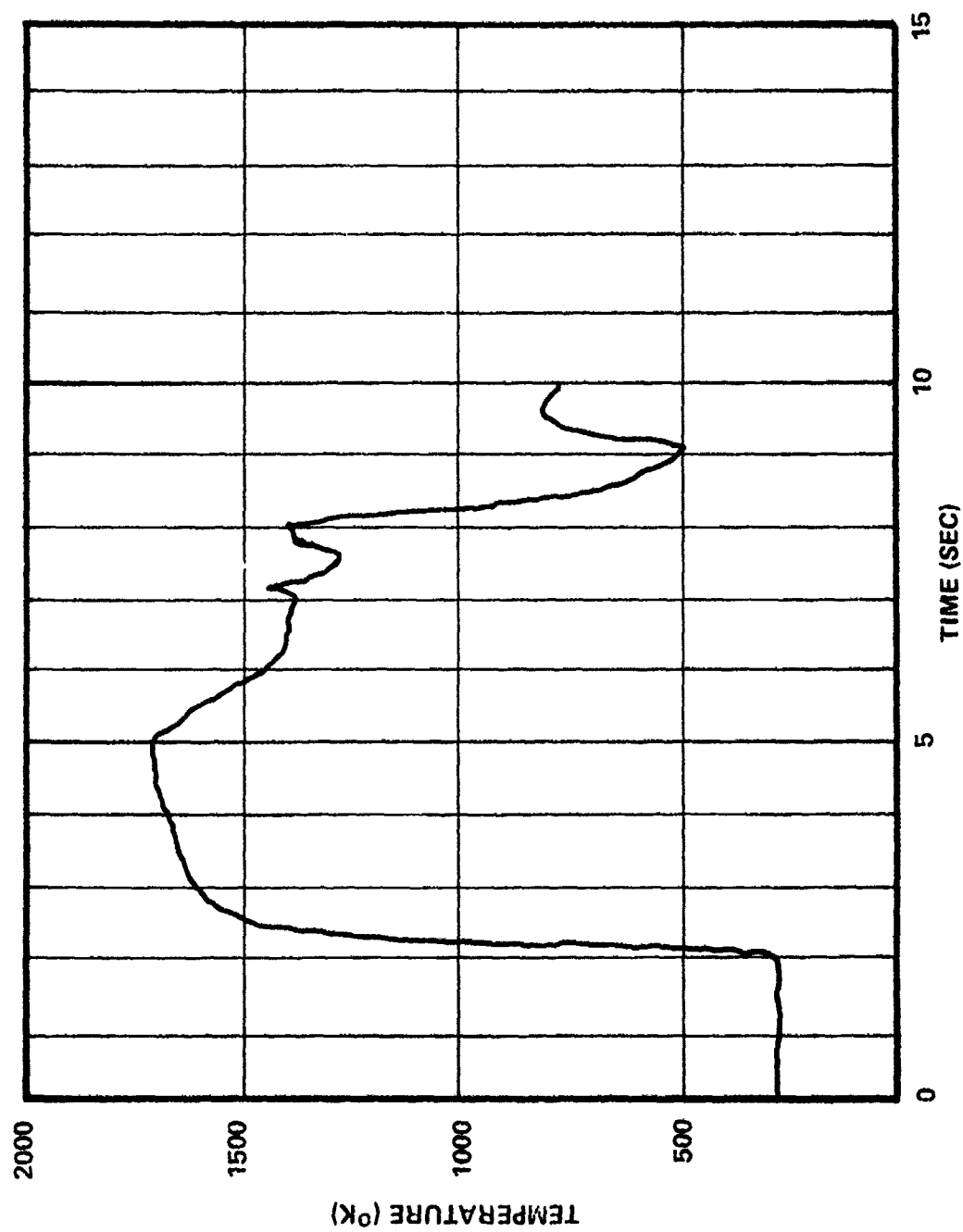


Figure 39. Chamber Temperature (°K) Run 13

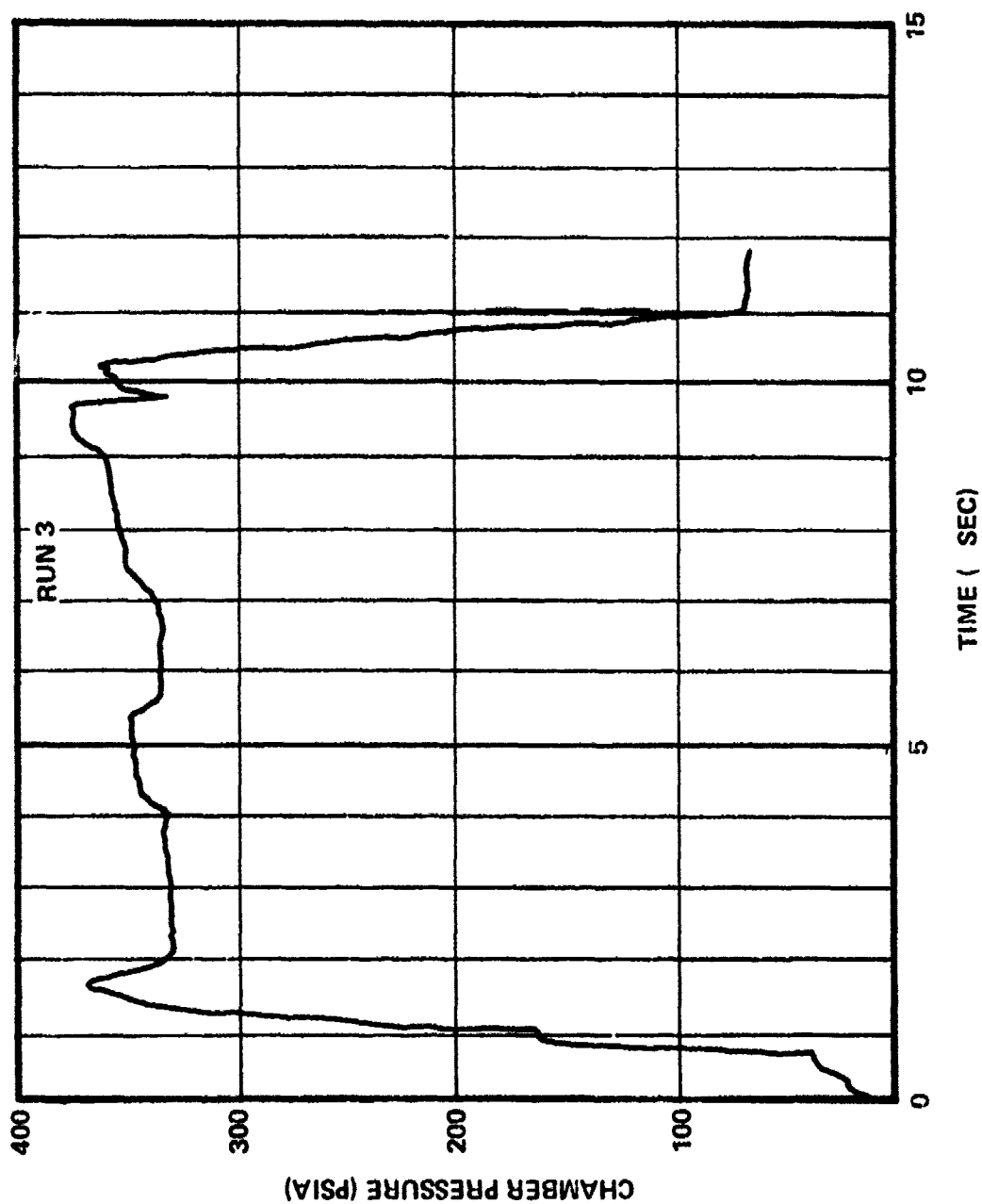


Figure 40. Chamber Pressure (Psia)

TABLE 11. TIMING OF EVENTS IN CDI FIRINGS

Run No.	Event	Time From Zero (Sec)									
		3	5	6	7	8	9	10	11	12	13
1A	CDI Prop Valve - On	3.69	2.00	3.20	3.20	5.51	5.51	5.52	4.02	4.02	4.02
1B	- Off	9.61	10.84	9.50	9.50	12.71	12.70	12.70	9.70	9.70	7.01
2	CDI Carriage - On	3.70	2.01	3.21	3.21	5.52	5.52	5.51	4.01	4.01	4.01
3A	Sample 1 - On	1.50	2.02	1.50	1.50	3.50	3.50	2.50	2.50	2.50	2.50
3B	- Off	4.00	3.50	3.19	3.19	5.50	5.50	5.50	4.00	4.00	4.00
4A	Sample 2 - On	5.20	7.30	7.30	7.30	7.50	7.50	7.50	6.00	6.00	4.90
4B	- Off	9.09	9.30	9.30	9.30	11.00	11.00	11.00	9.50	9.50	7.00
5A	CO Prop Valve - On	0.04	0.04	0.04	0.04	1.040	1.04	1.00	1.00	1.00	1.00
5B	- Off	9.80	10.50	10.50	10.50	13.70	13.70	13.70	9.71	9.71	7.02
6A	O <sub>2</sub> Prop Valve - On	0.30	0.30	0.30	0.30	1.30	1.30	1.01	1.01	1.01	1.01
6B	- Off	10.30	11.00	11.00	11.00	14.20	14.20	14.20	10.70	10.70	8.00
7A	Diluent Valve - On	0.50	0.50	0.50	0.50	1.50	1.50	1.50	1.50	1.50	1.50
7B	- Off	10.80	12.00	12.00	12.00	15.00	15.00	15.00	11.70	11.70	9.00
8A	Reactant Purge - On	9.50	10.41	10.41	10.41	11.01	11.01	11.01	2.02	2.02	2.02
8B	- Off	10.91	13.00	13.00	13.00	17.02	17.02	17.02	13.82	13.82	-
9A	CDI Purge - On	0.02	0.75	0.75	0.75	11.02	0.50	5.53	0.98	0.98	7.03
9B	- Off	12.03	11.01	11.01	11.01	17.01	17.01	17.01	13.81	13.81	10.96
10A	Sample Purge - On	0.01	0.01	0.01	0.01	0.01	0.01	0.01	0.99	0.99	0.99
10B	- Off	12.00	10.90	10.90	10.90	17.03	17.03	17.03	17.03	13.83	-
11A	Igniter - On	1.00	1.00	1.00	1.00	2.00	2.00	2.00	2.00	2.00	2.00
11B	- Off	1.20	1.20	1.20	1.20	2.20	2.20	2.20	2.20	2.20	2.20

arithmetic average ( $T_c$  AV), and chamber pressure. Two columns are presented for each firing; the "dash" 1 numbers refer to the non-CDI period, and the "dash" 2 numbers refer to the period when CDI is flowing. Between these columns a value for the temperature change ( $\Delta P_c$ ) between the two periods is given. The experimental characteristic exhaust velocity ( $C^*$ ) is calculated from the chamber pressure, throat area ( $A_t$ ), and total flow rate ( $\dot{w}$ ) from the usual relation.

The flow rate and the reactant formulas and heats of formation were used to calculate corresponding theoretical chamber temperatures and  $C^*$ 's using a chemical equilibrium model. These theoretical values are also presented in Table 12 and are further used to derive temperature and  $C^*$  efficiencies ( $\eta_t$  and  $\eta_{C^*}$ ).

The data may be summarized more compactly in statistical form, as shown in Tables 13 and 14.

Table 13 gives the chamber temperature efficiency and the  $C^*$  efficiency both with and without CDI flow. The values are averaged over the runs in which the gaseous diluent was injected at mid-chamber (runs 3-10).

The  $C^*$  efficiencies are lower than the temperature efficiencies due to the fact that they represent conditions existing at the throat. By this point, large heat losses have been incurred due to the passage through the heat sink instrumentation block. Actually, since the  $C^*$  is related to the square root of the temperature, the  $C^*$  values tabulated are consistent with temperature efficiencies at the throat of about 77 percent.

For the "without CDI" chamber temperatures, the averaging excluded run 6 because of a very noisy trace, and also run 10 because of a sagged temperature probe. For the "with CDI" chamber temperatures, run 6 was satisfactory, but run 10 was again excluded, as were runs 5, 8, and 9, which had CDI flow difficulties. For the  $C^*$  parameter, it was necessary to eliminate run 9 on the basis of a statistical test. The uncertainties indicated in the table are the standard deviation from the mean.



Table XIV gives the temperature efficiencies ( $T_{CAV}$ ) and  $C^*$  efficiencies for runs 11-13, where the gaseous diluent was injected at the head end of the chamber.

No  $T_c$  and  $C^*$  data are presented for the condition with CDI flow, since filter plugging problems and shortage of CDI prevented acquiring data with acceptable CDI flow rates.

It is evident from these tables that a loss in efficiency was experienced in going from mid-chamber injection to upper chamber injection of gaseous diluent. Apparently some quenching of the reaction occurred.

#### Species Sampling Results

The primary analytical tool employed in the quantitative analysis of gas samples collected from the firings was a CEC 21 490 mass spectrometer.

When the first two runs (3 and 5) were analyzed, it was discovered that no nitrogen was present in either the CDI or the non-CDI interval of the flow, when in fact, nitrogen was expected in both samples. In the non-CDI interval, nitrogen from the CDI injector purge should have been collected and during the CDI interval, nitrogen was expected as a decomposition product of CDI. Since both the purge and the CDI itself were injected at the centerline, and the sample was collected at the wall, the first explanation evident was that the combustor had a severe mixing problem. This prompted the redesigned probe, as discussed earlier. In subsequent samples, gas chromatographic analysis was also employed, and the nitrogen was found. Although the mass spectrometer was of the double focusing type and had successfully resolved  $N_2$  and CO in calibration mixtures, no mixtures with a large excess of one component over the other had been run. The CDI combustion samples thus revealed a limit on the ability of the mass spectrometer in resolving  $N_2$  and CO peaks. When the mass spectrometer was run at a slower scanning rate, the enhanced resolution revealed the  $N_2$  as a shoulder on the larger CO peak; and subsequent samples were analyzed for CO and  $N_2$  with both gas chromatographic and mass

TABLE 12. BALLISTIC DATA FROM CDI COMBUSTION TESTS

Run	3-1	3-2	5-1	5-2	6-1	6-2
$\dot{\omega}(\text{CDI}) \left(\frac{\text{gm}}{\text{sec}}\right)$	0	7.44	0	7.46	0	7.50
$\dot{\omega}(\text{Dil}) \left(\frac{\text{gm}}{\text{sec}}\right)$	45.3	45.3	45.7	46.0	45.0	45.0
$\dot{\omega}(\text{CO}) \left(\frac{\text{gm}}{\text{sec}}\right)$	2.4	2.4	2.4	2.4	2.35	2.35
$\dot{\omega}(\text{O}_2) \left(\frac{\text{gm}}{\text{sec}}\right)$	5.5	5.5	5.6	5.6	5.52	5.52
$T_{\text{C1}} (^{\circ}\text{K})$	1616	1380	1667	-	(1700)	1611
$T_{\text{C2}} (^{\circ}\text{K})$	-	-	-	-	(1450)	1356
$T_{\text{CAV}} (^{\circ}\text{K})$	-	-	-	-	(1575)	1483
$\Delta T_{\text{c}} (^{\circ}\text{K})$	-236		-		-92	
$T_{\text{c}} (\text{Theo.}) (^{\circ}\text{K})$	1772	1601	1784	1606	1785	1610
$\eta_{\text{t}} (\%)$	91.2	86.2	93.4	-	88.2	92.1
Time ( $T_{\text{c}}$ )	5.0	9.5	5.0	-	4.3	6.5
$P_{\text{c}} (\text{Psia})$	340	366	346	-	344	373
$\Delta P_{\text{c}} (\text{Psia})$	26		-		29	
Time ( $P_{\text{c}}$ )	6.0	9.0	5.0	-	4.5	8.0
$C^* (\text{ft/sec})$	3038	2869	3063	-	3093	2937
$C^* \text{ Theo.} (\text{ft/sec})$	3487	3320	3497	3325	3499	3329
$\eta_{\text{c}}^* (\%)$	87.1	86.4	87.6	-	88.4	88.2
Date	26 Oct 72		9 Nov 72		17 Nov 72	

TABLE 12. BALLISTIC DATA FROM CDI COMBUSTION TESTS

Run	7-1	7-2	8-1	8-2	9-1	9-2
$\dot{w}(\text{CDI}) \left(\frac{\text{gm}}{\text{sec}}\right)$	0	7.51	0	7.58	0	7.57
$\dot{w}(\text{Dil}) \left(\frac{\text{gm}}{\text{sec}}\right)$	44.5	44.5	45.7	46.0	46.0	46.0
$\dot{w}(\text{CO}) \left(\frac{\text{gm}}{\text{sec}}\right)$	2.4	2.4	2.4	2.4	2.4	2.4
$\dot{w}(\text{O}_2) \left(\frac{\text{gm}}{\text{sec}}\right)$	5.5	5.5	6.4	6.4	6.4	6.4
$T_{C1} (^{\circ}\text{K})$	1733	1567	1922	1655	1900	1811
$T_{C2} (^{\circ}\text{K})$	1533	1339	1678	1522	1744	1656
$T_{\text{CAV}} (^{\circ}\text{K})$	1633	1453	1800	1589	1822	1733
$\Delta T_c (^{\circ}\text{K})$	-180		-211		-89	
$T_c (\text{Theo.}) (^{\circ}\text{K})$	1793	1615	1980	1778	1972	1778
$\eta_i (\%)$	91.1	90.0	90.9	89.4	92.4	97.5
Time ( $T_c$ )	4.4	6.25	12.0	8.75	8.0	10.0
$P_c (\text{Psia})$	342	374	366	392	432	446
$\Delta P_c (\text{Psia})$	32		26		14	
Time ( $P_c$ )	4.0	8.0	6.5	8.0	8.0	10.0
$C^* (\text{ft/sec})$	3103	2968	3192	2987	3748	3400
$C^* \text{ Theo.} (\text{ft/sec})$	3504	3333	3637	3459	3630	3459
$\eta_{C^*} (\%)$	88.6	89.0	87.8	86.4	103.3	98.3
Date	20 Nov 72		8 Dec 72		12 Dec 72	

TABLE 12. BALLISTIC DATA FROM CDI COMBUSTION TESTS

Run	10-1	10-2	11-1	11-2	12-1	12-2
$\dot{\omega}(\text{CDI}) (\frac{\text{gm}}{\text{sec}})$	0	7.58	0	7.56	0	7.56
$\dot{\omega}(\text{Dil}) (\frac{\text{gm}}{\text{sec}})$	46.0	45.5	45.5	45.5	46.2	46.2
$\dot{\omega}(\text{CO}) (\frac{\text{gm}}{\text{sec}})$	2.4	2.4	2.4	2.4	2.4	2.4
$\dot{\omega}(\text{O}_2) (\frac{\text{gm}}{\text{sec}})$	6.2	6.2	5.9	5.86	5.9	5.9
$T_{C1} (^{\circ}\text{K})$	1778	1678	1589	1555	1583	1583
$T_{C2} (^{\circ}\text{K})$	1600	1378	1561	1533	1539	1555
$T_{\text{CAV}} (^{\circ}\text{K})$	1689	1528	1575	1544	1561	1569
$\Delta T_c (^{\circ}\text{K})$	-161		-31		+8	
$T_c (\text{Theo.}) (^{\circ}\text{K})$	1930	1750	1879	1685	1861	1678
$\eta_t (\%)$	87.5	87.3	83.8	91.6	83.9	93.5
Time ( $T_c$ )	6.5	9.5	5.5	9.5	5.0	9.5
$P_c (\text{Psia})$	342	373	342	356	341	352
$\Delta P_c (\text{Psia})$	31		14		11	
Time ( $P_c$ )	5.5	9.5	5.5	9.5	5.0	9.5
$C^* (\text{ft/sec})$	3129	3021	3175	2901	3125	2833
$C^* \text{ Theo.} (\text{ft/sec})$	3595	3435	3553	3376	3565	3393
$\eta_{c^*} (\%)$	87.0	87.9	89.4	85.9	87.6	83.5
Date	15 Dec 72		2 Jan 73		3 Jan 73	

TABLE 12. BALLISTIC DATA FROM CDI COMBUSTION TESTS

Run	13-1	13-1
$\dot{\omega}(\text{CDI}) \left(\frac{\text{gm}}{\text{sec}}\right)$	0	7.55
$\dot{\omega}(\text{Dil}) \left(\frac{\text{gm}}{\text{sec}}\right)$	46.0	46.0
$\dot{\omega}(\text{CO}) \left(\frac{\text{gm}}{\text{sec}}\right)$	2.36	2.36
$\dot{\omega}(\text{O}_2) \left(\frac{\text{gm}}{\text{sec}}\right)$	6.44	6.44
$T_{\text{C1}} (^{\circ}\text{K})$	1722	1622
$T_{\text{C2}} (^{\circ}\text{K})$	1703	1600
$T_{\text{CAV}} (^{\circ}\text{K})$	1712	1611
$\Delta T_{\text{c}} (^{\circ}\text{K})$	.101	
$T_{\text{c}} (\text{Theo.}) (^{\circ}\text{K})$	1982	1788
$\eta_{\text{t}} (\%)$	86.4	90.1
Time ( $T_{\text{c}}$ )	4.9	5.5
$P_{\text{c}} (\text{Psia})$	350	368
$\Delta P_{\text{c}} (\text{Psia})$		18
Time ( $P_{\text{c}}$ )	4.9	5.5
$C^* (\text{ft/sec})$	3190	2948
$C^* \text{ Theo. } (\text{ft/sec})$	3666	3491
$\eta_{\text{c}^*} (\%)$	87.01	84.4
Date	5 Jan 73	

TABLE 13. BALLISTIC EFFICIENCY FOR MID-CHAMBER  
INJECTION OF GASIOUS DILUENT

	<u>Without CDI</u>	<u>With CDI</u>
$T_c$ Eff	$91.8 \pm 1.0$	$89.4 \pm 2.4$
$C^*$ Eff	$87.8 \pm 0.6$	$87.6 \pm 1.0$

TABLE 14. BALLISTIC EFFICIENCY FOR UPPER CHAMBER  
INJECTION OF GASEOUS DILUENT

	<u>Without CDI</u>
$T_c$ Eff	$84.7 \pm 1.2\%$
$C^*$ Eff	$86.0 \pm 1.0\%$

spectrometric techniques. The results were in serious disagreement with each other, with the mass spectrometric measurements for  $N_2$  now being on the high side by a substantial factor, typically a factor of three. In view of the resolution difficulty with the mass spectrometer, it was decided to use the gas chromatographic results for CO and  $N_2$ . This decision created another difficulty in that the other species were not determined gas chromatographically, and a way of combining the gas chromatographic and mass spectrometric results had to be devised. The method adopted was to assume that the sum of the CO plus  $N_2$  concentrations determined mass spectrometrically was correct and then shift a portion of the  $N_2$  into the CO until the ratio determined gas chromatographically was achieved.

Several other corrections were necessary to the analysis. Most of the sample was helium, which was used in clearing the sampling lines in non-sampling intervals. It was thus necessary to subtract this component and re-normalize the remaining species to 100 percent.

Also, water was not analyzed for because of its tendencies to stick to the apparatus surfaces and cause poor analysis. It was thus calculated by totalling all the observed hydrogen species and subtracting the total from the total hydrogen computed theoretically. The added water, of course, necessitated a second re-normalization.

The results of these analyses are given in Table 15, as mole per cent. Runs 3, 5, 12, and 13, are not given, since a gas chromatographic determination was not made for them. The run numbers indicate the non-CDI intervals with a "dash" 1 (for example 6-1) and the CDI interval with a "dash" 2 (for example 6-2). The lack of  $N_2$  in the -1 series is an artifact of the data reduction technique. Since the  $N_2$  was only a purge specie, it followed the fate of the helium, and was subtracted. Most of the -1 samples were collected during a  $N_2$  purging interval, and  $N_2$  was actually found.

The data may be more compactly presented by combining the results into average values. This is done in Table 16 for the period without CDI flow. The nominal or average theoretical value over the valid experiments

TABLE 15. CHEMICAL ANALYSIS OF CDI COMBUSTION PRODUCTS

Run No.						
	6-1		6-2		7-1	
<u>Specie (Mol%)</u>	<u>EXPT</u>	<u>THEO</u>	<u>EXPT</u>	<u>THEO</u>	<u>EXPT</u>	<u>THEO</u>
CO	78.3	78.0	75.1	77.1	77.7	77.9
CO <sub>2</sub>	16.0	17.5	17.3	15.7	17.7	17.6
N <sub>2</sub>	0	0	3.8	3.3	0	0
H <sub>2</sub>	5.3	2.4	2.5	2.7	3.4	2.4
H <sub>2</sub> O	-	2.0	1.0	1.2	.9	2.0
O <sub>2</sub>	.26	0	.06	0	.7	0
HCN	0	0	.4	0	0	0
Ar	.18	.02	.04	.02	0	.02
Ne	-	-	-	-	-	-
Kr	-	-	-	-	-	-



TABLE 15. CHEMICAL ANALYSIS OF CDI COMBUSTION PRODUCTS

Run No.						
	7-2		8-2		9-1	
Specie (Mol %)	<u>EXPT</u>	<u>THEO</u>	<u>EXPT</u>	<u>THEO</u>	<u>EXPT</u>	<u>THEO</u>
CO	75.3	77.0	76.1	75.0	70.46	75.04
CO <sub>2</sub>	16.5	15.7	20.15	18.1	22.36	20.72
N <sub>2</sub>	3.8	3.3	.4	3.3	0	0.00
H <sub>2</sub>	2.3	2.6	2.14	1.6	3.76	1.76
H <sub>2</sub> O	1.3	1.2		1.4	.07	1.93
O <sub>2</sub>	.2	0	.30	0	2.07	0
HCN	.37	0	.20	0	0	0
Ar	.05	.02	.04	.02	.19	.03
Ne	-	-	.31	.27	.59	.31
Kr	-	-	.39	.33	.50	.38

TABLE 15. CHEMICAL ANALYSIS OF CDI COMBUSTION PRODUCTS

Run No.						
	9-2		10-1		10-2	
<u>Specie (Mol %)</u>	<u>EXPT</u>	<u>THEO</u>	<u>EXPT</u>	<u>THEO</u>	<u>EXPT</u>	<u>THEO</u>
CO	68.67	74.78	73.60	75.85	70.14	75.14
CO <sub>2</sub>	21.93	18.25	21.46	19.91	20.70	17.86
N <sub>2</sub>	5.55	3.30	0	0	4.57	3.34
H <sub>2</sub>	2.31	1.79	2.34	1.65	.74	1.84
H <sub>2</sub> O	.5	1.26	1.16	1.86	1.64	1.21
O <sub>2</sub>	.33	0	.12	0	.07	0
HCN	0	0	0	0	1.34	0
Ar	.055	.02	.06	.025	.04	.022
Ne	.33	.27	.36	.31	.35	.27
Kr	.33	.33	.90	.38	.40	.33

TABLE 15. CHEMICAL ANALYSIS OF CDI COMBUSTION PRODUCTS

Run No.				
	11-1		11-2	
Specie (Mol %)	EXPT	THEO	EXPT	THEO
CO	74.62	76.4	73.29	76.07
CO <sub>2</sub>	18.25	19.3	19.30	16.94
N <sub>2</sub>	0	0	3.18	3.32
H <sub>2</sub>	4.25	1.93	1.88	1.95
H <sub>2</sub> O	0	1.59	.78	1.10
O <sub>2</sub>	1.75	0	.30	0
H <sub>2</sub> CN	0	0	.77	0
Ar	.25	.024	.06	.02
Ne	.63	.31	.35	.27
Kr	.38	.38	.09	.33

is given in the first column for the various species found. In the second column, the difference between the individual theoretical values and the corresponding experimental values is averaged over the runs.

The standard deviation of the discrepancies from the average difference is given in the third column. The second column may be viewed as an expression of the magnitude of any trend away from the theoretically predicted concentration and the third column represents the precision with which the trend is known. In most cases there is no provable trend, and the experimental values agree with the nominal values within the precision of the data. The standard deviation is relatively large. Partly this is a consequence of the heavy dilution with helium from the sampling purge, which complicated analysis. There is a statistically significant excess of hydrogen which is not understood. The deficit of water is an artifact of the low hydrogen and the difference technique used in calculating the water. The surplus oxygen arose primarily from inclusion of run 11 and might only be an indication of an air leak in that run. The argon is also larger than expected, based on the amount known to be present in the O<sub>2</sub> tank, but is in a concentration range where detection and quantitative analysis is difficult. The ratio of neon to krypton is in the range expected, based on perfect mixing in the combustor; but again the precision of the data prevented definitive results.

A similar tabulation of averaged values for the samples collected during CDI flow is given in Table 17. In constructing this table, runs 8, 9, and 11 were excluded from the averaging. In run 8 there was evidence that mineral oil rather than CDI was being injected. The very low nitrogen supports this conclusion as well as the results of the photocell experiment described later. A review of the pre-firing events suggests the CDI was lost in a preceeding abort sequence. Run 9 was excluded because the unusually high  $P_c$  spoiled the effectiveness of the sampling purge and mixed in some sample from the non-CDI period. Run 11 was excluded because filter plugging prevented effective CDI flow.

TABLE 16. AVERAGED SAMPLING RESULTS (WITHOUT CDI FLOW)

<u>Specie (Mol %)</u>	<u>Nominal</u>	<u>(Expt - Theory)</u>	<u>Standard Deviation</u>
CO	76.64	-1.70	$\pm 1.7$
CO <sub>2</sub>	19.01	+ .15	$\pm .54$
H <sub>2</sub>	2.03	+ 1.78	$\pm .82$
H <sub>2</sub> O	1.88	-1.45(by diff)	$\pm 1.08$
O <sub>2</sub>	.00	+ .98	$\pm .79$
Ar	.02	+ .11	$\pm .09$
Ne	.19	+ .13	$\pm .14$
Kr	.23	+ .13	$\pm .2$

TABLE 17. AVERAGED SAMPLING RESULTS (WITH CDI FLOW)

<u>Specie (Mol %)</u>	<u>Nominal</u>	<u>(Expt - Theory)</u>	<u>Standard Deviation</u>
CO	76.40	-2.9	$\pm 1.49$
CO <sub>2</sub>	16.42	+1.75	$\pm .84$
N <sub>2</sub>	3.31	+ .74	$\pm .34$
H <sub>2</sub>	2.38	- .53	$\pm .40$
H <sub>2</sub> O	1.20	+ .11(by diff)	$\pm .26$
O <sub>2</sub>	.00	+ .11	$\pm .02$
HCN	.00	+ .70	$\pm .61$
Ar	.02	+ .02	$\pm .005$
Ne	.09	+ .06	$\pm .05$
Kr	.11	+ .023	$\pm .03$

The main predicted difference between this series and the non-CDI series is the presence of nitrogen from the pyrolysis of CDI, and this is verified by the results.

One unpredicted feature of the analysis is very consistent. In all intervals in which CDI was flowing, HCN was found in the products. Its presence is not likely an artifact of the sampling process, since it was never detected in any of the samples taken from the non-CDI sampling interval. It is not predicted to form in the equilibrium calculations, even though it is considered as a potential product in the course of the calculation. The amount found was usually small, typically 0.4 percent. However, it may be noted that the nitrogen in this amount of HCN is over 5 percent of the nitrogen expected from the CDI. The greatest amount of HCN found was 1.34 percent in run 10. This represents about 15 percent of the nitrogen present. The HCN was the only specie found which is not predicted theoretically and whose effect in a gas dynamic laser is completely unknown. Accordingly, the finding of HCN was one of the earliest concerns of the firing program.

A summary of the photocell results is given in Table 18. The purpose of this experiment was to check on possible formation of particulate matter from CDI by noting any increase in flame emissivity due to particulate black body radiation. The ratio of radiation intensity with and without CDI flow is shown in the final column of Table II for the runs where such data was taken. Also shown is the ratio expected, based on a correction for the measured temperature change. And finally, the ratio of calculated to measured values is presented in the middle column. This ratio will be near unity for equal emissivities between the CDI and non-CDI periods. Runs 10, 11, and 13 are suitably close to unity, whereas runs 3 and 8 would appear to show particulates arising from CDI. These latter runs are suspect, however. In run 3 the trace suggests that the photocell was "saturated" due to an improper choice of load resistor in the photocell amplifier circuit. Run 8, meanwhile, gives independent clues that mineral oil expulsion fluid was being injected rather than CDI. The low emissivity

in run 6 is also not believed to be real, but an artifact of a large uncertainty in the measured temperature change from which the temperature correction was computed. In summary, it is believed that runs 10, 11, and 13 are valid and indicate no change in flame emissivity on injection of CDI (no detectable particulate formation).

TABLE 18. RATIO OF PHOTOCELL INTENSITIES

\*C ( $I_{\text{without CDI flow}}/I_{\text{during CDI flow}}$ )

<u>RUN</u>	<u>CALCULATED</u>	<u>÷</u>	<u>MEASURED</u>
3	6.0	6.0	1.0
6	2.0	0.36	5.5
8	6.0	20	.3
10	6.0	1.0	6.0
11	1.2	0.6	2.0
13	2.0	1.0	2.0

\*C is a correction for the temperature change

In one way the injection of mineral oil was fortunate. The above analysis gives a ratio only, and it does not eliminate the possibility that both the non-CDI and the CDI flames are highly emissive. However the mineral oil-containing flame gives yet another reference point. This was at least two orders of magnitude more luminous than the non-mineral oil flame would have been at the same (lower) temperature, and it indicates that the flames without mineral oil (run 8 possible excepted) had emissivities less than a black body by that amount.

#### General Discussion of the Firing Results

It is of interest to consider how the foregoing results compare with various models other than chemical equilibrium. The possible ways in



which a non-equilibrium condition might express itself are limited only by the imagination, but a few of these are intrinsically more plausible than others; and it is useful to know if the effect on gross ballistic parameters is large enough to make the condition evident. Four models are considered below based on four different products species. The product species assumed are CDI vapor, HCN, HNCO, and NCO. A quasi-kinetic treatment was accomplished by forcing the CDI to form these species and allowing the remainder of the species in the medium to be in thermodynamic equilibrium with each other. The calculation was accomplished on the same chemical equilibrium computer program used to calculate full equilibrium theoretical performance. Necessary modifications were made to the thermodynamic library deck to allow the four species to form. The species HCN, HNCO, and NCO are already included in the JANNAF thermochemical tables and are normally considered. What was done to force the species to form was to create a fictitious specie having the same thermodynamic properties as the normal compound, and with the same formula, but with a dummy element replacing the nitrogen. The dummy element prevented chemical communication between the specie and all the other species available to the program. It was necessary to estimate high temperature thermodynamic functions for CDI. This was accomplished using both the statistical models summarized in the JANNAF thermochemical tables and estimated molecular frequencies. Four calculations were performed. All used the starting reactant flow rates which were experienced in combustion run number 7. In each calculation, one of the four species was forced to form. When the program is run in this way, the dominant reactions available to the CDI may be summarized as:

1.  $\text{C}_3\text{O}_3\text{N}_2 \longrightarrow \text{C}_3\text{O}_3\text{N}_2 \text{ (gas)}$
2.  $\text{C}_3\text{O}_3\text{N}_2 + 2 \text{H}_2 \longrightarrow 2\text{HCN} + \text{CO}_2 + \text{H}_2\text{O}$
3.  $\text{C}_3\text{O}_3\text{N}_2 + \text{H}_2 \longrightarrow 2\text{HNCO} + \text{CO}$
4.  $\text{C}_3\text{O}_3\text{N}_2 \longrightarrow 2\text{NCO} + \text{CO}$

The results of the calculation are summarized in Table 19. Of particular interest are the predicted temperature changes from the condition of no CDI flow to full CDI flow ( the row labeled  $\Delta T$ ) and the predicted chamber pressure changes (labeled  $\Delta P$ ). A conclusion that may be drawn from the table is that the actual course of the combustion might include a substantial fraction of CDI, HCN, or HNCO without causing extreme differences from the full equilibrium case (tabulated in the last column). It is interesting that the formation of HCN is accompanied by an increase in flame temperature over the full equilibrium case, leading to a decrease in the  $\Delta T$ . Since the  $\Delta T$  observed experimentally was larger, and not smaller, the full equilibrium case, HCN does not seem to fit the model as the sole non-equilibrium specie. All of the other species result in lower theoretical temperatures and could help to reconcile the HCN observed with the temperature that was found. The fact that none of the postulated species other than HCN were actually discovered in the products need not be taken as evidence that they were not indeed formed, since they are all very reactive. CDI and cyanic acid (HNCO) both polymerize on standing, to involatile products; whereas NCO is a radical and would be expected to react very rapidly, both with itself and other products in the medium. Thus the postulated products would remain in the sampling bottle during gas analysis. This line of reasoning led to a concerted effort to find condensible species in the sample bottles by rinsing them with water, and many of the common organic solvents. The only residue which could be recovered was about 0.5 gram of silicone grease. So the only non-equilibrium specie for which direct analytical evidence exists is HCN.

The non-equilibrium combustion of CDI is surprising in some ways. The experiment was not truly a combustion experiment so much as a pyrolysis experiment, because no thermal energy was expected from the CDI. Rather it was injected into an already established hot gas, and had only to break apart. Further, the CDI molecule seems only a few steps removed from the expected equilibrium products; all the carbon is attached to oxygen, and vice versa. No additional fuel or oxidizer are required,

TABLE 19. QUASI-KINETIC CALCULATIONS FOR RUN 7.

<u>Reactant</u>		<u>Flow Rate (g/sec)</u>			
O <sub>2</sub>		5.5			
CO Fuel		2.4			
CO/H <sub>2</sub> Diluent		44.5			
CDI		7.5			
<u>Specie</u>	<u>CDI/G</u>	<u>HCN</u>	<u>HNCO</u>	<u>CNO</u>	<u>CO/N<sub>2</sub></u>
C* (ft/sec)	3167	3306	3234	2990	3333
T <sub>C</sub> (°K)	1585	1677	1607	1284	1615
<u>Product Mole Fractions</u>					
Ar	.00022	.00021	.00021	.00020	.0002
CH <sub>4</sub>	.0001	-	-	.00042	
CO	.74816	.67245	.74294	.66284	.770
CO <sub>2</sub>	.17165	.25021	.17972	.19589	.157
H <sub>2</sub>	.02574	.00263	.00339	.02617	.026
H <sub>2</sub> O	.01728	.00324	.00248	.01310	.012
CDI	.03694	-	-	-	-
HCN	-	.07125	-	-	-
HCNO	-	-	.07125	-	-
CNO	-	-	-	.06886	-
Graphite	-	-	-	.03251	-
N <sub>2</sub>	o	o	o	o	.033
T (°K)	-208	-116	-186	-509	-178
P (psia)	+13	+30.6	21.5	-9.2	34.0

reducing the impact of any un-mixedness in the combustor. It was not expected that the kinetics would involve significant breakage of the strong C=O bond.

The weakest bonds in the CDI molecule are the two nitrogen - carbon single bonds joining the isocyanate groups to the carbonyl group. Their average bond strength is 62.5 kcal/mole, based on both the heat of formation of CDI reported earlier and the heat of formation for the NCO radical given in the JANNAF thermochemical Tables. This compares with 158.5 kcal per bond for the average of the remaining C=N and C=O bonds in the molecule. Thus, ignoring for the moment the possibilities for chemical attack, the most likely initial step is rupture of CDI into a carbon monoxide molecule and two NCO radicals. In principle the sequence could then be completed by the reaction between the NCO radicals



which is exothermic enough (-129 kcal) to return the heat absorbed by the original CDI breakup. This simple scheme might be an accurate accounting of events in a simple reaction medium containing only CDI and third bodies. However, the actual medium investigated contained significant quantities of elemental hydrogen, and also surplus oxygen from the oxidizer rich upper chamber. Thus the CDI was injected at a point where significant radical concentrations were being generated, and these doubtlessly increased the reaction possibilities of the CDI many fold. The change in liner configuration at test 11 was an attempt to eliminate some of those reaction possibilities by completing the reaction before the point of CDI injection. As the product analysis showed, the strategy failed, at least as measured by HCN formation.

## SECTION VII

### CONCLUSIONS AND RECOMMENDATIONS

The pyrolysis of CDI was found to exhibit a non-equilibrium feature in the formation of HCN, which accounted for about 10 percent of the total nitrogen introduced by the CDI. This is considered to be a real effect, and not an artifact of the combustor or procedure. The HCN, once formed, is persistent and survives a nominal 1800°K environment for at least 25 milliseconds. In an actual  $N_2O$ /benzonitrile/CDI gas generator, the amount of HCN would be limited by the total hydrogen present, either as  $H_2$  or  $H_2O$  and could not exceed, therefore, about 4 percent. The effect of this HCN on laser performance is presently unknown. In other respects the combustion was normal, yielding no evidence of particulates or other non-equilibrium species.

Whatever its effects on lasing, HCN is patently undesirable as an exhaust product owing to its toxicity. It is worthwhile to inquire how its formation might be avoided. Obviously it cannot form if no hydrogen, elemental or bound, is present. This might be arranged by sacrificing the energy available from benzonitrile and burning only CDI (the lower curve of Figure 1.). Alternatively, a non-hydrogen fuel might be used instead of benzonitrile. DCFO heavily diluted with CDI would probably be safe to handle, and the two compounds are in fact compatible. Still again, it might be possible to arrange a staged combustion in which CDI is pyrolyzed by burning a portion to  $CO_2$  and the final temperature then boosted with a small benzonitrile/ $N_2O$  stage. Implicit in all these suggestions, of course, is the assumption that CDI would, in the absence of hydrogen, not form some other non-equilibrium product -- one persistent enough to await the final arrival of water, or other hydrogen species. The data collected here do not shed any light on this possibility.

Whether any further work on this GDL reactant scheme is justified rests on the answers to yet other questions. The basic suitability of CO as a diluent molecule remains unsettled. The supposed storage advantages of

CDI over cryogenic nitrogen need further study in view of the finding that it must be stored either as a mild cryogen or a meltable solid. Its favorable density (60 percent greater than  $\text{LN}_2$ ) should not be overlooked here. And finally, any user of CDI must contend with its lack of commercial availability.

Nevertheless these questions are deserving of attention for any GDL application which imposes severe volume and weight constraints, such as is the case in airborne applications.

## REFERENCES

1. E. Gerry "Gas Dynamic Lasers" IEE Spectrum p 51-8. Nov 1970
2. J. Wilson "Exploratory Development Work in Support of the High Power/Energy Laser Program" Final Report Contract F29601-70-C-0073, AFWL-TR-70-152 (July 1971)
3. F. A. Cotton, and G. Wilkinson Advanced Inorganic Chemistry, Interscience Publishers (1962)
4. S. Coffey, "Compilation of Data on Organic Explosives", OSRD Report (1944)
5. F. D. Marsh and M. E. Hermes, J. Am. Chem. Soc. 87, 1819 (1965)
6. F. D. Marsh and M. E. Hermes, J. Am. Chem. Soc. 86, 4506 (1964)
7. W. J. Linn, O. W. Webster, and A. E. Benson, J. Am. Chem. Soc. 87, 3651 (1965)
8. E. Nachbaur, Monatshefte Für chemie Vol 97 p 361-7 (1966)
9. Rodd's Chemistry of Carbon Compounds. El Elseveier Publishing Co (1965)
10. E. Ciganel and C. Krespam, J. Org. Chem. 33, 541 (1968)
11. R. W. Begland, et. al. J. Am. Chem. Soc. 93 (19) 4953-5 (1971)
12. K. Wallenfels & G. Bachmann Angew. Chem. 73, 142-3 (1961)
13. C. O. Parker, et. al., Tetrahedron, 17, 79 (1962)
14. H. Wieland, Z. Kitasato & L. Vtzing, Ann. 1, 43 (1930)
15. C. L. Dickinson, US Patent 2,942,022.
16. Smirnova et al Biol Aktion Soldin Alead, Navle SSR 1965 102-8
17. A. J. Saggiomo, J. Org. Chem. 22 1171-5 (1957)
18. Bailey and Evans Chem Ind (1964) (32) 1424-5
19. A. S. Bailey and J. R. Case Tetrahedron 3 (1131) (1958)
20. E. I DuPont Patent Neth Appl 298295

21. C. D. Weis J. Org Chem 27 3514-20 (1962)
22. S. Trofimenko & B. C. McKusick, J. Am. Chem. Soc. (84) 3677-8 (1962)
23. Webster J. Am. Chem. Soc. 87 (8) 1820 (1965)
24. C. R. Noller Chemistry of Organic Compounds 3rd Ed W. B. Saunders Company (1966)
25. Webster J. Am. Chem. Soc. 86 (14) 2898-902 (1964)
26. M. Constantine, Monthly Progress Report, 16 Dec 1971, Contract FO4611-71-C-0035, Rocketdyne.
27. P. R. Hammond Science 142 (3591) 502 (1963)
28. K. Wallenfels and K. Friedrich, Tetrahedron Letters 1963 (19) 1223-7
29. T. L. Cairns, et al, J. Am. Chem. Soc. 80 (2775-80) (1957)
30. P. Liany "Organic Syntheses, Collective Vol III" Ed by E. C. Horning, John Wiley and Sons p 805.
31. H. Wieland, Ann, 444, 7 (1925)
32. N. Kornblum, Org Reactions, 12, 101 (1962)
33. C. Grundmann, Fortsch Chem Forsch. 7, 62 (1968)
34. G. B. Bachmann and L. E. Strom, J. Org. Chem. 28, 1150 (1963)
35. C. Grundmann, Ber., 97, 575 (1964)
36. M. Frankel, Rocketdyne, Private Communication.
37. D. E. Elrich et al, Allegheny Ballistics Laboratory Technical Report 69-20 p 5 (1969)
38. A. S. Bailey, B. R. Hemm, and J. M. Langdon, Tetrahedron 19, 161 (1963)
39. C. D. Veis, J. Org. Chem., 27, 3514 (1962)
40. E. Yamato and S. Sugawara, Tetrahedron Letters 1970, 4383.
41. F. Eloy, Fortsch Chem Forsch. 4 807 (1965)
42. F. Eloy, J. Org. Chem., 26, 952 (1961)



43. C. Grundmann and H. D. Franmold, J. Org. Chem. 31, 157 (1969)
44. C. I. Merrill and R. N. Watson "The Synthesis of 4, 5- Dicyanooxazole, A Low Hydrogen Content Fuel", AFRPL-TR-72-68, (June 1972).
45. Compt Rendu, 239, 816-818 (1954); Ber 1414-23 (1964)
46. Ber., 21, 2197 (1888); J. Chem. Soc., 95, 2167 (1909)
47. V. Krukonis, AVCO, Letter of 1 April 1971
48. R. Homewood, AVCO, Letter of 5 May 1970.
49. B. Goshgarian, G. Shoemaker, B. Goff, "Physical Properties of DCFO" Informal AFRPL Report February 1971
50. B. Goff, Test Report 133P, 17 February 1971
51. T. Owens, Test Report 267, 12 May 1970
52. T. Owens, Test Report 15, 19 January 1970
53. T. Owens, Test Report 1030, 5 January 1970
54. B Goff, Test Report 153P, 3 March 1971
55. Avanzino, Test Report 403, 26 May 1971
56. E. C. Lupton, G. Hess, Test Report 71T-2, 28 May 1971
57. B. Goff, Test Report 645, 19 March 1971
58. M. Constantine, Monthly Progress Report, 13 October 1971, Contract FO4611-71-C-0035
59. J. Siegel, US Navy Toxicology Unit, Letter of 18 May 1971
60. Dr. Back, AMRI., Private Communication
61. M. Constantine, Monthly Progress Report, 12 November 1971, Contract FO4611-71-C-0035
62. M. Constantine, Monthly Progress Report, 14 September 1971, Contract FO4611-71-C-0035
63. M. Constantine, Monthly Progress Report, 12 August 1971, Contract FO4611-71-C-0035
64. G. Shoemaker, Test Report 112P, 11 January 1971

65. Van Meter and Denson, Letter of 18 May 1971
66. Olin Matheson Chemical Co, US Patent 2,990,412
67. "Development and Demonstration of Inert Gas Pressurization System", Aerojet Report 8160-01Q-6F, November 1960.
68. "Design, Fabrication, and Test of a Breadboard Hybrid Pressurization System", Northrop Report NOR 69-129, May 1970.
69. J. Wilson Laser and Technology Program (U), Quarterly Interim Report, AVCO Everett Research Laboratory, November 1970, Confidential Report.
70. C.A. Brau, High Power Laser Techniques (U), AVCO Everett Research Laboratory, October 1969, Secret Report.
71. M. Constantine, Monthly Progress Report, 14 February 1972, Contract FO4611-71-C-0035, Rocketdyne
72. E. C. Lupton, Letter of 24 January 1972.
73. Watson and Hess, Test Report 460, 5 April 1972.
74. R. C. Mitchell Monthly Progress Reports, dated 13 June 1972, 10 July 1972, 11 September 1972, and 12 October 1972, Contract FO4611-71-C-0035, Rocketdyne.
75. E. C. Lupton, Private Communication.
76. B. Goshgarian, Test Report 127P, 12 January 1971.
77. Hess & Lupton, Test Report 71T-3, 29 June 1971.
78. B. Goshgarian, Private Communication.
79. L. A. Dee, Test Report 692, 27 April 1971.
80. W. H. McAdams, Heat Transmission McGraw-Hill Book Company Inc (1954)
81. Bird, Stewart and Lightfoot, "Transport Phenomena", John Wiley and Sons, Inc. (1960)
82. R. Svehla "Estimated Viscosities and Thermal Conductivities of Gases at High Temperatures". NASA-TR-R-132 (1962)

83. C.R. Wilke, J. Chem. Physics 18 517-19 (1950)
84. Forstall, Walton, and Shapior, J of Appl. Mech. 399 (December 1950)
85. T. Fanciullo "RE-283 Swirl Injector Design Program" (1970)
86. C. Merrill, M. Barnes, R. Watson, "An Improved and Economical Process for the Production of Dicyanofuroxan", USAF Invention #8098.

## AUTHOR'S BIOGRAPHY

Curtis C. Selph  
Air Force Rocket Propulsion Laboratory  
Edwards, California

Project Engineer, Gas Dynamic Section, Engine Components Branch, Liquid Rocket Division. B.S. Chemical Engineering, University of South Carolina, 1958. M.S. Chemistry, Georgia Institute of Technology, 1970. Authored: "Boron Nitride Producing Reactions" Presented at 3rd meeting of the JANAF-ARPA-NASA Thermochemical Panel: "The Effect on Specific Impulse of Uncertainties in the Heat of Formation of Beryllium Subfluoride", presented at the 5th meeting of the JANAF-ARPA-NASA Thermochemical Panel; "The Thermodynamic Properties of Beryllium Compounds. X. Heats of Formation and Entropies of  $\text{BeCl}_2(\text{g})$  and  $\text{Be}_2\text{Cl}_4(\text{g})$ ." J. of Physical Chemistry 71, 254 (1967); "More-Storable Reactants for Gas Dynamic Lasers" presented at AIAA 10th Combustion Symposium.

Member: American Institute of Aeronautics and Astronautics.

## AUTHOR'S BIOGRAPHY

Michael F. Powell  
Air Force Rocket Propulsion Laboratory  
Edwards, California

Senior Project Engineer, Gas Dynamic Section, Engine Components Branch, Liquid Rocket Division. B.S. in Aeronautics and Astronautics, University of Washington, 1964. Senior AFRPL Project Engineer on a joint AFWL/AFRPL High Power Chemical Laser Program. Authored: Design & Experimental Evaluation of a Direct Combustion HF Chemical Laser (DCL II) AFRPL-TR-72-67; "Injector/Chamber Scaling Evaluation, Rocketdyne Injector Development" - AFRPL-TR-70-34; "Injector/Chamber Scaling Evaluation, TRW Injector Evaluation; - AFRPL-TR-69-199; - "Injector/Chamber Scaling Evaluation Facility Checkout" - AFRPL-TR-69-83; and "Development of Electroformed Water-Cooled Thrust Chamber Assemblies" - AFRPL-TM-66-32.

Member: American Institute of Aeronautics and Astronautics.